İSTANBUL TECHNICAL UNIVERSITY ★ INSTITUTE OF SCIENCE AND TECHNOLOGY

REDUCTION OF GAS-PHASE REACTION MECHANISM OF ISOOCTANE FOR THE DESCRIPTION OF PARTIAL OXIDATION OF SURROGATES OF GASOLINE AND DIESEL

M.Sc. Thesis by

Hüseyin KARADENİZ

Department : Mechanical Engineering

Programme : Automative

Thesis Supervisor: Prof. Dr. Cem Soruşbay

SEPTEMBER 2010

ACKNOWLEDGEMENTS

TABLE OF CONTENTS

ABBREVIATIONS

APU	**:**	Auxiliary Power Unit
CFD	**:**	Computational Fluid Dynamics
CPOX	**:**	Catalytic Partial Oxidation
CPU	**:**	Central Processing Unit
CSP	**:**	Computational Singular Perturbation
DRG	**:**	Directed Relation Graph
DRGEP	**:**	Directed Relation Graph With Error Propagation
DRGASA	**:**	Directed Relation Graph Aided Sensitivity Analysis
DRGEPSA	**:**	Directed Relation Graph With Error Propagation And Sensitivity Analysis
ILDM	**:**	Intrinsic Low-Dimensional Manifolds
OCM	**:**	Oxidative Coupling of Methane
ODE	**:**	Ordinary Differential Equation
LLNL	**:**	Lawrence Livermore National Laboratory
POX	**:**	Partial Oxidation
PMSR	**:**	Pairwise Mixing Stirred Reactor
PSR	**:**	Perfectly Stirred Reactors
QSS	**:**	Quasi-Steady-State
QSSA	**:**	Quasi-Steady-State-Approximation
RR	**:**	Reaction Rate
SI	**:**	Spark Ignition
SR	**:**	Steam Reforming

LIST OF TABLES

LIST OF FIGURES

LIST OF SYMBOLS

A   **:** Frequency factor

          Area

$\overline{A}^0$ **:** Free energy

$\dot{A}_{ijk}$ **:** Elemental flux of atom A from species j to species k through reaction i

b   **:** Exponent factor

c_i **:** Concentration of species i

c_{ij} **:** Consumption of species i to species j through all atoms through forward and backward reactions

$c_{ij}^{\ a}$ **:** Consumption of species i to species j through atom a

$c_{ij\ f}^{a}$ **:** Consumption of species i to species j through atom a multiplied with sum of both species' sensitivity coefficients (species i and species j) through forward reactions

$c_{ij\ b}^{a}$ **:** Consumption of species i to species j through atom a multiplied with sum of both species' sensitivity coefficients (species i and species j) through backward reactions

C_P **:** Heat capacity at constant temperature

D_{im} **:** Averaged diffusion coefficient

E_a **:** Activation energy

$E_{i,r}$ **:** Absolute sensitivity

$E_{i,r}^{rel}$ **:** Relative sensitivity

f_{fast} **:** Fast modes

f_{slow} **:** Slow modes

f_{ij} **:** Formation of species i from species j through all atoms through forward and backward reactions

f_{ij}^{a} **:** Formation of species i from species j through atom a

$f_{ij\ f}^{a}$ **:** Formation of species i from species j through atom a multiplied with sum of both species' sensitivity coefficients (species i and species j) through forward reactions

$f_{ij\ b}^{a}$ **:** Formation of species i from species j through atom a multiplied with sum of both species' sensitivity coefficients (species i and species j) through backward reactions

Gz   **:** Graetz number

h   **:** Enthalpy

h_{k} **:** Mass transfer coefficient

$I_{(i)}$ **:** Predefined importance value of species i

$I_{k,i}$ **:** Index of the *i*th reaction to the production rate of the *k*th species in the *j*th reaction

J   **:** Jacobian Matrix

k   **:** Reation rate constant

K_{c} **:** Equilibrium constant

k_{r} **:** Parameter of the system

m   **:** Molecular mass

M   **:** Molecular weight

n_{j}^{a} **:** Number of atoms in species j

n_{k}^{a} **:** Number of atoms in reaction k

$n_{A,j}$ **:** Number of atoms in species j

N_{i} **:** Necessity of species i

$N_{i,0}$ **:** Initial necessity of species i

$N_{A,i}$ **:** Total number of atoms in reaction i

N_{i} **:** Number of species

Nu_{T} **:** Nussult number

P	: Pressure
$\underline{P}$	: Steric factor
q_i	: Instantaneous rate of reaction i
q_{ifwd}	: forward reaction rate
q_{irev}	: backward reaction rate
R	: Universal gas constant
r_k	: Rate of reaction k
$S_{A,B}$	: Sensitivity of species A on species B
S_{ji}	: Sensitivity of species j on species i
$S_{(i,k)}$	: Sensitivity of species i in reaction k
Sh	: Sherwood numbers
$\dot{s}_k$	: surface reaction rate
T	: Temperature
U	: Internal energy
	Velocity
ν'	: Stoichiometric coefficient (reactant)
ν''	: Stoichiometric coefficient (product)
X^+	: Activated complex
ω_i	: production rate of species i
$\dot{\omega}_k$	: gas phase reaction rate
V	: Volume
Y	: Variable
σ_{BC}	: collision radius of species B and C
μ	: Reduced mass

[ ]   **:** Concentration

$\Delta_R \overline{A}^0$ **:** Change of free energy in a reaction

Λ **:** Diagonal matrix

τ_c **:** Characteristic time scale

ϕ **:** Composition space

ψ **:** Vector

ρ **:** Density

α **:** Surface relaxation factor

REDUCTION OF GAS-PHASE REACTION MECHANISM OF ISOOCTANE FOR THE DESCRIPTION OF PARTIAL OXIDATION OF SURROGATES OF GASOLINE AND DIESEL

SUMMARY

Development of reformers to produce hydrogen and/or synthesis gas from liquid hydrocarbon fuels (e.g., gasoline, diesel, or jet fuel) offers potential for NOx abatement in diesel engines, engine combustion enhancement, and for electricity production in fuel cell auxiliary power units (APUs) on-board of vehicles. Conventional fuels are attractive due to their high energy density, large amount of hydrogen (elementary) stored, widespread production, and distribution and retailing infrastructure [1]. Further, they do not require carrying an additional fuel for on-board vehicle applications.

There are three chemical processes using primary fuels to make fuel-cell hydrogen: steam reforming (SR), catalytic partial oxidation (CPOX) and autothermal reforming (ATR). Due to its slow start-up and endothermic operation, traditional steam reforming (SR) is not attractive for efficient mobile applications. Catalytic partial oxidation (CPOX) and autothermal reforming (ATR), which combines CPOX and SR, are considered to be thermally more efficient for reforming [2].

Extensive efforts have been made to develop compact reforming reactors for reformate/hydrogen production from a variety of hydrocarbon sources including diesel and gasoline. The reactors consist of monolithic structures coated with noble metal catalysts, on which the hydrocarbons are partially oxidized. Aside from the heterogeneous conversion, homogeneous reactions seem to be significant, in particular for higher hydrocarbons and real fuels. The reactors are fed with hydrocarbon/air mixtures and can be operated autothermally. Coking and aging of the catalyst under reforming conditions are major challenges in the reactor development. Therefore, a profound knowledge of the CPOX for complex hydrocarbon fuels is required to improve the overall behavior of the reformer and predict coking of the reforming catalyst.

Numerical simulations have become an important tool for enhancing our understanding of oxidation processes in reforming reactors. Homogeneous chemistry is found to play the important role in the formation of soot in the gas phase and coking of reforming catalyst. In particular, the formation of soot precursors is likely through homogeneous gas-phase reactions at fuel rich operating conditions and high temperature.

Recent advancements in detailed descriptions of combustion and partial oxidation processes have led to a drastic increase in the total number of chemical species and steps in the detailed chemical mechanisms. For gasoline engine applications, the detailed i-octane mechanism developed by Lawrence Livermore National Laboratory (LLNL) contains 857 species and 7193 reactions [3]. This mechanism was used for the numerical study of catalytic partial oxidation of isooctane over a

rhodium/alumina coated honeycomb monolith in flow reactor at short-contact times [4]. Although the new numerical approach [5] allows us to speed up the treatment of large-scale 2D fluid dynamics by using a detailed gas-phase and surface chemistry in DETCHEM software [6], a typical run with the detailed LLNL mechanism in plug-flow reactor configuration takes many hours. In order to significantly cut down the computational time, a reduced description of homogeneous chemistry with fewer species and steps is necessary [7]. Hence a reduced description can be used for speedy CFD- simulations of reforming systems with complex geometry to support mobile fuel-cell-based APU systems operating on logistics fuels.

The objective of this study is the coupling of mechanism reduction procedures with DETCHEM software and development of i-octane reduced mechanism for fast and accurate prediction of soot precursors in CPOX reformer at fuel rich operating conditions.

BENZİN VE DİZEL TEMSİLİ YAKITLARIN KISMI OKSİDASYONUNU TANIMLAYAN IZOOCTAN'IN GAZ FAZINDAKİ REAKSİYON MEKANİZMASININ İNDİRGENMESİ

ÖZET

Sıvı hidrokarbon yakıtlarından (benzin, dizel, jet yakıtları vb.) hidrojen ve/veya sentez gazı (hidrojen ve karbonmonoksit içeren gaz) üretimi dizel motorlarında NOx emisyonunun azaltılması, motor yanmasının iyileştirilmesi ve araçlarda yerleşik olarak yakıt hücresi yardımcı güç ünitelerinde elektrik üretimi gibi olanaklar sunmaktadır. Geleneksel yakıtlar yüksek enerji yoğunlukları, içermekte oldukları büyük miktarlarda hidrojen kaynağı, yaygın üretim, dağıtım ve satış alt yapıları gibi avantajları nedeniyle bu amaç için oldukça kullanışlıdırlar [1]. Ayrıca, araçlardaki yerleşik uygulamalarda ilave yakıt taşınmasını gerektirmemektedirler.

Temel yakıtları yakıt hücresi hidrojenine dönüştürmek amacıyla üç kimyasal proses kullanılmaktadır: buharla yeniden düzenleme (SR), kısmı katalitik oksidasyon (CPOX) ve ototermal olarak yeniden düzenleme (ATR). Geleneksel buharla yeniden düzenleme (SR) yavaş başlangıç çalışma koşulları ve endotermik çalışma gibi dezavantajları nedeniyle verimli mobil uygulamalarda çok kullanışlı değildir. Katalitik kısmı oksidasyon (CPOX) ve katalitik kısmı oksidasyon ile buharla yeniden düzenleme yöntemlerinin bir birleşimi olan ototermal olarak yeniden düzenleme (ATR) yeniden düzenleme prosesinde termal olarak daha verimli çalışmaya olanak sağlamaktadırlar [2].

Dizel ve benzin gibi hidrokarbon kaynaklarından hidrojen üretmek amacıyla uygun yeniden düzenleme reaktörlerinin üretilmesi amacıyla birçok çalışma yapılmıştır. Reaktörler, üzerlerinde hidrokarbonların kısmi olarak okside edildiği soy metal katalizörleriyle kaplı monolitik yapıya sahiptirler. Homojen reaksiyonların özellikle yüksek hidrokarbonlar ve gerçek yakıtlar için heterojen dönüşümden daha fazla öneme sahip oldukları görülmektedir. Reaktörler hidrokarbon/hava karışımlarıyla beslenmektedirler ve ototermal olarak çalıştırılabilirler. Hidrokarbonların yeniden düzenlenmesi prosesi esnasında kok oluşumu ve katalizörün yaşlanması reaktör geliştirilmesindeki en büyük güçlüklerdir. Bu yüzden yeniden düzenleyici reaktörlerin geliştirilmesi ve katalizördeki kok oluşumunun tahmin edilebilmesi amacıyla kompleks hidrokarbonların katalitik kısmı oksidasyonu ile ilgili detaylı bilgiye ihtiyaç duyulmaktadır.

Yeniden düzenleyici reaktörlerin oksidasyon proseslerinin davranışlarını anlayabilmek amacıyla nümerik hesaplamalar önemli bir araç haline gelmiş durumdadır. Gaz fazında is oluşumunda ve yeniden düzenleyici katalizörde kok oluşumunda en önemli etkinin homojen reaksiyon kimyasından geldiği anlaşılmaktadır. Özellikle, is öncülerinin oluşumu çoğunlukla homojen gaz kimyası reaksiyonlarında yakıtça zengin karışım ve yüksek sıcaklık koşullarında gerçekleşmektedir.

Yanma ve kısmi oksidasyon proseslerindeki son gelişmeler detaylı kimyasal mekanizmalarındaki toplam kimyasal bileşen ve reaksiyon sayılarında önemli miktarlarda artışlara neden olmuştur. Lawrence Livermore Ulusal Laboratuarı

(LLNL) tarafından benzin motoru uygulamaları için geliştirilen detaylı i-oktan mekanizması 857 bileşen ve 7193 reaksiyon içermektedir [3]. Bu mekanizma i-oktanın rodyum/alüminyumoksit kaplı bal peteği şeklindeki monolit akış reaktöründe kısa reaksiyon sürelerindeki katalitik kısmı oksidasyon olayının nümerik olarak incelenmesi amacıyla kullanılmıştır [4]. Her ne kadar DETCHEM [6] yazılımında geliştirilen yeni nümerik yaklaşım [5] büyük ölçeklerdeki 2 boyutlu akış dinamiklerinin gaz fazı ve yüzey kimyası koşulları için incelenmesini hızlandırmış olsa da, detaylı LLNL mekanizmasıyla plug-akış reaktör konfigürasyonu saatler boyu sürmektedir. Hesaplama süresini önemli miktarlarda azaltabilmek amacıyla, daha az sayıda bileşen ve reaksiyon içeren indirgenmiş homojen mekanizma kimyasının kullanımı gereklidir [7]. Bu yüzden, lojistik yakıtların kompleks yapıdaki yeniden düzenleme sistemlerinin yakıt hücresine dayanan yardımcı güç ünitesi sistemlerindeki kullanımı sırasında daha hızlı hesaplamalı akışkanlar mekaniği (CFD) simülasyonlarının yapılabilmesi amacıyla indirgenmiş reaksiyon mekanizmalarının yardımına başvurulabilir.

Bu çalışmanın amacı ise DETCHEM yazılımı ile mekanizma indirgeme tekniklerini birleştirerek katalitik kısmi oksidasyon yeniden düzenleyicisinde i-oktan indirgenmiş mekanizmasını yakıtça zengin karışımlarda kullanmak ve de is öncülerinin doğru ve hızlı bir şekilde tahminini yapabilmektir.

1. INTRODUCTION

Increasing industrialization results in increasing fuel consumption. Because most of the energy requirement is obtained by fossil fuels, it is a great interest of increasing the efficiency of combustion of these fuels and decreasing the emissions omitted from them. Alternative processes are investigated in order to achieve these objectives.

Hydrogen is an alternative energy carrier that has great environmental advantages. Production of hydrogen and syngas (H_2 and CO) from liquid hydrocarbons such as gasoline, diesel and natural gas by catalytic partial oxidation (CPOX) and steam reforming (SR) is currently in the focus of both academic and industrial research [4]. Hydrogen is the simplest and the most plentiful element in the universe. Despite its simplicity and abundance, hydrogen does not occur naturally as a gas on Earth, it is always combined with other elements. Water, for example, is a combination of hydrogen and oxygen. Hydrogen is also found in many organic compounds, notably the "hydrocarbons" that make up many of our fuels such as gasoline, natural gas, methanol and propane [8]. Hydrogen has a very high flame speed and good ignitibility, thus enables extremely lean operation, so lean that engines have been run down to 30% of full load without any throttling [9]. High flame speed enables to operate in lean mixture which leads to improved efficiency and decrease NO_x and CO emissions.

There are generally three ways to store hydrogen in an automobile: as a gas "dissolved" in a metal (metal hydride), as a cryogenic liquid or as a compressed gas. Hydride storage is the simplest and the safest, but it increases vehicle weight and results in a severe fuel economy penalty. Liquid hydrogen is light, but due to its low energy density occupies three times as much volume as gasoline. Storage as a compressed gas is inexpensive and provides for ease of operation but its weight and bulk are the main problems [10].

On-board hydrogen generation from a suitable high energy density fuel such as gasoline is an alternative to obtain hydrogen. However, a problem is how to generate

hydrogen from such fuels. Most common techniques for this generation process are partial oxidation (POX), steam reforming (SR) and autothermal reforming (ATR).

Partial oxidation (POX) technique involves the exothermic reaction of feed fuel in the presence of a small amount of air, such that incomplete combustion should occur. The generation of hydrogen from gasoline may be represented as,

$$CH_{1.86} + 1/2(O_2 + 79/21\ N_2) \rightarrow 0.93\ H_2 + CO + 79/42\ N_2$$
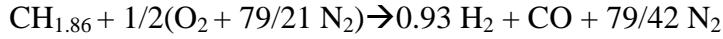
where the oxygen is supplied in air. Carbon in the fuel is converted in to carbon monoxide, and hydrogen in the fuel is released as free hydrogen. The product gas now contains the residual nitrogen from air [10]. Partial oxidation is an exothermic reaction.

Steam reforming (SR) enables to produce hydrogen from hydrocarbons with or without the presence of a catalyst. The use of catalyst may result in low enough temperatures and short contact times. The objective of a catalytic steam reforming process is to liberate the maximum quantity of hydrogen held in water and the feed stock fuel. Steam reforming of gasoline may be represented by the following idealized chemical reaction,

$$CH_{1.86} + H_2O \rightarrow 1.93\ H_2 + CO$$
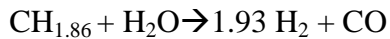
Carbon in the fuel is converted in to CO by oxidation with oxygen supplied in the steam, and hydrogen in the fuel, together with hydrogen in the steam, is released as free hydrogen. In other words, the resulting hydrogen comes from fuel as well as from the steam. The reaction is endothermic, i.e. it requires external heat input through a heat exchanger surface [10].

Autothermal reforming (ATR) is known as simultaneous conversion of hydrocarbons with steam and oxygen [11]. It offers advantages of small unit size, and lower operational temperature, easier startup, and wider choice of materials. Moreover, it has a higher energy efficiency compared to SR and POX. The overall ATR of methane is ideally expressed by the following reaction equation,

$$CH_4 + x(O_2) + (2-2x)H_2O \rightarrow CO_2 + (4-2x)H_2$$
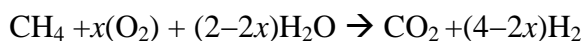
where x is the O/C molar ratio. This ratio is the key stoichiometric parameter that determines the theoretical S/C molar ratio required to convert CH_4 in to CO_2 and H_2,

the maximum H_2 yield, and the heat of reaction at adiabatic conditions at defined temperature [12].

Steam-reforming reaction of hydrocarbons usually taking place at temperatures around 700°C seems to show the highest reforming efficiency. But the drawback is that this reaction is endothermic and therefore the reactor needs to be heated by combustion of fuels itself. POX and ATR systems do not require external heating like steam-reforming system and can be heated up internally relatively quickly by exothermic reaction of fuels. Hence, they are much dynamic than a steam reforming system [13].

Catalytic reactors are generally characterized by the complex interaction of various physical and chemical processes. Monolithic reactors can serve as example, in which partial oxidation and reforming of hydrocarbons, combustion of natural gas, and the reduction of pollutant emissions from automobiles are frequently carried out. Figure 1.1 illustrates the physics and chemistry in a catalytic combustion monolith that glows at a temperature of about 1300 K due to the exothermic oxidation reactions [14].
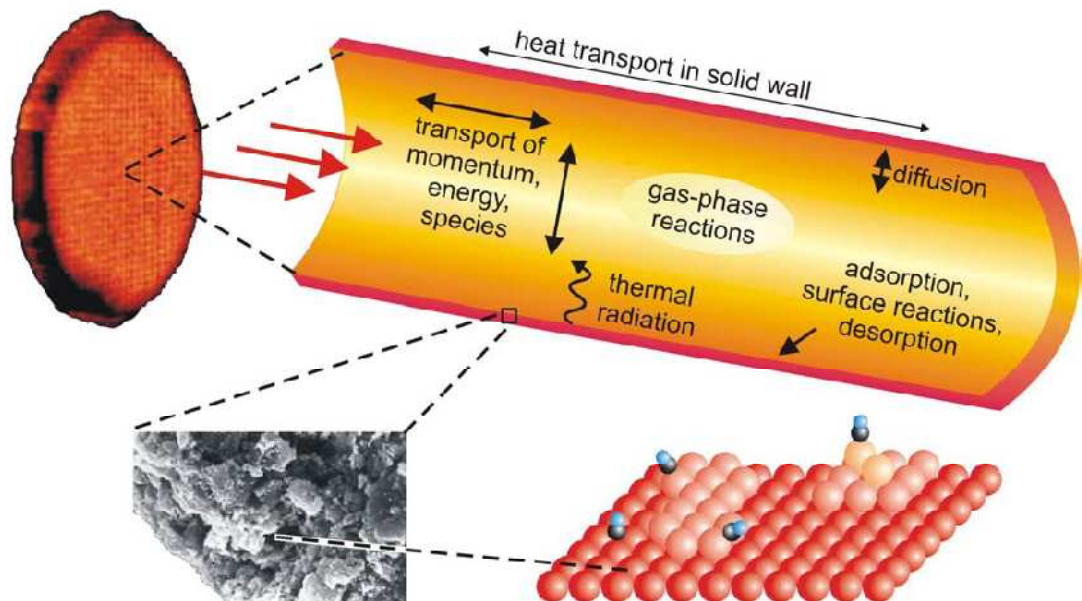
Figure 1.1 : Catalytic combustion monolith and physical and chemical process occurring in the single monolith channel [14]

In each channel of the monolith, the transport of momentum, energy, and chemical species occurs not only in flow (axial) direction, but also in radial direction. The

reactants diffuse to the inner channel wall, which is coated with the catalytic material, where the gaseous species adsorb and react on the surface. The products and intermediates desorb and diffuse back in to the bulk flow. Due to high temperatures, the chemical species may also react homogenously in the gas phase. In catalytic reactors, the catalyst material is often dispersed in porous structures like washcoats or pellets. Mass transport in the fluid phase and chemical reactions are then superimposed by diffusion of the species to the catalytic centers in the pores. The temperature distribution depends on the interaction of heat convection and conduction in the fluid, heat release due to chemical reactions, heat transport in the solid material, and thermal radiation. If the feed conditions vary in time and space and/or heat transfer occurs between the reactor and the ambiance, a non-uniform temperature distribution over the entire monolith will result, and the behavior will differ from channel to channel [14].

The reactors for the catalytic partial oxidation process consist of monolithic structures coated with noble metal catalyst being on the order of a quarter to one millimeter in diameter, on which the hydrocarbons are partially oxidized. High conversion of hydrogen ($YH_2 > 90\%$) can be achieved in rhodium catalyst at short contact times upon low ignition temperatures [15-16]. Aside from the heterogeneous conversion, homogenous reactions seem to be significant, in particular for higher hydrocarbons and real fuels. At the operating temperatures around 1000 K and higher, homogenous gas phase reactions are likely [4]. Coking and aging of the catalyst under reforming conditions are major challenges in the reactor development. Therefore, a profound knowledge of the CPOX for complex hydrocarbon fuels is essential to improve the overall behavior of the reformer and predict coking of the reforming catalyst. Homogenous chemistry is found to play an important role in the formation of soot in the gas phase and coking of reforming catalyst. In particular, the formation of soot precursors is likely through homogenous gas-phase reactions at fuel rich operating conditions and high temperature.

Multipurpose commercial CFD codes can simulate very complex reactive flows. There are several software packages for the modeling of complex reaction kinetics in CFD such as CHEMKIN [17] and DETCHEM [6].

DETCHEM software package [6] allows modeling and simulation of reactive flows. It enables modeling and simulation of homogenous gas phase reactions as well as heterogeneous reactions on catalyst. Numerical study of different catalytic combustion and partial oxidation processes were applied in DETCHEM software package such as partial oxidation of methane to synthesis gas at short contact times in rhodium coated monoliths [18], catalytic combustion of methane [19], catalytic partial oxidation of i-octane over rhodium catalysts [4] and catalytic reforming of higher hydrocarbons [20].

Hartmann et al. [20] displayed the selectivity of the major by-products, methane, ethylene, propylene, and iso-butylene as a function of C/O ratio (carbon-to-oxygen ratio). Their results show that full conversion of i-octane on rhodium catalyst is obtained at fuel lean and stoichiometric conditions (up to C/O=1). Because the amount of oxygen is not enough to ensure full conversion of i-octane, the amount of fuel that is partially and totally oxidized on the surface decreases. Therefore, temperature decreases with the increasing C/O ratios. In addition, less oxygen content in the feed reduces the amount of fuel that can be heterogeneously converted by exothermic surface reactions forming CO, CO_2, H_2 and H_2O. Therefore, higher C/O ratios leave more fuel for homogenous conversion occurring further downstream. They proved that the best selectivity for syngas production can be achieved at C/O=1, 98% for H_2 and 99% for CO. At lower C/O ratios, the amount of the total combustion products, CO_2 and H_2O increases but no other products are observed. As the C/O ratio increases, the selectivity towards H_2 and CO decreases and the selectivity for olefins (C_2-C_4) increases. Major by-products explained in their study are methane, i-butylene, propylene, and ethylene. No olefins are detected at C/O=1, as the C/O ratio increases, the concentration of olefins increases rapidly and reach maximum at the end of monolith channel [4].

Solutions performed through CFD simulations require much computation time. Nonlinearity, large number of chemical species and reactions, and the fact that chemical reactions exhibit a large range of time scales make the solution of those equation systems challenging. Turbulent flows as well as sometimes laminar flows require too much of CPU time with current numerical algorithms and computer capacities. This challenging fact asks for the application of reduction of large reaction mechanisms.

2. FUNDAMENTALS OF CHEMICAL KINETICS

If the initial state of a reactive gas mixture is known, the final state of this mixture after chemical equilibrium can be determined. Chemical kinetics allows us to determine how the mixture gets from its initial state to final state. It allows us to determine some properties such as reaction rates, temperature, pressure and concentrations of chemical species. Here, a brief summary of the required formulae will be given [21, 22].

2.1 Rates of Reaction and Reaction Orders

Chemical reactions take place at a certain rate that depends on the conditions of the system such as concentrations of the chemical compounds, pressure, temperature, existence of a catalyst or inhibitor. Rate of reaction is defined as the consumption rate of a reactant or formation rate of a product whose unit is defined as mol/m^3s.

A one-step chemical reaction can be expressed in terms of stoichiometric coefficients:

$$\sum_{i=1}^{N} \nu'_i M_i \rightarrow \sum_{i=1}^{N} \nu''_i M_i \qquad (2.1)$$

where ν'_i is the stoichiometric coefficient of reactants, ν'' is the stoichiometric coefficient of products, M_i is the specification of the molecule of the ith species, and N is the total number of compounds involved in the reaction. The meaning of this equation can be illustrated by the following example.

$$5H \rightarrow 2H_2 + H \qquad (2.2)$$

In this example,

N=2, M1=H, M2=H2, $\nu'_1 = 5$, $\nu''_1 = 1$, $\nu'_2 = 0$, $\nu''_2 = 2$

The chemical reaction (2.2) is balanced with the stoichiometric coefficients. But equation (2.1) does not provide a detailed information about the reaction mechanism.

Reaction rate of a chemical product species is proportional to the products of the concentrations of the reacting chemical species where each concentration is raised to a power equal to the corresponding stoichiometric coefficient. Thus, reaction rate is given as,

$$RR = \frac{d[\ ]_{product}}{dt} = \frac{d[\ ]_{reactant}}{dt} = k \prod_{i=1}^{N} ([\ ])^{v_i'} \qquad (2.3)$$

$$\frac{d[\ ]}{dt} = (v_i'' - v_i')RR = (v_i'' - v_i')k \prod_{i=1}^{N} ([\ ])^{v_i'} \qquad (2.4)$$

where [ ] is the concentration of species, k is the reaction rate constant. Rate constant is independent of the concentrations of species [ ] and depends on the temperature. In most cases it can be expressed as,

$$k = AT^b \exp\left(-\frac{E_a}{RT}\right) \qquad (2.5)$$

where AT^b represents the collision frequency and exponential term is called as the Boltzmann factor. If this factor is explained in more detail,

$$D = AT^b \qquad (2.6)$$

where b is the exponent between 0 and 1. Then equation (4) becomes

$$k = D \exp\left(-\frac{E_a}{RT}\right) \qquad (2.7)$$

$$A = \sigma_{BC}^2 \left(\frac{8\pi KT}{\mu}\right)^{1/2} \underline{P} \qquad (2.8)$$

where K is the Boltzmann constant, μ is the reduced mass of colliding molecules of B and C [$\mu \equiv m_B m_C / (m_B + m_C)$], σ_{BC} is the collision radius of species B and C, m_B and m_C are the molecular masses and $\underline{P}$ is the steric factor whose order is about 0.01.
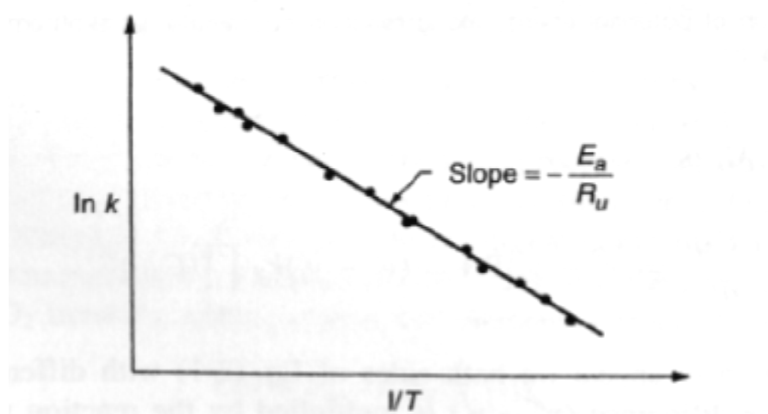
Figure 2.1 : Temperature dependence of reaction rate constant k [22]

The term E_a corresponds to activation energy. Chemical reactions occur only if the reacting molecules have an energy level above activation energy. In other words, there is an energy barrier for chemical reactions to occur. When we consider two reactant molecules react and form C and D molecules. Products are preceded by the activated complex, which is symbolized as X^+. Thus,

$$A + B \rightleftarrows X^+ \rightleftarrows C + D \tag{2.9}$$

For instance, considering the equation (2.9), when a free atom B reaches to the molecule A_2, then an activated complex BA_2^+ may be formed. This activated complex always has more energy than the separate molecules or atoms and it may separate in to BA and A molecules or the initial components B and A_2. And there is a path during the reaction from reactants to products and activated complex is at the point where exist highest energy. If we consider a reaction as shown below,

$$A+B+C+\ldots \rightarrow D+E+F+\ldots \tag{2.10}$$

where A,B and C denote the different reactants involved in the reaction. Since the species A is a reactant, the consumption rate of this species is written in terms of reaction rate as,

$$\frac{d[A]}{dt} = -k \cdot [A]^a [B]^b [C]^c \ldots$$

$$k_{exp} = k [B]^b [C]^c \ldots \tag{2.11}$$

$$\frac{d[A]}{dt} = -k_{exp} \cdot [A]^a$$

where a, b and c are reaction orders with respect to species A,B and C,… and k is the rate coefficient of the reaction. The sum of these coefficients gives the overall order of the reaction, such as first order or second order reaction. Here concentrations of species, e.g. [B], [C] shall remain almost constant during the reaction, in other words they do not change noticeably.

Unit of the reaction rate constant is expressed in terms of overall reaction order, m, as

$$\frac{mole}{cm^3 \cdot s} \frac{1}{\left(mole / cm^3 \right)^m} = mole^{1-m} cm^{3m-3} s^{-1}$$

If the overall order of reaction m=1 is, then unit of the reaction is a frequency, since $mole^{1-m} cm^{3m-3} s^{-1} = mole^{1-1} cm^{3-3} s^{-1} = s^{-1}$. A second order reaction has a unit of $mole^{1-2} cm^{6-3} s^{-1} = cm^3 / (mole \cdot s)$.

Considering equation (2.11), first order reaction gives a first-order (a=1) time behavior,

$$\ln \frac{[A]_t}{[A]_0} = -k_{exp} \left(t - t_0 \right) \tag{2.12}$$

where $[A]_t$ and $[A]_0$ are concentrations of species A at time t and t_0, respectively.

Second-order (a=2) time behavior of the reaction is determined as,

$$\frac{1}{[A]_t} - \frac{1}{[A]_0} = k_{exp} \left(t - t_0 \right) \tag{2.13}$$

Third-order time behavior of the reaction is determined as,

$$\frac{1}{[A]_t^2} - \frac{1}{[A]_0^2} = 2k_{exp} \left(t - t_0 \right) \tag{2.14}$$
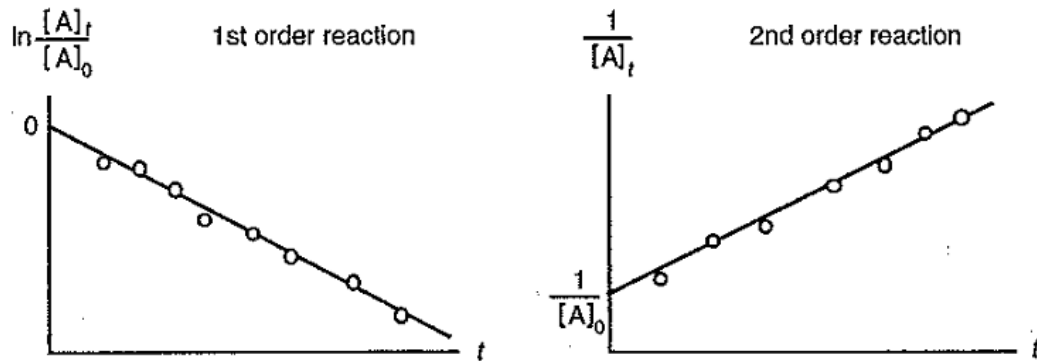
Figure 2.2 : Time behavior of the concentrations for first and second order reactions [21]

2.2 Reverse Reactions

In a chemically reacting system backward reactions also occur in addition to forward reactions. The rate law for backward reactions can be written based on equation (2.11) as,

$$\frac{d[A]}{dt} = k^{(r)}[D]^d[E]^e[F]^f .....$$ (2.15)

Forward and backward reactions have the same rate,

$$\frac{d[A]}{dt} = k^{(f)}[A]^a[B]^b[C]^c ..... = k^{(r)}[D]^d[E]^e[F]^f .....$$

or (2.16)

$$\frac{[D]^d[E]^e[F]^f ...}{[A]^a[B]^b[C]^c ...} = \frac{k^{(f)}}{k^{(r)}}$$

This relation corresponds to equilibrium constant, K_c,

$$K_c = \frac{k^{(f)}}{k^{(r)}} = \exp(-\Delta_R \overline{A}^0 / RT)$$ (2.17)

2.3 Elementary Reactions, Reaction Molecularity

Chemical reactions occur in different steps. While some of them occur in hundreds of reactions, others can occur in thousands of reactions. Such reactions are called elementary reactions. Occurrence of a CO_2 product in a combustion system can be given as an example for this phenomenon. In other words, CO_2 molecule does not

10

evolve only by the collision of C atom and O_2 molecules in one reaction. Such reactions are called as overall reactions. Overall reactions have complicated rate laws comparing to elementary reactions. And they consist of a large number of elementary reactions.

Reaction molecularity is transition state between reactants and products during the reaction and it corresponds to number of species. Three different reaction molecularities are considered here, respectively: unimolecular reactions, bimolecular reactions, trimolecular reactions.

$$A \rightarrow \text{products}\} \text{unimolecular}$$

$$\left.\begin{array}{l} A + B \rightarrow \text{products} \\ A + A \rightarrow \text{products} \end{array}\right\} \text{bimolecular} \tag{2.18}$$

$$\left.\begin{array}{l} A + B + C \rightarrow \text{products} \\ A + A + B \rightarrow \text{products} \\ A + A + A \rightarrow \text{products} \end{array}\right\} \text{trimolecular}$$
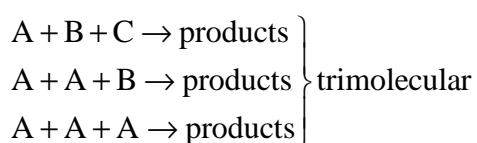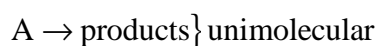
2.4 Consecutive Reactions

One-step elementary reactions are observed correlated to first-order and second-order reactions in the previous sections. Another reaction type that can occur in a reaction system is consecutive reactions. In this type of reaction product of one reaction takes place in another reaction and forms another products. For instance,

$$A + B \xrightarrow{k_1} AB \xrightarrow{k_2} C + D \tag{2.19}$$

If the rate law is written in terms of product and reactant for the species AB,

$$\begin{align} \frac{d[AB]}{dt} &= k_1[A][B] = -\frac{d[A]}{dt} = -\frac{d[B]}{dt} \\ \frac{d[AB]}{dt} &= -k_2[AB] = -\frac{d[C]}{dt} = -\frac{d[D]}{dt} \end{align} \tag{2.20}$$

if two of these rates are considered together,

$$\left(\frac{d[AB]}{dt}\right)_{net} = k_1[A][B] - k_2[C][D] \tag{2.21}$$

2.5 Competitive Reactions

Competitive reactions take place when different products are formed from the same reactants.

$$A + B \xrightarrow{\ k_1\ } AB$$
$$A + B \xrightarrow{\ k_2\ } E + F$$

(2.22)

If the rate laws are written for the first and the second reactions,

$$\left(\frac{d[A]}{dt} \right) = -k_1[A][B]$$
$$\left(\frac{d[A]}{dt} \right) = -k_2[A][B]$$

(2.23)

When these two reactions are considered together the rate law for species A is obtained as,

$$\left(\frac{d[A]}{dt} \right)_{net} = -(k_1 + k_2)[A][B]$$

(2.24)

2.6 Chain Reactions

Chain reactions are common in chemical reaction mechanisms and have complex structure that contains a series of consecutive, competitive and reverse reactions.

2.7 Free Radicals

In a chemically reacting system there exist very reactive atoms such as O, H, N or very reactive species which have unpaired electrons that can react with other species very actively. These atoms or species are called as "free radicals" or simply "radicals".

Hydrogen atom is a free radical, and the dots shown below symbolize electrons,

$$H:H \rightarrow H \cdot + H \cdot$$
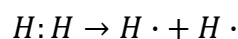
CH_4 is normally a stable species. If one hydrogen atom is removed from the compound then CH_3 and H free radicals are obtained,

$$H : \overset{\overset{\displaystyle H}{..}}{\underset{..}{C}} : H \;\rightarrow\; H : \overset{\overset{\displaystyle H}{..}}{\underset{..}{C}} \cdot \;+\; \cdot H$$
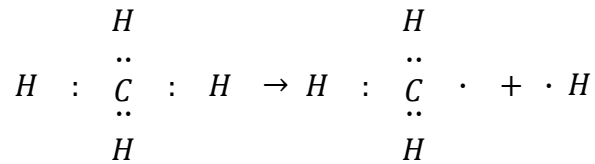
Radical chain reactions may contain different kinds of chain reactions. The most important ones of these are shown below,

$$
\begin{aligned}
&H_2 + O_2 && = \;2OH\bullet && \text{chain initiation} && \left.\right\}\text{chain initiation reaction}\\
&OH\bullet + H_2 && = \;H_2O + H\bullet && \text{chain propagation} && \left.\right\}\text{chain carrying reaction}\\
&H\bullet + O_2 && = \;OH\bullet + O\bullet && \text{chain branching} && \left.\right\}\\
&O + H_2 && = \;OH\bullet + H\bullet && \text{chain branching} && \text{chain branching reactions}\\
&H\bullet && = \;1/2\,H_2 && \text{chain termination} && \left.\right\}\\
&H\bullet + O_2 + M && = \;HO_2 + M && \text{chain termination} && \text{chain termination reactions}
\end{aligned}
$$
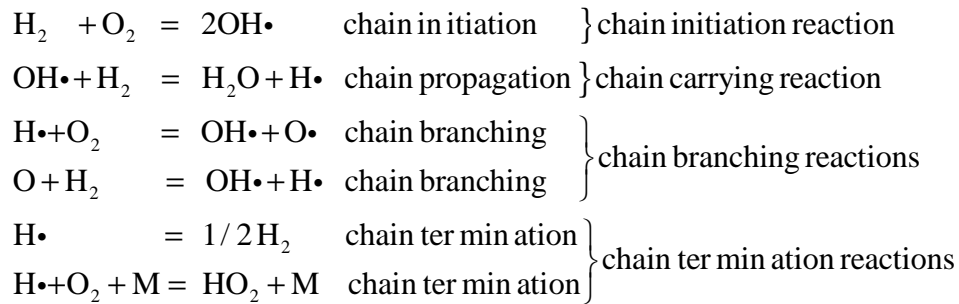
Free radicals are formed from stable species in chain-initiating reactions. Chain carrying reactions can be classified in to two different reaction kinds; chain propagation reactions where reactive species react and form another reactive species and chain branching reactions where the number of reactive species (free radicals) increases. Finally, chain terminating reactions consume the free radicals and form stable species.

2.8 Surface Reactions

Surface reactions play an important role in combustion applications, e.g., in wall recombination processes during autoignition, in coal combustion, in soot formation and oxidation, in catalytic combustion or in metal combustion.

The main feature of this phenomenon is the existence of surface sites and adsorption of species in to these sites. Surface sites (catalyst) increase the reaction rate without being consumed. Surface sites and species have a concentration measured in mol/cm^2. This phenomenon takes place in different steps:

- Transport of the reactant molecule to the surface by convection and/or diffusion
- Adsorption of the reactant molecules on the surface
- Elementary reaction steps, involving various combinations of adsorbed molecules, the surface itself and gas-phase molecules
- Desorption of the product molecules from the surface

- Transport of the product molecules away from the surface by convection and/or diffusion

These processes are illustrated in the below schema.
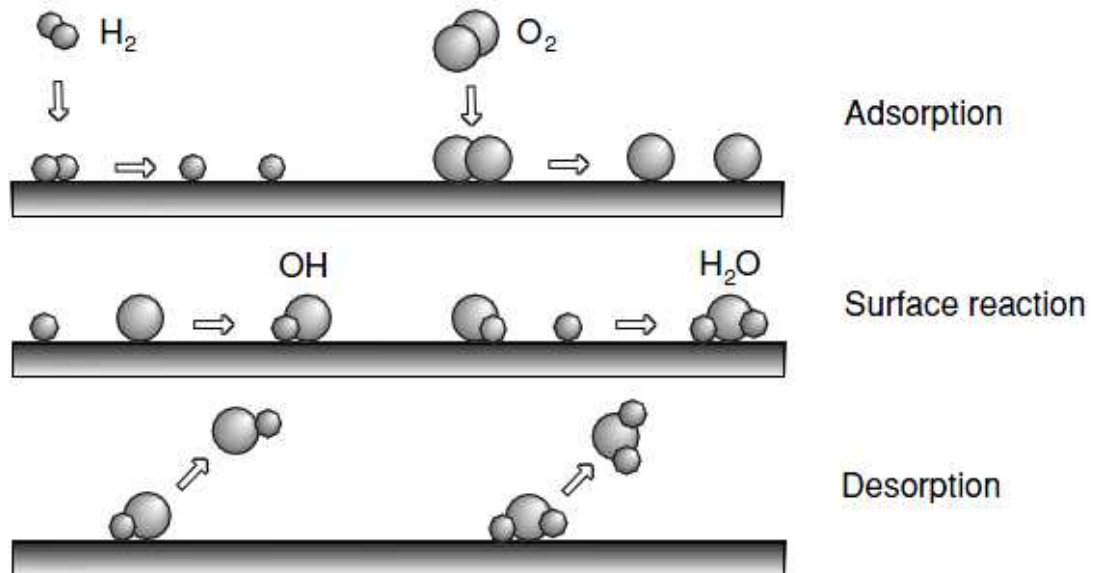
Figure 2.3 : Processes of catalytic surface reaction of hydrogen oxidation [21]

3. REACTION MECHANISMS

Combustion of hydrocarbons contains hundreds of reactions for simple hydrocarbons such as CH_4, thousands of reactions for larger hydrocarbons. The interaction of these elementary reactions governs the whole reaction mechanism. Even though there are large amount of reactions, they have characteristic properties which will be explained further.

3.1 Detailed Mechanisms

Detailed mechanisms consist of hundreds of species and from hundreds to thousands of reactions. These mechanisms contain all the important species and elementary reactions. They also contain as much as possible fundamental information. Different detailed reaction mechanisms have been proposed for different kinds of hydrocarbons such as methane, i-octane for the last decades.

Generation of reaction mechanisms starts with the estimation of necessary species and reactions which are likely to occur in the observed conditions. Reactants, large number of intermediate species and products must be included in the mechanism. Increasing databases of rate parameters of elementary reactions enable to create more detailed "complete" mechanisms which have more complex structures. Development of detailed mechanisms is time-consuming and iterative. Validation against experimental data is necessary, and usually several independent research groups are involved in the process [23]. Thermodynamic data constitute is an additional requirement.

The above detailed mechanism generation is so complex and there may always exist human errors. In order to automate this challenging process, computers have become to play an important role in the last two decades [23-26].

A mechanism generation program follows the below steps to create reaction mechanisms:

1- Storage of chemical species which can be easily used by the reaction generator that predicts products of each chemical reaction

2- Production of a feasible set of elementary reactions for the given species

3- Searching kinetic parameters of the generated reactions in a database

4- Defining the unimportant reactions that will be removed from the mechanism

After the mechanism is constructed and rate parameters are incorporated, differential rate equations are integrated.

The next step is comparing numerical integration and experiments. But it is not so easy and in order to gain more information about the detailed mechanisms very few variables are required from the analysis.

The problem of the simulation of such detailed mechanisms is "stiffness" of the mechanism which increases the computation time. Elementary reactions occur in a reaction mechanism in different time scales. The ratio of fastest time scale to slowest time scale is the stiffness of the system. Because of stiffness, too small time steps are necessary to achieve stability and using standard integration methods such as Runge-Kutta method become inapplicable in detailed mechanisms. Therefore, it is necessary to reduce detailed mechanisms through some methods which will be explained further in section 3.5.

3.2 Skeletal Mechanisms

Applying detailed reaction mechanisms in CFD applications, and making a detailed investigation on these mechanisms require too much computational time. Coupling physical processes such as transport phenomena in the flow field with the chemical kinetics makes the systems even more complicated to solve. For instance, the i-octane LLNL detailed mechanism developed by Lawrence Livermore National Laboratory (LLNL) contains 857 species and 7193 reactions [3]. Different time scales exist in such a big mechanism that corresponds to the stiffness of the mechanism which makes the solution of the numerical integration harder. Therefore, simplification of such big mechanisms without much loss of information allows making more detailed investigations on the system in considerably much less computation time. A useful technique to simplify reaction mechanisms from a

detailed mechanism and then to reduced mechanism as long as the predictability of the kinetic model is still acceptable [27].

Some species and reactions in the detailed reaction mechanism play less important role on the system than other species. These species can be defined as redundant. Removing redundant species from the detailed mechanism does not give considerable error on the calculations such as mole fractions of species. These species and reactions are defined by the mechanism simplifying techniques which will be explained further in section 3.5. For instance, applying a necessity analysis allows deleting up to 55% of all species from the detailed mechanism.

3.3 Reduced Mechanism

There are numbers of approaches to generate reduced mechanisms. They can be classified in to two different categories: static and dynamic approaches. Static approaches are analyses such as reaction flow analysis and sensitivity analysis. Sensitivity analysis gives the reactions and species with high sensitivities and defines them as non-redundant, which cannot be removed from the detailed reaction mechanism. After adding fuel, oxidizer, and products to this non-redundant list, reaction flow analysis gives the atomic mass flow through the given reactions. This is used to detect redundant species that are considered unimportant for the mechanism, due to small amounts of formation and destruction, for differently defined levels of mass flow [28].

Dynamic approaches take a detailed or skeletal mechanism as reference and then to select only the most important species and reactions for the reduced mechanism. Reduced mechanisms can be generated by applying the steady state assumptions to a detailed or skeletal mechanism without any significant loss of accuracy. A measure of species lifetimes is taken from the diagonal elements of the Jacobian matrix of the chemical source terms. The species with a lifetime shorter than and mass-fraction below specified limits are assumed to be in steady state and selected for removal from the skeletal or detailed mechanism [28].

The details of sensitivity, reaction flow and species lifetime analysis will be explained futher.

3.4 Reaction Mechanism Analyzing Techniques

Reaction mechanisms have characteristic properties as mentioned before. For instance, only some of the reactions determine the overall rate of reactions. If a knowledge can be obtained about these properties then just the important reactions or species which dominate characteristics of reaction mechanism (such as rate limiting reactions) can be kept and the reactions or species which are irrelevant to these properties can be removed from the mechanism which finally results in simplifying of the reaction mechanism.

3.4.1 Quasi-Steady-State-Approximation (QSSA)

Quasi-steady-state approximation assumes that production rate of some chemical species is close to their consumption rate where it can be assumed that they are both equal. This allows us to neglect the concentrations of these species, and they can be removed from the reaction mechanism which finally results in the simplification of mechanisms. The biggest drawback of this method is that it needs a profound knowledge of the user about the species which are likely to be a good candidate of this assumption.

In order to explain this method the below equation can be considered,

$$A \xrightarrow{k_1} B \xrightarrow{k_2} C \tag{3.1}$$

The rates laws for these species is given as,

$$\frac{d[A]}{dt} = -k_1[A] \tag{3.2}$$

$$\frac{d[B]}{dt} = k_1[A] - k_2[B] \tag{3.3}$$

$$\frac{d[C]}{dt} = k_2[C] \tag{3.4}$$

One can assume that only the species A exist at time t=0 and the other species (B and C) have a concentration of zero. Based upon this assumption, $[A]_{t=0}=[A]_0$, $[B]_{t=0}=0$ and $[C]_{t=0}=0$ can be written which leads to the below solution.

$$\frac{d[A]}{dt} = -k_1[A]$$

$$\frac{d[A]}{[A]} = -k_1 dt$$

$$\ln[A] = -k_1 t$$

$$[A] = [A]_0 \exp(-k_1 t) \tag{3.5}$$

$$[B] = [A]_0 \frac{k_1}{k_1 - k_2} \{\exp(-k_2 t) - \exp(-k_1 t)\}$$

$$[C] = [A]_0 \left\{1 - \frac{k_1}{k_1 - k_2} \exp(-k_2 t) + \frac{k_2}{k_1 - k_2} \exp(-k_1 t)\right\}$$

If B is assumed to be a very reactive species whose formation and consumption rates are almost equal, quasi steady state approximation can be written as,

$$\frac{d[B]}{dt} = k_1[A] - k_2[B] \cong 0 \tag{3.6}$$

which leads to

$$k_1[A] = k_2[B] \tag{3.7}$$

This relation can also be used for the solution of C,

$$\frac{d[C]}{dt} = k_1[A] \tag{3.8}$$

$$\frac{d[C]}{dt} = k_1[A]_0 \exp(-k_1 t) \tag{3.9}$$

$$[C] = [A]_0 \left[1 - \exp(-k_1 t)\right] \tag{3.10}$$

3.4.2 Partial Equilibrium

Some of the forward and backward reactions are so fast at high temperatures in reaction mechanisms where partial equilibrium can be assumed for these reactions. If hydrogen combustion at high temperatures is considered as an example,

$$H + O_2 \quad = OH + O$$
$$O + H_2 \quad = OH + H$$
$$OH + H_2 = H_2O + H$$
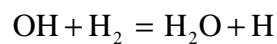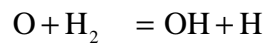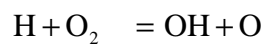
Because these reactions are so fast, forward and backward reaction rates are assumed to be equal which leads to,

$$k_1[H][O_2] = k_2[OH][O]$$
$$k_3[O][H_2] = k_4[OH][H]$$
$$k_5[OH][H_2] = k_6[H_2O][H]$$
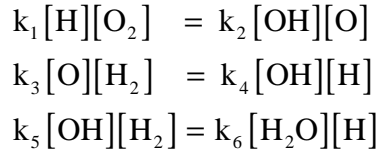
This equation system can be solved for O,H and OH intermediates and concentrations of the species are obtained as,

$$H + O_2 = OH + O$$
$$O + H_2 = OH + H$$
$$OH + H_2 = H_2O + H$$
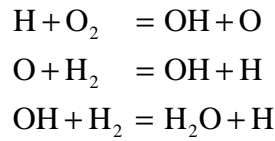
Partial equilibrium assumption provides satisfactory results only at high temperature regimes.

3.4.3 Sensitivity Analysis

Sensitivity analysis is used for three main purposes with respect to chemical kinetics: (1) reducing the number of reactions in a given problem, (2) identifying the rate-limiting steps in the system, (3) understanding the relative importance of reactions in the system.

Sensitivity analysis is one of the oldest skeletal reduction techniques which identify the rate limiting reaction steps. Rate law for a reaction mechanism consisting of R reactions and S species can be written as a system of first order ordinary differential equation (ODE) as [21],

$$\frac{dc_i}{dt} = F_i(c_1,...,c_s;k_1,...,k_R)$$
$$i = 1,2,...,S \tag{3.11}$$
$$c_i(t = t_0) = c_i^0$$

where the time t is independent variable, the concentration of species, c_i are dependent variable and k_r the parameters of the system, c_i^0 are initial conditions at t_0. System parameters can be defined as reaction rates, initial concentrations or pressure etc. Solution of the differential equation system (3.11) depends on the initial conditions and on the system parameters. Most of the reactions do not have a large affect on the solution, i.e. concentrations of species at time, t. These reactions are

related to quasi steady state or partial equilibrium phenomena. However, some of the reactions effect deeply the solution, i.e. concentrations of species at time, t. These reactions are defined as rate-determining steps. The dependence of the solution c_i on the parameter k_r is called as sensitivity. Absolute and relative sensitivities are defined as,

$$E_{i,r} = \frac{\partial c_i}{\partial k_r} \tag{3.12}$$

$$E_{i,r}^{rel} = \frac{k_r}{c_i} \frac{\partial c_i}{\partial k_r} = \frac{\partial \ln c_i}{\partial \ln k_r} \tag{3.13}$$

Sensitivity analysis is numerically performed by generating a differential equation system for the sensitivity coefficients by formally differentiating (3.11),

$$\frac{\partial}{\partial k_r}\left(\frac{\partial c_i}{\partial t}\right) = \frac{\partial}{\partial k_r} F_i\left(c_1,...,c_s; k_1,...,k_R\right)$$

$$\frac{\partial}{\partial t}\left(\frac{\partial c_i}{\partial k_r}\right) = \left(\frac{\partial F_i}{\partial k_r}\right)_{c_l, k_{l\neq r'}} + \sum_{n=1}^{s}\left\{\left(\frac{\partial F_i}{\partial c_n}\right)_{c_{l\neq n'}, k_l}\left(\frac{\partial c_n}{\partial k_r}\right)_{k_{l\neq j}}\right\} \tag{3.14}$$

$$\frac{\partial}{\partial t} E_{i,r} = \left(\frac{\partial F_i}{\partial kj}\right)_{c_l, k_{l\neq r}} + \sum_{n=1}^{s}\left\{\left(\frac{\partial F_i}{\partial c_n}\right)_{c_{l\neq n}, k_l} E_{n,r}\right\}$$

where c_l after the partial derivatives means that all c_l are held constant during the differentiation, and $c_{l\neq n}$ after the partial derivatives means that all c_l are held constant except c_n.
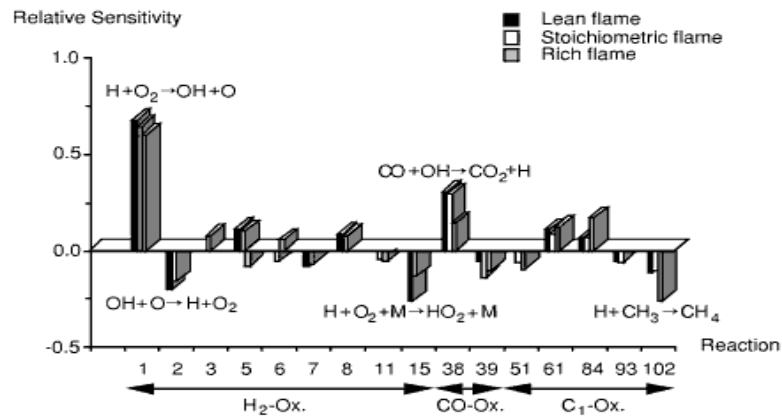
Figure 3.1 : Sensitivity analysis for the laminar flame velocity of a stoichiometric methane/air flame at p=1 bar T_u=298 K [29]
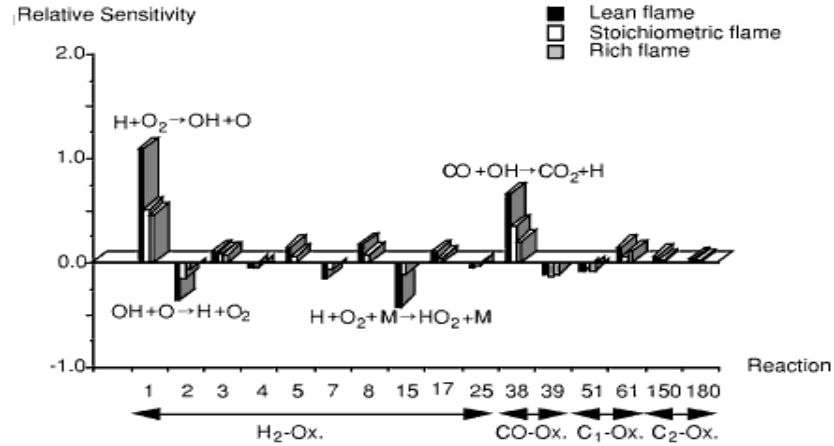
Figure 3.2 : Sensitivity analysis for the laminar flame velocity of a stoichiometric propane/air flame at p=1 bar and T_u=298 K [29]

Finally sensitivity analysis gives the most sensitive species and reactions on the entire reaction mechanism.

3.4.4 Reaction Flow Analysis

Reaction flow analysis can be divided in to two major categories: integral reaction flow analysis and local reaction flow analysis [21].

Integral reaction flow analysis considers the overall formation or consumption during the combustion processes.

Table 3.1 : Schematic illustration of the output of a reaction flow analysis [21]

Reaction	Species →					
↓	1	2	3	. . . .	S-1	S
1	30%	4%	1%	. . . .	0%	0%
2	0%	0%	0%	. . . .	0%	0%
3	0%	5%	0	. . . .	100%	80%
.	.	.	.		.	.
.	.	.	.		.	.
.	.	.	.		.	.
.	.	.	.		.	.
R-1	68%	91%	97%	. . . .	0%	5%
R	0%	7%	0%	. . . .	1%	0%

A reaction can be considered as unnecessary, if all entries in a row is lower than a certain limit, e.g. 1%. For instance, the row of reaction 2 is 0% and it can be removed from the reaction mechanism, on the other hand the row of reaction 2 is more than, say 1%, and it cannot be removed.

Local reaction flow analysis considers the formation and consumption of species locally, i.e., at specific times in time-dependent problems or at specific locations in steady processes. According to this analysis, a reaction is unimportant, if reaction rate RR satisfies the following condition,

$$\left| RR_{t,r,s} \right| < \varepsilon \left| \underset{r=1}{\overset{R}{Max}} \ RR_{t,r,s} \right| \ , \quad s=1,...,N \ , \quad t=0,...,T \tag{3.15}$$
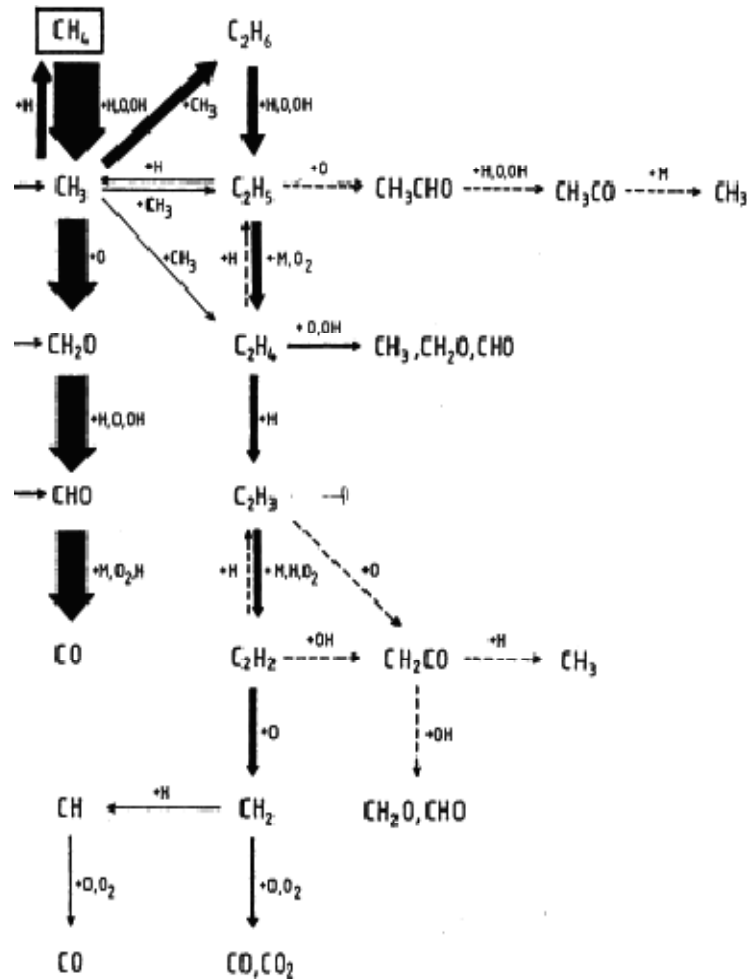
Figure 3.3 : Integral reaction flow analysis in a premixed stoichiometric CH$_4$/air flame at p=1 bar and T$_u$=298 K [30]

23

Figure 3.4 : Integral reaction flow analysis in a premixed rich CH_4/air flame at p=1 bar and T_u=298 K [30]; the analysis of acetylene is left out due to its complexity

3.5 Reaction Mechanism Simplifying Techniques

Practical fuels such as gasoline and diesel contain complex mixtures of different hydrocarbons. In order to predict the behavior of such complex fuels in combustion and partial oxidation processes surrogates of these fuels such as single component reference fuels like i-octane, n-heptane and characteristic fuel components such as aromatic, naphthenic, olefinic and paraffinic species have been developed and validated over a wide range of different parameters. The mechanisms used to describe the oxidation of such surrogates are called detailed mechanism. Even though these detailed mechanisms represent the behavior of surrogates, they still contain large amount of species and reactions. Mathematical model of such chemical reaction systems consists of a set of partial differential equations that describes the time dependent development of all properties of the system such as mole fractions, pressure and velocity. Computational simulation of these detailed mechanisms requires too much time. Even super computers are not able to make these simulations speedily because of the coupling the chemical kinetics with physical conditions.

There have been quite a lot of attempts to reduce the number of species and reactions of these detailed mechanisms for certain conditions in the last two decades.

Different mechanism simplifying methods have been improved to reduce number of species and reactions of detailed oxidation mechanisms. These methods can be classified in to two major categories: skeletal reduction and life time analysis. Examples of these methods will be explained briefly but in a very explanatory way in this chapter.

3.5.1 Skeletal Reduction Techniques

Skeletal reduction eliminates number of species and reactions which are unimportant for the particular conditions. There are different skeletal reduction techniques which will be summarized briefly further.

Sensitivity analysis which was explained in section 3.1.3 is one of the oldest skeletal reduction techniques which identify the rate limiting reaction steps.

Reaction flow analysis which was explained in section 3.1.4 gives characteristic reaction pathways in a reaction and allows neglecting unimportant reactions from the mechanism.

Necessity analysis proposed by Soyhan et al. [31,32] which is based on simultaneous use of sensitivity analysis and reaction flow analysis to predict accurately the occurrence of autoignition in the end gas of a spark ignition (SI) engine. Redundant species are detected by simultaneous use of sensitivity and reaction flow analysis in this method. Sensitivity analysis gives important species due to their high sensitivities by making small changes of system parameters. These important species are kept in the mechanism. Each species is assigned a necessity value according to the importance of the species itself and the flow of atoms to the important species and from the important species in a reaction mechanism. Important species are sensitive species which are detected by the sensitivity analysis, and the species that are needed to describe the global combustion process, such as final products and fuels. Skeletal mechanism is obtained after removal of redundant species from the detailed mechanism according to the simultaneous use of sensitivity and reaction flow analysis. And after the skeletal mechanism is obtained, the detailed and skeletal mechanism is compared for some considered parameters as mentioned above

(ignition delay time, combustion duration etc.). The flow diagram of this method is shown in Figure 1.
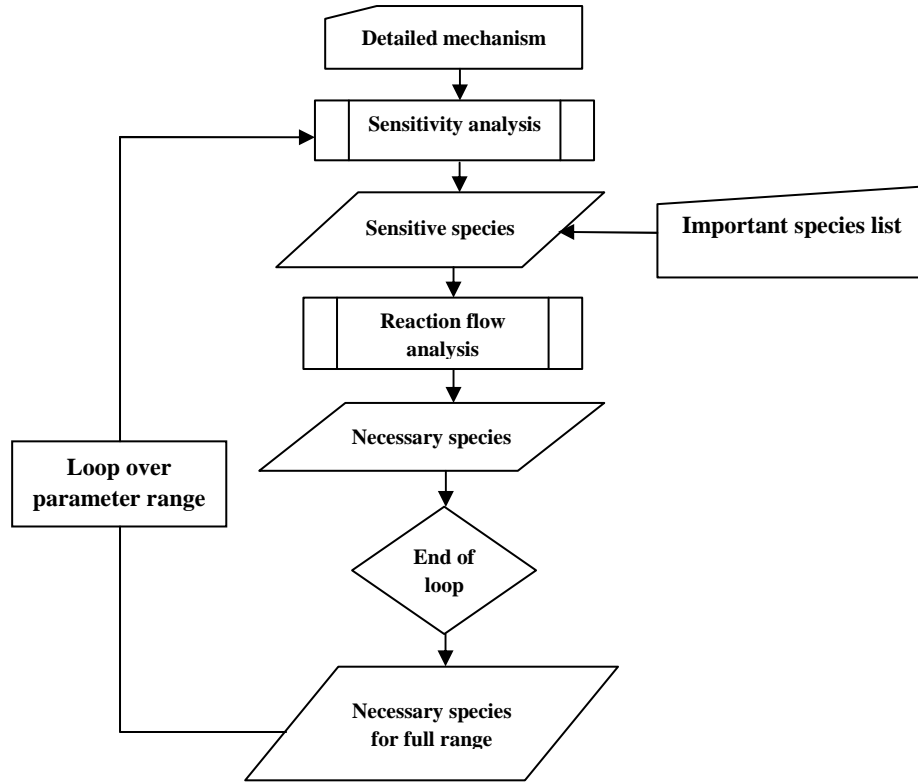
Figure 3.5 : Flow chart of the necessity analysis method

In this method, sensitivity coefficients have been used to determine the species that are most sensitive on the overall combustion process. Therefore a sensitivity analysis is performed,

$$S_{A,B} = \frac{\partial [A]}{\partial [B]} \approx \sum_{k=1}^{N_R} \frac{d[A]}{d[B]} \cdot \frac{dr_k}{d[B]} \qquad (3.16)$$

where $S_{A,B}$ is the sensitivity of the species A on species B. For the rate expression, the below equation is used,

$$r_k = \prod_{i=1}^{N_s} c_i^{v'_{ik}} k_k \qquad (3.17)$$

By using the above rate expression, the following rate expression is derived and used for the sensitivity analysis.

$$S_{A,j} = \sum_{k=1}^{N_R} \left| \frac{d[A]}{dr_k} \frac{v'_{kj}}{c_j} r_k \right| \qquad (3.18)$$

The transfer rates of atoms such as C, O and H through the species in the reaction mechanism are calculated by the reaction flow analysis. The flow of atom a between species i and j through formation or consumption is calculated as follows;

$$f_{ij}^{a} = \frac{\sum\limits_{k=1}^{N_R} r_k v'_{jk} v''_{ik} \frac{n_j^{a}}{\Delta n_k^{a}}}{\sum\limits_{k=1}^{N_R} r_k v''_{ik}} \tag{3.19}$$

$$c_{ij}^{a} = \frac{\sum\limits_{k=1}^{N_R} r_k v''_{jk} v'_{ik} \frac{n_j^{a}}{\Delta n_k^{a}}}{\sum\limits_{k=1}^{N_R} r_k v'_{ik}} \tag{3.20}$$

where f_{ij}^{a} is the relative transfer of atom a through formation of species i from species j and c_{ij}^{a} is the relative transfer of atom a through consumption of species i to species j.

The number of atoms n_j^{a} are normalized to the total number of atoms transported in the reaction;

$$\Delta n_k^{a} = \sum\limits_{i=1}^{N_s} v'_{ik} n_k^{a} \tag{3.21}$$

The relative necessity that a species needs in order to be included in the reaction mechanism, N_i, is defined as;

$$N_i = max(N_{i,0}, N_j f_{ij}^{a}, N_j c_{ij}^{a}; j = 1, N_s, a = 1, N_a) \tag{3.22}$$

Equation (3.22) must be solved iteratively. And the initial value, $N_{i,0}$, used in equation (3.22) is defined as the relative species sensitivity coefficients:

$$N_{i,0} = \frac{S_{ji}}{max_{k=1,N}(S_{jk})} \tag{3.23}$$

Some important species in the mechanism have a relative initial necessity level of 100%. They are species such as fuel, products. If a species is found to be important either formation or consumption of an important species, it is given a relative necessity by using equation (3.22). All of the species are ranked according to their relative importance level after calculation of equation (3.23). Different cutoff levels

are implemented after that and the species which have a relative importance level lower than the cutoff level are defined as unimportant and they are removed from the reaction system. Different skeletal mechanisms are obtained according to the removal of unimportant species from the reaction mechanism based on different cutoff levels.

F. Mauss et al. [33] derived skeletal mechanism from n-heptane LLNL detailed reaction mechanism and validated it by the simultaneous use of sensitivity and reaction flow analysis which was also used by Soyhan et al. [31,32].

Directed relation graph is another skeletal reduction technique. Lu et al. [34] used directed relation graph (DRG) to derive skeletal and reduced mechanisms from a detailed ethylene oxidation mechanism consisting of 70 species and 463 elementary reactions for high temperature chemistry for the PSR performance and autoignition delay for low-to-moderately high temperature chemistry. Skeletal mechanism is generated in this method by identifying unimportant species and thereby unimportant elementary reactions associated to these species based upon a preset numerical criterion. A set of target species A_i are specified in this method and the other species in the mechanism which are significant for the formation or consumption of these target species are specified by the value of ε, and whose removal from the mechanism will result in target species' concentrations an exceed. Each node in this DRG represents a species in the detailed mechanism, and there is an edge from vertex A to vertex B, and removal of species B causes a significant error to the production rate of species A. And, an edge from A to B means that B has to be kept to correctly evaluate the production rate of A. Thus, species A depends on species B only if there is a directed path from A to B. Finally, the direct influence of one species (B) to another species is calculated by an intermediate error to the production rate of the other species (A), r_{AB}, which is calculated as,

$$r_{AB} = \frac{\sum\limits_{i=1,l} \left| v_{A,i} \omega_i \delta_{Bi} \right|}{\sum\limits_{i=1,l} \left| v_{A,i} \omega_i \right|} \tag{3.24}$$

$$\delta_{Bi} = \begin{cases} 1 & \text{if the } i \text{ th elementary reaction} \\ & \text{involves species B,} \\ 0 & \text{otherwise} \end{cases} \tag{3.25}$$

If $r_{AB} \geq \varepsilon$, then there is a direct edge from A to B, A→B.

Consequently, if A has to be kept, B should also be kept, because strongly dependency of species A on species B. Even if two species do not directly depend on themselves, they can be coupled indirectly with the coupling of intermediate species. For instance, if A→B and B→C, then A requires C.
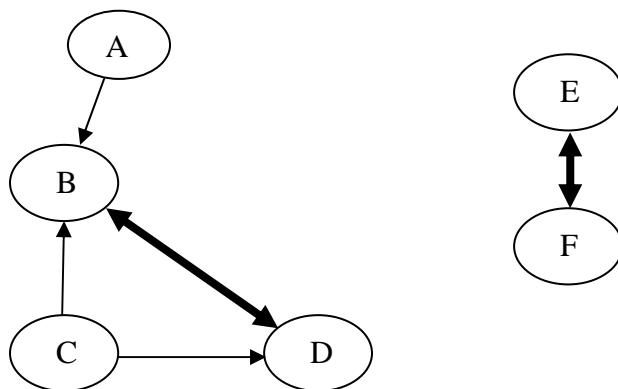
Figure 3.6 : Direct relation graph showing typical relations of the species [34]

They derived a skeletal mechanism that contains 33 species and 205 elementary reactions, and a reduced mechanism that contains 20 species and 16 global reactions by using this method. And they validated their derived skeletal and reduced mechanisms through the comparison of results of PSR and autoignition with the detailed mechanism for entire pressure, equivalence ratio and residence time range of the reduction processes.

Yu et al. extended their method to the reduction of large mechanisms with hundreds of species and thousands of reactions, namely for n-heptane and i-octane mechanisms [35]. They derived skeletal mechanisms with 188 and 233 species for n-heptane and i-octane in a two stage reduction process respectively. They reduced number of the species with the first-stage DRG reduction process to 290 species for n-heptane and 347 species for i-octane respectively. Furthermore, they eliminated the skeletal mechanisms of n-heptane and i-octane to 188 species and 233 species respectively by performing a second-stage DRG. Moreover they validated their mechanisms to represent well the performance of the detailed mechanism for the autoignition, PSR and independent system of jet-stirred reactor.

Xin et al. [36] used DRG method for mechanism reduction in the oxidative coupling of methane (OCM). They used GRI-Frenklach detailed mechanism that contains 71 species and 486 reactions and derived a skeletal mechanism that contains 39 species.

And they proved that the skeletal mechanism they derived costs 30 % CPU time of the detailed mechanism. Simulations were performed for isothermal and constant pressure plug flow reactor at different temperatures and CH_4/O_2 ratios for the mechanism reduction. They selected CH_4, O_2, C_2H_6 and C_2H_2 as target species and their concentrations are required to have less than 5% differences from those of the complete mechanism.

Lu et al. explained the background of directed relation graph in detail, as well [37].

Directed relation graph error propagation method (DRGEP) that is based on DRG is a new method improved by Desjardins et al. [38]. Apart from DRG, DRGEP considers the length between species. This approach is illustrated in the below figure,
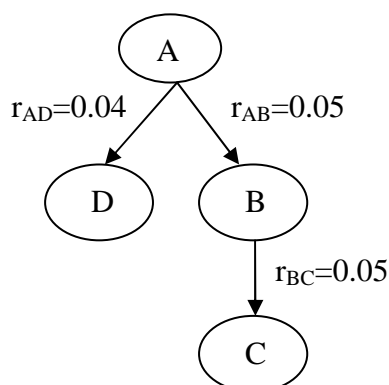
Figure 3.7 : Part of a directed relation graph involving four species. Although the link between species B and C is not the weakest in the graph, removing C should introduce the smallest error in the prediction of the target A [38]

A is selected as a target species in the above figure, and species B and D are directly linked to target species A with the coefficients of 5% and 4%, respectively. C is not directly linked to target species A, but species B with the coefficient of 5%. Species D is the first removed species in conventional DRG method because it gives the minimum error for target species A. The difference between DRGEP and DRG is introduced here. It is proposed in DRGEP that removing species C before removing D gives less error because it is not directly linked to target species A. Finally, the farther away a species is from target species, the less error gives it due to DRGEP method. They validated their method for the oxidation of detailed LLNL i-octane mechanism through predicting autoignition at constant volume in a large range of conditions relevant for engine related applications. They proved that DRGEP method gives better results comparing to DRG method for the considered parameters.

Directed relation graph sensitivity analysis (DRGASA) is another skeletal reduction method. The species which were not removed by DRG reduction process are further reduced by applying sensitivity analysis to them. This method was performed by some researchers [39,40]. Lu et al. [39] applied DRGASA to a skeletal mechanism that contains 188 species and 909 reactions which was derived from n-heptane detailed mechanism that contains 561 species and 2539 reactions by using DRG method. They selected ignition delays, extinction times of perfectly stirred reactors (PSR) and laminar flame speeds as the targets parameters for examining. They obtained a skeletal mechanism with 78 species and 359 reactions which gives 30% for the worst case. Niemeyer et al. [40] also performed DRGASA for the reduction of n-heptane, i-octane and n-decane for the prediction of ignition delay time. They also performed another method called as directed relation graph with error propagation and sensitivity analysis (DRGEPSA) in the same study and validated the new method which combines two different method described previously: directed relation graph with error propagation (DRGEP) and directed relation graph aided sensitivity analysis (DRGASA). DRGEPSA method covers weakness of DRGASA and DRGEP methods, and it allows removing more unimportant species from the detailed mechanisms. For instance, skeletal mechanisms were derived for the same conditions from the detailed mechanism of n-heptane by applying DRGEPSA, DRGEP and DRGASA methods resulting in containing 108 species, 173 species and 153 species skeletal mechanisms, respectively. Skeletal mechanisms were derived for the same conditions from the detailed mechanism of i-octane by applying DRGEPSA, DRGEP and DRGASA methods resulting in containing 165 species, 232 species and 211 species skeletal mechanisms, respectively.

On the fly reduction of kinetic mechanisms using elemental flux analysis is another skeletal reduction technique [41]. This method is based on element flux analysis [42]. Instantaneous elemental flux of atom A from species j to species k through reaction i, denoted as A_{ijk}, is defined in equation (3.26). Total instantaneous flux between species j and k can be calculated by summing A_{ijk} over all the reactions in which species j and k are evolved, as represented in equation (3.27).

$$\dot{A}_{ijk}(t) = q_i(t) \frac{n_{A,j} n_{A,k}}{N_{A,i}} \qquad (3.26)$$

$$\bar{\dot{A}}_{ijk}(t) = \sum_{i=1}^{N_R} \dot{A}_{ijk}(t) \qquad (3.27)$$

where $q_i(t)$ is instantaneous rate of reaction i (mol/s), $n_{A,j}$ is the number of atoms in species j, $n_{A,k}$ is the number of atoms in species k, $N_{A,i}$ is the total number of atoms in reaction i, and N_R is the number of the reactions these species appear as reactants or products. The atomic fluxes of each atom (C, H, O, N etc.) between sources and sinks are sorted in descending order and a user-defined cutoff level is applied on the flux list and reduced mechanisms are obtained according to cutoff levels. Forward and backward reactions are taken into account separately when calculating flux according to equation (3.28).

$$\dot{A}_{ijk}(t) = (|q_{ifwd}(t)| + |q_{irev}(t)|) \frac{n_{A,j} n_{A,k}}{N_{A,i}} \qquad (3.28)$$

where q_{ifwd} and q_{irev} are forward and backward reaction rates, respectively. After flux is calculated, reduction scheme is integrated in to reactive flow simulation. In the on-the-fly scheme, reduced mechanism is updated dynamically when the conditions change. Their idea for using on-the-fly scheme was taking into account of reaction and mixing effects during each time step when reactive flow model divides the simulation in to discrete time steps. They validated their method for a pairwise mixing stirred reactor (PMSR) model [43] and a plug-flow reactor (PFR) model.

3.5.2 Life Time Analysis

Life time analysis can be divided in to two major groups: *computational singular perturbation (CSP)* and *intrinsic low-dimensional manifolds method (ILDM)*.

The idea of time scales in a set of ordinary differential equation (ODE) system describing reaction kinetics stems is the fact that elementary reactions occur at different rates which finally results in different time scales due to the elementary reactions.

Computational singular perturbation (CSP) method separates QSS species from the fast species induced by reactions in partial equilibrium [44]. Lu et al. [44] used this method to develop a reduced mechanism for methane oxidation. Skeletal mechanism with 30 species is obtained from a detailed methane oxidation mechanism with 35

species by the application of directed relation graph. CSP method is further applied to the skeletal mechanism later. ODE in a chemically reacting system is given as,

$$\frac{dy}{dt} = g(y) \tag{3.29}$$

where y is the vector of dependent variables, e.g. species concentrations, and g is the source term. The way to capture different time scales due to the elementary reactions is to find the eigenvalues of the Jacobian of the ODE system. Jacobian matrix J can be derived by the chain rule as,

$$\frac{dg}{dt} = J \cdot g(y), \quad J = \frac{dg}{dy} \tag{3.30}$$

In the CSP theory the rates in g can be combined to modes, f, through the below change,

$$\frac{df}{dt} = \Lambda \cdot f, \quad f = B \cdot g,$$

$$\tag{3.31}$$

$$\Lambda = \left(\frac{dB}{dt} + B \cdot J \right) \cdot A, \quad A = B^{-1}$$

where A and B are matrices consisting of the column and row basis vectors respectively. Jacobian matrix, J, is time independent for linear systems and time dependent for nonlinear systems. In addition, a diagonal Λ can be easily obtained for linear systems readily, however it is not so easy to obtain a diagonal Λ for nonlinear systems. A CSP refinement procedure is applied to find a pair of A and B iteratively when it is not easy to find a diagonal, Λ. This results in a block-diagonal Λ such that the fast modes, f_{fast}, can be decoupled from the slow ones:

$$\frac{df_{fast}}{dt} = \Lambda_{fast} f_{fast}, \quad \frac{df_{slow}}{dt} = \Lambda_{slow} f_{slow},$$

$$\Lambda = \begin{pmatrix} \Lambda_{fast} & \\ & \Lambda_{slow} \end{pmatrix}, \quad A = \begin{pmatrix} A_{fast} & A_{slow} \end{pmatrix},$$

$$B = \begin{pmatrix} B_{fast} \\ B_{slow} \end{pmatrix}, \tag{3.32}$$

$$\Lambda_{fast} = \left(\frac{dB_{fast}}{dt} + B_{fast} \cdot J \right) \cdot A_{fast},$$

$$\Lambda_{slow} = \left(\frac{dB_{slow}}{dt} + B_{slow} \cdot J \right) \cdot A_{slow}$$

Eigenvalues of Λ_{fast} are negative, and with large quantities compared to Λ_{slow}. Fast and slow subspaces are separated here, and the fast modes in f_{fast} vanish in a rapid period, i.e. $f_{fast} = 0$. A characteristic time scale τ_c is introduced here and it separates the fast and slow subspaces. They chose ignition delay time of autoignition as the characteristic time for ignition processes, and time scales shorter than the ignition delay are assumed exhausted. In addition, they chose extinction residence time in PSR for extinction processes, and fast modes faster than the extinction processes are assumed exhausted.

After separating fast and slow subspaces, the *i*th species is presumed as a good quasi steady state (QSS) species if it satisfies the below equation,

$$|Q_i| < \varepsilon, \quad Q = \mathrm{diag}\left(A_{slow} B_{slow}\right) \tag{3.33}$$

where ε is a threshold value, say 0.1, that limits the relative error in the concentration of the *i*th species induced by the QSSA. Q consists of the diagonal elements of the matrix of the slow subspace. If Q_i can be neglected comparing to the threshold value ε, then *i*th species is mostly within the fast subspace with exhausted fast modes and it is assumed to be in QSS. Main property of the QSS species is low concentrations and sparsely coupling. Further, there are two different types of fast species in a large mechanism: one with low reaction rate and a high destruction rate, which means that is consumed fast and remains in small concentrations, and the other type is with large creation and destruction that balances each other. The first type of species are good candidates for QSS, and the second type is a good candidate for partial equilibrium species. These two different types of species are distinguished through by introduced CSP method. QSS species exist only in the fast subspace, whereas fast species induced by partial equilibrium exist both in fast and slow subspaces [10].

By considering these assumptions, they derived a 15 step reduced mechanism from the detailed mechanism and validated it for PSR and autoignition conditions. Ignition delay prediction comprises very good with the detailed mechanism. They compared species profiles in autoignition and PSR conditions and they proved that their reduced mechanism comprises well with the detailed mechanism. They also compared laminar premixed flames and non-premixed opposed-jet flames. They

compared laminar flame speeds as an important system parameter in the study of chemistry-diffusion interaction, and it is shown that reduced mechanism predicts the flame speeds well within the range of entire pressure and equivalence ratios.

Finally, they compared a 17-step reduced mechanism and detailed mechanism for NO formation. They proved that their reduced mechanism gives acceptable results for NO mass fraction comparison in an opposed-jet nonpremixed flame and three premixed flames with different equivalence ratios.

Lu et al. performed CSP method to a skeletal mechanism derived by a detailed mechanism of n-heptane [10]. They improved the below definition for the elimination of the reactions which is based on CSP method.

$$I_{k,i} = \frac{\left| v_{k,i} \omega_i \right|}{\sum\limits_{j=1,N} \left| v_{k,j} \omega_j \right|} \tag{3.34}$$

where $I_{k,i}$ is the importance index of the ith reaction to the production rate of the kth species in the jth reaction, N number of the reactions, and ω_i is the net rate of the ith reaction. The ith reaction is considered to be unimportant for a reaction state if,

$$I_{k,i} < \varepsilon, \quad k = 1,...,M, \tag{3.35}$$

condition is satisfied, where ε is a threshold value, i.e. 0.1.

They reduced the number of the reactions from 359 to 317 by applying this method while number of the species remained constant. However, they further reduced the number of species by applying CSP to define QSS species which was explained above [15]. The number of the species in the skeletal mechanism is decreased from 68 to 55 by applying this technique.

Intrinsic low dimensional manifold method (ILDM) is the second major life time analysis method introduced and implemented by Maas et al. [16-19].

Chemical time scales ranges from 10^{-9} to 10^{-2} s and they cover larger range than physical time scales (molecular transport e.g.) [45,46]. Aside from CSP method, Maas et al. [45] improved a method to distinguish fast and slow time scales that needs just detailed kinetic mechanism and number of degrees of freedom as input. It does not rely on experience from the user. But it is not as easy as QSS technique to

understand ILDM. However, the input required by ILDM is easier, and no assumptions about the reaction rates at which species are consumed of produced are necessary. This finally makes ILDM easier to accurately apply. It must also be mentioned here that QSSA can not cover low temperature regime results, but in contrast ILDM covers this regime calculations quite well.

Degrees of freedom mentioned above correspond to number of steps of mechanism. For instance, four degrees of freedom means a four-step mechanism. The user doesn't need to provide extra information as it is in CSP method, for instance which species are assumed to be in quasi steady state. The system is changed by reducing the mechanism in CSP, but instead of reducing the system, the most important part of the solution is found in its phase space in ILDM technique. It must be pointed out that they decoupled fast time scales from slow time scales for homogenous, adiabatic, isobaric closed system.

The state of the reaction is described by a set of n_s ordinary differential equations, where n_s is the number of the species. Thus n_s different time scales govern the process and n_s variables are needed to describe the state of the system. It must be clarified that other state variables such as total enthalpy, the pressure must also be included in this set of ordinary differential equation. For instance, if total enthalpy and pressure are also added to this set then n_s+2 set of ordinary differential equations are obtained. Since they use constant h and P in their system, n_s set of ordinary differential equations are obtained.

Very fast time scales usually correspond to equilibrium processes in chemical kinetics. If the number of these fast time scales are named as n_f and removed from the solution, then remaining time scales are given by (remaining time scales are named as n_g) $n_{g=}$ n_{s-} n_f. Making such an assumption allows describing the system with less amount of variable numbers such as n_g degrees of freedom. It means that number of equations to be solved to describe the system is reduced and n_g number of manifold is obtained and the reduced n_g step mechanism yields trajectories on this manifold. If all solution trajectories reaches the same equilibrium point, this equilibrium point means zero-dimensional manifold for the system. When the slowest time scales dominates all other time scales at each point, then one-dimensional manifold is obtained. When the next slowest time scale dominates all other time scales, then the solution trajectories reaches to a two-dimensional

manifold. From the same point of view higher order manifolds are obtained, respectively. The method improved by Maas et al [45] defines an intrinsic n_g dimensional manifold, n_f local conditions that generate the manifold stem from the eigenvalue-eigenvector representation of the local Jacobian matrix. The Jacobian contains the necessary information to define the solution of the local behavior of a linearized system. Real parts of the eigenvalues correspond to time scales associated to the system, and imaginary parts of the eigenvalues correspond to frequency where the solution oscillates at a point. They use similar methods to CSP but their method has different approach. For instance, fast time scales are detected and removed then the stiffness of the ordinary differential equation system is decreased and solved by explicit methods in CSP method. However, they do not decrease the stiffness of the system they develop a scheme that reduces the state space of a reaction system which can then be tabulated for the following purposes such as combustion calculations.

In this method chemical reaction system is treated in terms of element and reaction vectors. Number of atoms of element i in a species j is called as "element composition vectors" denoted as $\mu_{j,i}$. Similarly, each elementary chemical reaction is defined in terms of a "reaction vector" denoted as v_i. Reaction subspace R is the space spanned by the reaction vectors v_i. The dimension of this space is defined by, $n_r = n_s - n_e$. Inert species are also treated as elements. This spanned composition space is shown as Φ. And as explained above this space is represented by such a set of vectors.

If a chemical system has a state that corresponds to a point on the manifold, the state of the system is given by a point on this manifold for all times. Movements in the state space according to reaction vectors results in a change of state due to chemical reaction. This change means a movement parallel to the manifold. Movements in element vectors results in the change of element composition. They are perpendicular to the manifold. All the trajectories on the manifold approaches equilibrium point of the system. Sample plots of trajectories are shown in the below figures that were obtained from a numerical solution of a detailed reaction mechanism for the water-gas system for specific values of pressure, enthalpy and element composition. These plotted trajectories are obtained for CO_2/H_2O and CO_2/OH planes, respectively. Finally chemical reaction is regarded as a movement along those trajectories.
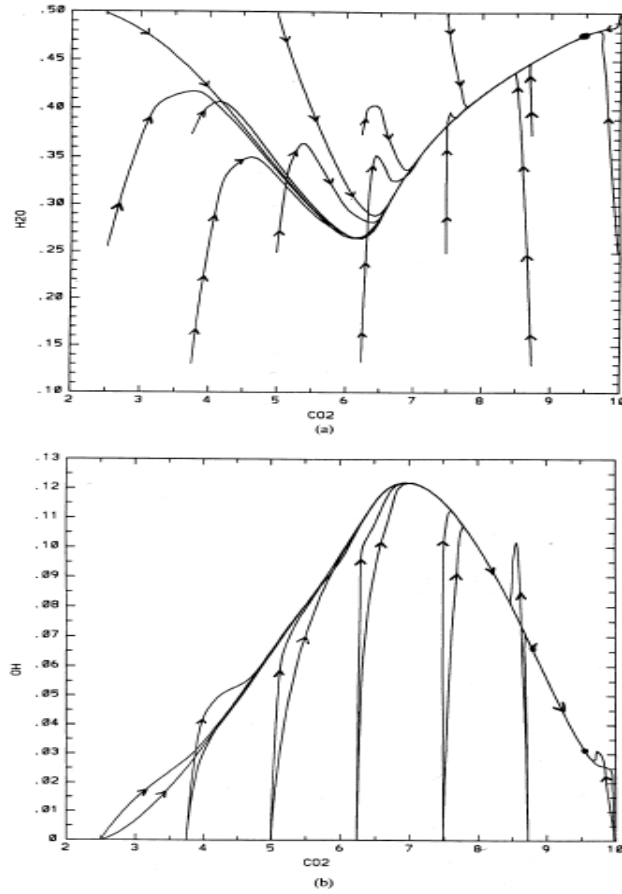
Figure 3.8 : Sample trajectories in the state space for a CO/H$_2$/air system. • denotes the equilibrium value. (a) Projection in to the CO2-H2O plane. (b) Projection in to the OH-CO2 plane [45]

Trajectories that are seen on the graphics branch before equilibrium is reached. A low-dimensional manifold, which is represented by a line in this projection, has the property that all trajectories tend to approach that manifold, and only slow time scales govern the chemical reaction on this manifold [45]. Low-dimensional manifold in the state space represents slow time-scale processes, and the systems that do not lie on this manifold occur fast in time in the direction of the manifold.

If a chemical reaction system with the below governing equations is considered,

$$\frac{\partial h}{\partial t} = 0 \tag{3.36}$$

$$\frac{\partial P}{\partial t} = 0 \tag{3.37}$$

$$\frac{\partial \phi_i}{\partial t} = \frac{\dot{\omega}_i(h, P, \phi)}{\rho(h, P, \phi)} \quad i = 1, 2, ..., n_s \tag{3.38}$$

in terms of vector notation,

$$\frac{\partial \psi}{\partial t} = F(\Psi) \tag{3.39}$$

where $\Psi = (h, P, \phi_1, \phi_2, ..., \phi n_s)^T$

Eigenvalues of the Jacobian $F(\Psi)$ identifies $n_s + 2$ different time scales associated with the movement in the state space. And corresponding eigenvectors describe "characteristic directions" associated with time scales. The main idea of looking for the points in the state space for which components in the directions of certain eigenvectors (in this case those associated with fast time scales) vanish [45].

4. DEVELOPMENT OF THE REDUCTION METHOD

Necessity analysis with simultaneously combined sensitivity and reaction flow analysis through each reaction reduction method that is compatible with DETCHEM [6] is proposed in this study. This method is based on necessity analysis developed by Soyhan et al. [31] which was described in detail in section 3.2. A FORTRAN code is written based on this method. The new FORTRAN code is compatible with DETCHEM^{BATCH} [6]. It correlates with DETCHEM^{BATCH} via DETCHEM Interface and the Batch Library.

In this study, reduction of CPOX (catalytic partial oxidation) of detailed LLNL i-octane mechanism in homogenous gas phase and exhaust gases after catalyst is investigated.

In order to reduce catalytic partial oxidation of detailed LLNL i-octane reaction mechanism, necessity analysis which was performed by Soyhan et al. [31] that is explained before, is chosen as the starting reduction method. Necessity analysis with simultaneously combined sensitivity and reaction flow analysis through each reaction reduction method is proposed further.

4.1 Implementation of the Necessity Analysis Method

Necessity analysis was implemented via a FORTRAN code that is compatible with DETCHEM^{BATCH}. The improved FORTRAN code receives basic information from DETCHEM software library, such as stoichiometric coefficients of species, atomic composition of species and reaction numbers, and makes the calculations according to the necessity analysis method. After the FORTRAN code was improved and correlated with DETCHEM^{BATCH}, it was found that this analysis can be improved for this study. It was seen that necessity analysis overestimates some species' relative necessity values. For example, in a methane CPOX reaction mechanism, CH_2 (s) appears in 6 reactions and contributes to the formation and consumption of CH_2, CO, OH, H, C_2H_4 and CH_3 species. In contrast, CH_3 appears in 24 reactions and contributes to the formation and consumption of H_2, CH_2 (s), C_2H_4, CH_2, H, CHO,

CH$_4$, CH$_2$O, OH, CH$_3$O, C$_2$H$_4$, C$_2$H$_6$, H$_2$O, HO$_2$, H$_2$O$_2$ and CH$_2$OH species. Sensitivity values of CH$_3$ are also higher than sensitivity values of CH$_2$ (s). So, it can easily be said that CH$_3$ must have a higher relative necessity than CH$_2$ (s). But, in contrast, necessity analysis calculation assigns a higher relative necessity to CH$_2$ (s) than CH$_3$, and deletes it from the mechanism before CH$_2$ (s) is deleted.

From this point of view, it is decided to improve necessity analysis method for this study. And a new method is proposed which is called as necessity analysis with simultaneously combined sensitivity and reaction flow analysis through each reaction which is explained in the following chapter. Comparison of the results of necessity analysis and newly proposed method based on necessity analysis is given in section 5.4.3.

4.2 Necessity Analysis With Simultaneously Combined Sensitivity And Reaction Flow Analysis Through Each Reaction Method

Sensitivity analysis is performed at first in necessity analysis method, improved by Soyhan et al. [31], then reaction flow analysis is performed and finally sensitivity analysis and reaction flow analysis are combined with an iterative method (sensitivity and reaction flow analysis were considered simultaneously). After these steps, species are eliminated according to cutoff levels and skeletal mechanisms are obtained.

In the necessity analysis with simultaneously combined sensitivity and reaction flow analysis through each reaction method, simultaneous use of sensitivity and reaction flow analysis is performed for each reaction separately. The difference between necessity analysis improved by Soyhan et al. [31] and necessity analysis with simultaneously combined sensitivity analysis and reaction flow analysis through each reaction method is introduced at this point. They performed sensitivity analysis at first and summed all species' sensitivity values through all reactions and then coupled them with reaction flow analysis. On the other hand, sensitivity coefficients of each species' in each reaction are considered separately (they are not summed through all reactions) and coupled with reaction flow calculations through each reaction, in the new approach proposed in this thesis study.

By applying these simultaneous sensitivity and reaction flow analysis, necessity species are detected, and new skeletal mechanisms are derived based on these necessary species. Each species is assigned a necessity value according to the flow of atoms from or to each species that it contributes to formation or consumption in a reaction mechanism multiplied with each species sensitivity coefficients through each reaction. The flow diagram of this proposed method is shown in Figure 2.

```
                    ┌─────────────────────┐
                    │ Detailed mechanism  │
                    └─────────────────────┘
                              │
                              ▼
              ┌──────────────────────────────┐
        ┌────▶│      Sensitivity analysis      │
        │     └──────────────────────────────┘
        │                   │
        │                   ▼
        │            ╱─────────────╲
        │           ╱  Sensitivity  ╲
        │           ╲  coefficients  ╱
        │            ╲─────────────╱
        │                   │
        │                   ▼
        │     ┌──────────────────────────────┐
┌──────────┐  │       Sensitivity             │
│ Loop over │  │       coefficients            │
│ parameter │  │            +                  │
│  range    │  │       Reaction Flow           │
└──────────┘  │       analysis                │
        │     └──────────────────────────────┘
        │                   │
        │                   ▼
        │            ╱─────────────╲
        │           ╱   Necessary   ╲
        │           ╲    species     ╱
        │            ╲─────────────╱
        │                   │
        │                   ▼
        │              ╱────────╲
        └─────────────╱  End of   ╲
                      ╲   loop     ╱
                       ╲────────╱
                              │
                              ▼
                   ╱──────────────────╲
                  ╱  Necessary species  ╲
                  ╲   for full range     ╱
                   ╲──────────────────╱
```
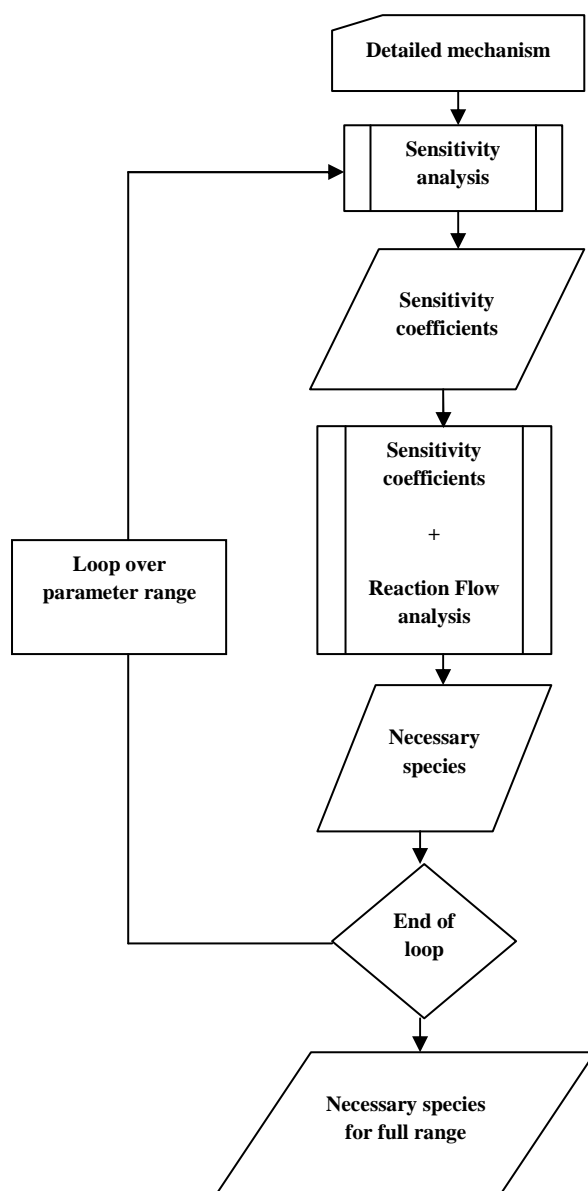
Figure 4.1 : Flow chart of necessity analysis with simultaneously combined sensitivity and reaction flow analysis through each reaction method

The details of necessity analysis with simultaneously combined sensitivity and reaction flow analysis through each reaction method is described in the following sections.

4.2.1 Sensitivity Analysis:

In this method, sensitivity coefficients are used to determine the species that are most sensitive on the overall CPOX process. Therefore, a sensitivity analysis is performed in DETCHEM^{BATCH} with respect to all or reduced number of kinetic parameters. Absolute and relative sensitivity values were calculated using the following expressions [6]:

$$E_{i,j} = \frac{dn_i}{dp_j} \qquad \text{absolute sensitivities} \qquad (4.1)$$

$$E_{i,j}^{rel} = \frac{p_j}{n_i}\frac{\partial n_i}{\partial p_j} = \frac{\partial \ln n_i}{\partial \ln p_j} \qquad \text{relative sensitivities} \qquad (4.2)$$

In order to improve the accuracy of the computed relative sensitivities, an option for sensitivity analysis with respect to $\ln p_j$ is also introduced:

$$E_{i,j}^{\ln p_j} = p_j \frac{\partial n_i}{\partial p_j} = \frac{\partial n_i}{\partial \ln p_j} \qquad (4.3)$$

Standard implicit solvers LIMEX and DAESOL can be used to solve the coupled governing equations.

Sensitivity analysis in DETCHEM^{BATCH} gives a matrix that contains the information of each species' sensitivity coefficients through each reaction. An example of output of sensitivity analysis is shown in the below table,

Table 4.1: Output of sensitivity analysis of DETCHEM^{BATCH}

Reaction	Sensitivity Coefficient of CH_4	Sensitivity Coefficient of O_2	Sensitivity Coefficient of O	Sensitivity Coefficient of H_2O	Sensitivity Coefficient of H
1	-2.29E-04	-2.95E-04	8.69E-11	3.46E-04	1.42E-10
2	-4.47E-08	-1.12E-07	-6.70E-13	1.71E-07	5.38E-13
3	-1.20E-05	-3.13E-05	4.83E-12	4.66E-05	1.36E-10
4	0.00E+00	-7.45E-09	-3.75E-13	1.49E-08	2.66E-14
5	0.00E+00	0.00E+00	0.00E+00	0.00E+00	-1.78E-15
…	…	…	…	…	…
…	…	…	…	…	…
108	-2.87E-05	-3.64E-05	9.09E-13	4.13E-05	3.30E-11

As it can be seen from the table, each species has a sensitivity coefficient in each reaction.

4.2.2 Reaction Flow Analysis With Simultaneous Use of Sensitivity Analysis Through Each Reaction

As mentioned in the last section, the difference between necessity analysis with simultaneously combined sensitivity and reaction flow analysis through each reaction method and necessity analysis method proposed by Soyhan et al. [31] is introduced at this point: the transfer rates of atoms such as C,O and H through the species in the reaction mechanism are calculated through the reaction flow analysis in necessity analysis method. The flow of atom a between species i and species j through formation or consumption is calculated through the equations (3.19) and (3.20).

In order to consider sensitivity values of each species' (sensitivity coefficients) in the new approach proposed in this study, sensitivity coefficients are considered simultaneously with the reaction flow analysis as shown in the below equation (for the forward reactions);

$$f_{ij\,f}^{a} = \frac{\sum_{k=1}^{N_R} r_k v'_{jk} v''_{ik} \dfrac{n_j^a}{\Delta n_k^a}[S_{(i,k)} + S_{(j,k)}][I_{(i)} + I_{(j)}]}{\sum_{k=1}^{N_R} r_k v''_{ik}} = \frac{f\_1\_1}{f\_2\_1} \qquad (4.4)$$

$$c_{ij\,f}^{a} = \frac{\sum_{k=1}^{N_R} r_k v''_{jk} v'_{ik} \dfrac{n_j^a}{\Delta n_k^a}[S_{(i,k)} + S_{(j,k)}][I_{(i)} + I_{(j)}]}{\sum_{k=1}^{N_R} r_k v'_{ik}} = \frac{c\_1\_1}{c\_2\_1} \qquad (4.5)$$

where $f_{ij\,f}^{a}$ is relative transfer of atom a through formation of species i from species j multiplied with sum of both species' sensitivity coefficients (species i and species j) through forward reactions (the f notation in the equation points out forward reactions), $c_{ij\,f}^{a}$ is the relative transfer of atom a through consumption of species i to species j multiplied with sum of both species' sensitivity coefficients (species i and species j) through forward reactions (the f notation in the equation points out forward reactions), r_k is the reaction rate coefficient of reaction k, v'_{jk} is the stoichiometric

coefficient of species j in reaction k, $\dfrac{n_j^a}{\Delta n_k^a}$ is the ratio of the number of atoms n_j^a to

the total number of atoms transported in the reaction, v_{ik}'' is the stoichiometric

coefficient of species i in reaction k, $S_{(i,k)}$ is the sensitivity coefficient of species i in

reaction k, $S_{(j,k)}$ is the sensitivity coefficient of species j in reaction k, $I_{(i)}$ is

predefined importance value for species i, $I_{(j)}$ is predefined importance value for

species j.

If there is not any backward reaction in the reaction mechanism, equations (4.4) and
(4.5) can be used to calculate formation and consumption values of species.
However, in a reaction system, backward reactions may also occur. In order to
consider the backward reactions, the following equations are improved,

$$f_{ij\,b}^{a} = \frac{\displaystyle\sum_{k=1}^{N_R} r_k v_{jk}'' v_{ik}' \frac{n_j^a}{\Delta n_k^a}[S_{(i,k)} + S_{(j,k)}][I_{(i)} + I_{(j)}]}{\displaystyle\sum_{k=1}^{N_R} r_k v_{ik}'} = \frac{f\_1\_2}{f\_2\_2} \tag{4.6}$$

$$c_{ijb}^{a} = \frac{\displaystyle\sum_{k=1}^{N_R} r_k v_{jk}' v_{ik}'' \frac{n_j^a}{\Delta n_k^a}[S_{(i,k)} + S_{(j,k)}][I_{(i)} + I_{(j)}]}{\displaystyle\sum_{k=1}^{N_R} r_k v_{ik}''} = \frac{c\_1\_2}{c\_2\_2} \tag{4.7}$$

where $f_{ij\,b}^{a}$ is relative transfer of atom a through formation of species i from species j

multiplied with sum of both species' sensitivity coefficients (species i and species j)
through backward reactions (the b notation in the equation points out backward

reactions), $c_{ij\,b}^{a}$ is the relative transfer of atom a through consumption of species i to

species j multiplied with sum of both species' sensitivity coefficients (species i and
species j) through backward reactions (the f notation in the equation points out
forward reactions).

If both forward and backward reactions occur in the reaction mechanism, the total
amount of formation and consumption values that a species has can now be summed
considering both forward and backward reactions as follows;

$$f_{ij} = \sum_{a=1}^{n} \frac{f\_1\_1 + f\_1\_2}{f\_2\_1 + f\_2\_2} \tag{4.8}$$

$$f_{ij} = \sum_{a=1}^{N_a} \left(\frac{\sum\limits_{k=1}^{N_R} r_k v'_{jk} v''_{ik} \dfrac{n_j^a}{\Delta n_k^a}[S_{(i,k)} + S_{(j,k)}][I_{(i)} + I_{(j)}] + \sum\limits_{k=1}^{N_R} r_k v''_{jk} v'_{ik} \dfrac{n_j^a}{\Delta n_k^a}[S_{(i,k)} + S_{(j,k)}][I_{(i)} + I_{(j)}]}{\sum\limits_{k=1}^{N_R} r_k v''_{ik} + \sum\limits_{k=1}^{N_R} r_k v'_{ik}} \right) \qquad (4.9)$$

$$c_{ij} = \sum_{a=1}^{n} \frac{c\_1\_1 + c\_1\_2}{c\_2\_1 + c\_2\_2} \qquad (4.10)$$

$$c_{ij} = \sum_{a=1}^{N_a} \left(\frac{\sum\limits_{k=1}^{N_R} r_k v''_{jk} v'_{ik} \dfrac{n_j^a}{\Delta n_k^a}[S_{(i,k)} + S_{(j,k)}][I_{(i)} + I_{(j)}] + \sum\limits_{k=1}^{N_R} r_k v'_{jk} v''_{ik} \dfrac{n_j^a}{\Delta n_k^a}[S_{(i,k)} + S_{(j,k)}][I_{(i)} + I_{(j)}]}{\sum\limits_{k=1}^{N_R} r_k v'_{ik} + \sum\limits_{k=1}^{N_R} r_k v''_{ik}} \right) \qquad (4.11)$$

In this equation, sensitivity coefficients are multiplied with reaction flow calculations through each reaction, and summed in the end considering both forward and backward reactions. It can be seen that not only one species' sensitivity coefficients, but both species' (species i and species j) sensitivity coefficients are considered together. There is also another control parameter in this equation that is called as I (importance). Some important species, such as products, reactants and by-products are assigned a pre-defined high importance value, and all the other species are assigned an importance value of 1. The basic idea of introducing an importance value for each species is to give a high formation f_{ij} or consumption c_{ij} values to the species which contributes to the formation or consumption of important species. After this calculation, each species is assigned a necessity value according to maximum of its formation or consumption value,

$$N_i = \max(f_{ij}, c_{ij}) \qquad (4.12)$$

Finally, all of the species are ranked according to their necessity values. Different cutoff levels are implemented for necessity values, and a species which have a necessity level lower than the cutoff level is defined as unimportant and removed from the reaction mechanism. Different skeletal mechanisms are obtained according to the removal of unimportant species from the reaction mechanism based on different cutoff levels. And skeletal mechanism that gives the most consistent results is defined as "reduced mechanism".

During the simulations and observations of the results it was seen that the new improved method gives very consistent results in small time intervals such as 4.2 e-2

miliseconds (shown in the following chapter), but it gives considerably worse results for longer time intervals such as 1.0 second for the same cutoff levels. After this problem had been seen, it was decided to improve equations between (4.4 – 4.11), and it was seen that removing normalization section of equations (4.4-4.7) (denominator parts of equations 4.4-4.7) and also removing "important parameter" from the equations ($I(i)$ and $I(j)$) gives better results not also for small time intervals such as 4.2 E-02 but also for longer time intervals such as 1.0 s. The idea of removing normalization part of the equations was creating an equation without considering just one species' stoichiometric coefficient values. As it is seen in equations (4.4-4.7), just one species' stoichiometric coefficient values are considered for the normalization. In contrast, both species' stoichiometric coefficient values are considered in the numerator part of the same equations. The idea of removing the importance parameter from the equation is relying on the sensitivity analysis and reaction flow analysis results instead of intervention the reaction mechanism by adding another control parameter.

The new derived equations based on the above assumptions are explained below;

The flow of atom "a" between species i and species j through formation or consumption multiplied with the sum of each species' sensitivity coefficients (species i and species j) are calculated for forward reactions as follows;

$$f_{ij\,f}^{a} = \sum_{k=1}^{N_R} r_k v'_{jk} v''_{ik} \frac{n_j^a}{\Delta n_k^a} [S_{(i,k)} + S_{(j,k)}] \tag{4.13}$$

$$c_{ij\,f}^{a} = \sum_{k=1}^{N_R} r_k v''_{jk} v'_{ik} \frac{n_j^a}{\Delta n_k^a} [S_{(i,k)} + S_{(j,k)}] \tag{4.14}$$

And the flow of atom a between species i and j through formation or consumption multiplied with the sum of each species' sensitivity coefficients (sensitivity coefficients) are calculated for backward reactions as follows;

$$f_{ij\,b}^{a} = \sum_{k=1}^{N_R} r_k v''_{jk} v'_{ik} \frac{n_j^a}{\Delta n_k^a} [S_{(i,k)} + S_{(j,k)}] \tag{4.15}$$

$$c_{ij\,b}^{a} = \sum_{k=1}^{N_R} r_k v'_{jk} v''_{ik} \frac{n_j^a}{\Delta n_k^a} [S_{(i,k)} + S_{(j,k)}] \tag{4.16}$$

If both forward and backward reactions occur in the reaction mechanism, the total amount of formation and consumption values that a species has can now be summed considering both forward and backward reactions as follows;

$$f_{ij} = \sum_{a=1}^{n} \left(f_{ij\,f}^{a} + f_{ij\,b}^{a} \right) \tag{4.17}$$

$$f_{ij} = \sum_{a=1}^{N_a} \left(\sum_{k=1}^{N_R} r_k v'_{jk} v''_{ik} \frac{n_j^a}{\Delta n_k^a} [S_{(i,k)} + S_{(j,k)}] + \sum_{k=1}^{N_R} r_k v''_{jk} v'_{ik} \frac{n_j^a}{\Delta n_k^a} [S_{(i,k)} + S_{(j,k)}] \right) \tag{4.18}$$

$$c_{ij} = \sum_{a=1}^{n} \left(c_{ij\,f}^{a} + c_{ij\,b}^{a} \right) \tag{4.19}$$

$$c_{ij} = \sum_{a=1}^{N_a} \left(\sum_{k=1}^{N_R} r_k v''_{jk} v'_{ik} \frac{n_j^a}{\Delta n_k^a} [S_{(i,k)} + S_{(j,k)}] + \sum_{k=1}^{N_R} r_k v'_{jk} v''_{ik} \frac{n_j^a}{\Delta n_k^a} [S_{(i,k)} + S_{(j,k)}] \right) \tag{4.20}$$

At the end, each species is assigned a necessity value according to maximum of its formation or consumption value multiplied with sensitivity coefficients via using equation (4.12).

Different cutoff levels are implemented for necessity values, and the species which have a necessity level lower than the cutoff level is defined as unimportant and removed from the reaction mechanism. The implementation of the cutoff levels is illustrated in the below figure. After necessity values of each species is calculated, the cutoff procedure begins and deletes the species which has a lower necessity value assigned by the user. For example, seven different cutoff levels are defined in the below figure, and according to these cut off levels, cutoff 1 deletes the species which has a necessity value lower than 1.0E-40, cutoff 2 deletes the species which has a necessity value lower than 1.0E-36, cutoff 3 deletes the species which has a necessity value lower than 1.0E-31, cutoff 4 deletes the species which has a necessity value lower than 1.0E-29, cutoff 5 deletes the species which has a necessity value lower than 1.0E-27, cutoff 6 deletes the species which has a necessity value lower than 1.0 E-25, and finally cutoff 7 deletes the species which has a necessity value lower than 1.0E-21. Continuous lines on the graphs correspond to the cutoff levels.
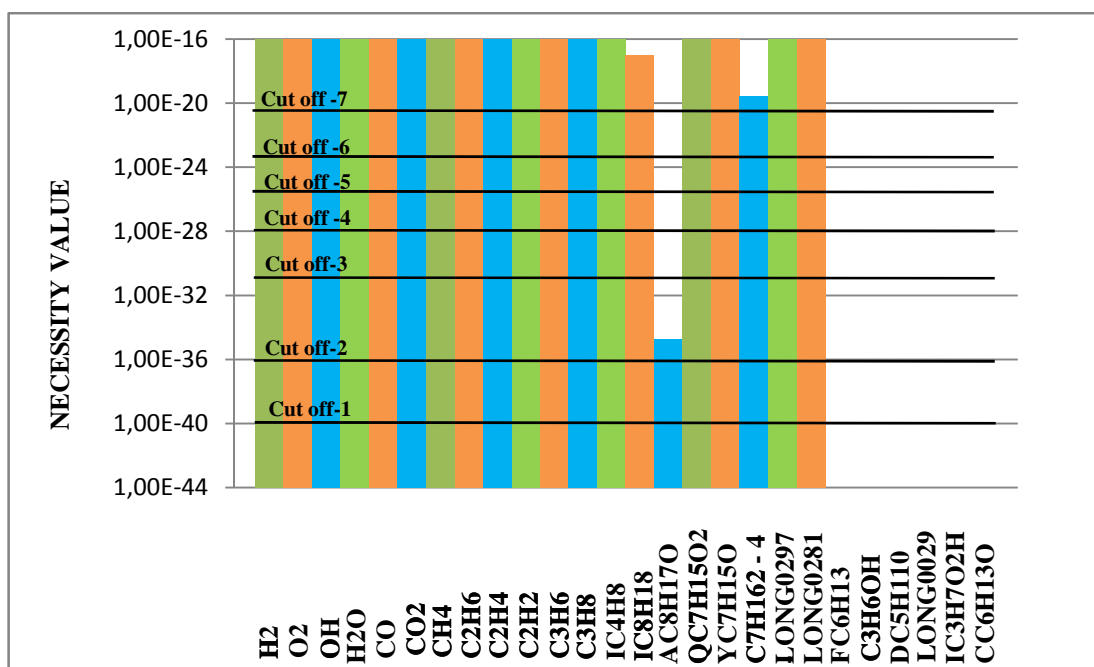
Figure 4.2 : Implementation of the cut-off levels according to the necessity values of the species

Different skeletal mechanisms are derived according to the removal of unimportant species from the reaction mechanism based on different cutoff levels. Consistencies of the skeletal mechanisms are validated by comparing the predictions of the distribution of important species in the batch reactor. During the simulations C/O ratio, temperature and contact times are changed. And skeletal mechanism that gives the most consistent results is defined as "reduced mechanism".

5. RESULTS

5.1 Implementing "Necessity Analysis With Simultaneously Combined Sensitivity And Reaction Flow Analysis Through Each Reaction" Method

Before getting started with i-octane reaction mechanism, the new improved method is validated with a smaller mechanism (with methane reaction mechanism consisting of 26 species and 108 reactions). The main idea of using a smaller mechanism is to save the computation time for the validation of the code. I-octane detailed mechanism (LLNL detailed mechanism) that will be used in this study consists of 857 species and 7193 reactions [3]. Making a simulation and observing the results of such a big mechanism requires much time. For instance, performing a sensitivity analysis for such a big mechanism may require days of calculation according to the conditions. As mentioned before, in order to save the validation time of the method, the FORTRAN code is first tested with the methane reaction mechanism. This reaction mechanism consists of 26 species and 108 reactions. Thus making a calculation with such a smaller mechanism (comparing to i-octane mechanism) requires considerably much less time.

The simulations of catalytic partial oxidation of methane and i-octane for homogenous gas phase are performed in DETCHEM^{BATCH} [6], and the simulations of the gases after catalyst are performed in DETCHEM^{PLUG} [6]. The details of DETCHEM^{BATCH} and DETCHEM^{PLUG} are explained in the following two sections.

5.2 DETCHEM^{BATCH} Code

The batch code simulates homogenous gas-phase and heterogeneous surface reactions in a batch reactor. Time dependent pressure, volume and temperature profiles can be specified by the user. Governing equations used in Batch code are as follows;

$$\frac{dn_k}{dt} = V \dot{\omega}_k + A \dot{s}_k \qquad \text{gas-phase species} \qquad (5.1)$$

$$\frac{dn_k}{dt} = A \dot{s}_k \qquad \text{surface species} \tag{5.2}$$

$$pV = nRT \qquad \text{ideal gas equation} \tag{5.3}$$

where $\dot{\omega}_k$ is the gas phase reaction rate, $\dot{s}_k$ is the surface reaction rate, A is the catalytic surface area, and V is the reactor volume, respectively. The species concentrations n_k are expressed in terms of mole numbers. As it was explained in the sensitivity analysis calculation section, sensitivity calculations can also be performed in DETCHEM$^{\text{BATCH}}$.

5.3 DETCHEM$^{\text{PLUG}}$ Code

DETCHEM$^{\text{PLUG}}$ code simulates the behavior of plug flow chemical reactors. And the code is improved for the non-dispersive one dimensional flow of chemically reacting ideal gas mixture. Governing equations used in Plug code are as follows;

$$\frac{d(\rho u A_c)}{dz} = A_s \sum_{k=1}^{kg} \dot{s}_k M_k \tag{5.4}$$

$$\rho u A_c \frac{dY_k}{dz} + Y_k A_s \sum_{k=1}^{kg} \dot{s}_k M_k = M_k (A_s \dot{s}_k + A_c \dot{\omega}_k) \tag{5.5}$$

$$\rho u A_c \frac{d(C_P)}{dz} + \sum_{k=1}^{kg} \dot{\omega}_k h_k M_k A_c + \sum_{k=1}^{kg} \dot{s}_k h_k M_k A_s = U A_s (T_W - T) \tag{5.6}$$

$$pM = \rho RT \tag{5.7}$$

The above equations represents total continuity, species continuity, energy, and the equation of state respectively. In addition to these equations, residence time of gas is calculated through the below differential equation,

$$\frac{d\tau}{dz} = \frac{1}{u} \tag{5.8}$$

In order to compensate model limitations, mass transfer coefficients can be used additionally. They approximate the "resistance" to species mass transport between the mean composition and the composition at the reacting channel surface. The mass transfer coefficients are defined by the following relationship,

$$\dot{s}_k M_k = h_k (\rho_s Y_{k,s} - \rho_{k,m}) \tag{5.9}$$

where h_k is the mass transfer coefficient, which can be represented in non-dimensional form using the Sherwood numbers,

$$Sh = \frac{h_k d}{D_{im}} \tag{5.10}$$

The Sherwood numbers are calculated locally using standard correlations.

For the constant wall temperature, the Nussult number is defined as,

$$Nu_T = 3.657 + 8.827 \left(\frac{1000}{Gz} \right)^{-0.545} \exp\left(\frac{-48.2}{Gz} \right) \tag{5.11}$$

For the case of constant heat flux,

$$Nu_H = 4.364 + 13.18 \left(\frac{1000}{Gz} \right)^{-0.545} \exp\left(\frac{-60.2}{Gz} \right) \tag{5.12}$$

where Gz is the Graetz number for the heat transfer. In the case of mass transfer, Sherwood numbers are expressed by the same equation with the Gz replaced by the Greatz number for mass transfer. Since the Greatz number number is calculated as a function of reactor position, the mass and heat transfer coefficient calculated in DETCHEM^{PLUG} are the local values.

In DETCHEM^{PLUG} the standard implicit code LIMEX is used to solve the coupled governing equations. DETCHEM^{PLUG} offers various options to solve the problem. The temperature solution offers isothermal, non-isothermal, adiabatic and non-adiabatic conditions. In addition to these, the axial temperature profile can be specified by a subroutine. In isothermal as well as in the axial temperature profile case the energy equation is not solved. The species transport can be modeled for Gas-phase and the Surface reactions. As a special case, the surface reactions can be specified to take place on washcoat.

Though DETCHEM^{PLUG} is essentially a one dimensional model, it supports a number of geometrical configuration (The mass and heat transfer coefficients are specific to the flow geometry). The configurations supported currently are cylindrical, cylindrical with gradually increasing cross-sectional area, triangular, square, hexagonal and a sinusoidal geometry.

5.4 Simulations

Simulations are performed at first for methane reaction mechanism then they are performed for i-octane LLNL detailed reaction mechanism.

5.4.1   Results of The Batch Simulation With Methane Mechanism

The list of the species of detailed methane reaction mechanism is shown in the below table:

Table 5.1 : All species in the detailed methane reaction mechanism

CH_4	O_2	O	H_2O	H	HO_2	H_2O_2	H_2
CO	CO_2	CH_2O	CH_2OH	CH_3OH	CH_3O	CH_2	C_2H_2
CH_3O_2H	C_2H_6	CHO	OH	CH_3	CH	$CH_2 (s)$	CH_3O_2
C_2H_4	N_2						

Initial conditions and initial mole fractions that are used in methane partial oxidation simulation for C/O=1.0 is shown in table 5.2 and table 5.3.

Table 5.2 : Initial parameters of methane simulation for C/O=1.0

Parameter	Value
Volume (m^3)	2.8 e-6
C/O	1
Pressure (bar)	10
Temperature (K)	1005.78

Table 5.3 : Gas phase composition for C/O=1

Species	Mole Fraction
O_2	0.1477
CH_4	0.2954
N_2	0.5569

After the simulation was performed according to the inlet conditions (table 5.2 and 5.3) through improved FORTRAN code based on the proposed reduction method, the below relative necessity values for each species are obtained as follows:

Table 5.4 : Relative necessity values of each species in CPOX of methane

Species	Necessity Value
CH_4	5.06E-10
O_2	4.31E-08
O	3.92E-13
H_2O	2.59E-10
H	1.06E-12
H_2O_2	3.83E-11
H_2	2.23E-12
CO	2.31E-11
CO_2	4.51E-12
CH_2O	3.42E-10
CHO	5.68E-11
CH_2OH	9.32E-12
OH	3.48E-10
CH_3OH	1.53E-11
CH_3	5.89E-10
CH_3O	1.35E-11
CH	1.10E-24
CH_2	6.36E-17
$CH_2(S)$	1.03E-17
C_2H_2	1.86E-35
CH_3O_2	4.31E-08
CH_3O_2H	7.54E-14
C_2H_4	2.60E-20
C_2H_6	1.72E-12
N_2	4.31E-08

Different cutoff levels are defined according to relative necessity values of species, different skeletal mechanisms are obtained based on these cutoff levels. These cutoff levels can be seen in the below diagram. Cutoff 1 removes the species from the mechanism which have a necessity value lower than 1.0E-24, cutoff 2 removes the species from the mechanism which have a necessity value lower than 1.0E-17, cutoff 3 removes the species from the mechanism which have a necessity value lower than 1.0E-16, cutoff 4 removes the species from the mechanism which have a necessity value lower than 1.0E-13 and cutoff 5 removes the species from the mechanism which have a necessity value lower than 1.0E-12.
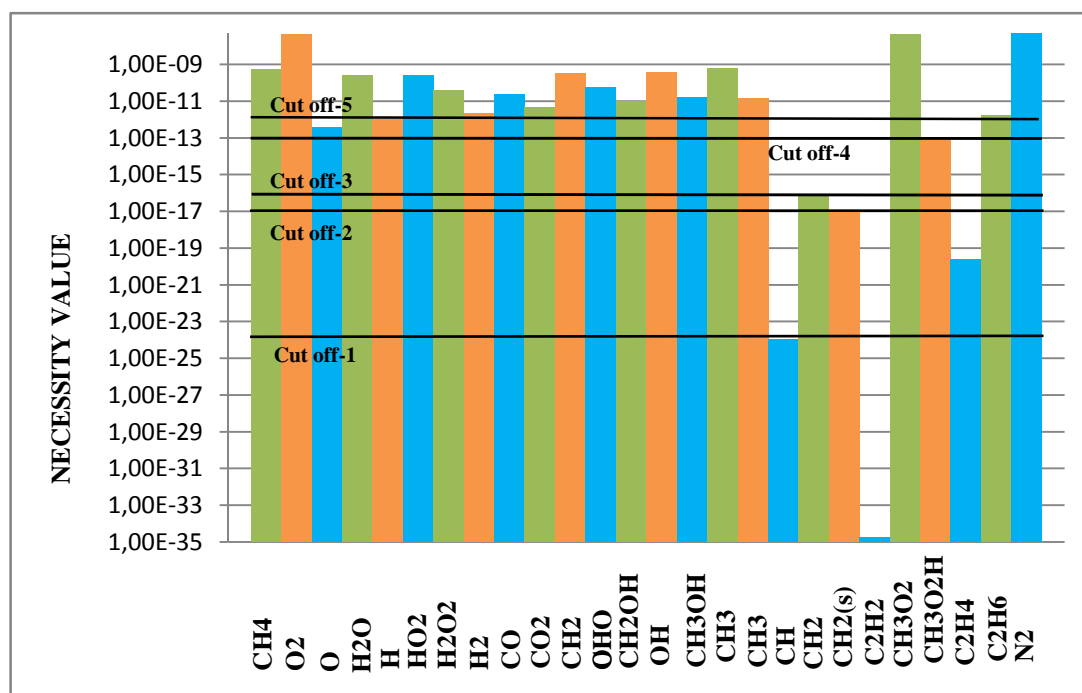
Figure 5.1 : Implementation of the cutoff levels according to the necessity values of the species for CPOX of methane

The list of the removed species numbers and the remaining total reaction numbers are shown in table 5.5.

Table 5.5 : Remaining species numbers and reaction numbers for different skeletal mechanisms for CPOX of methane: C/O=1.0

Mechanism	Number of Remaining Species	Number of Reactions
Detailed	26	108
Skeletal_1	24	97
Skeletal_2	22	89
Skeletal_3	21	84
Skeletal_4	20	78
Skeletal_5	19	61

The list of the deleted species are shown in table 4.7.

Table 5.6 : The list of the deleted species according to each skeletal mechanism

Mechanism	Deleted Species						
Skeletal_1	C_2H_2	CH					
Skeletal_2	C_2H_2	CH	C_2H_4	CH_2 (s)			
Skeletal_3	C_2H_2	CH	C_2H_4	CH_2 (s)	CH_2		
Skeletal_4	C_2H_2	CH	C_2H_4	CH_2 (s)	CH_2	CH_3O_2H	
Skeletal_5	C_2H_2	CH	C_2H_4	CH_2 (s)	CH_2	CH_3O_2H	O

Predictions for the distribution of important species in the batch reactor of the detailed and skeletal mechanisms are shown in the following graphics.
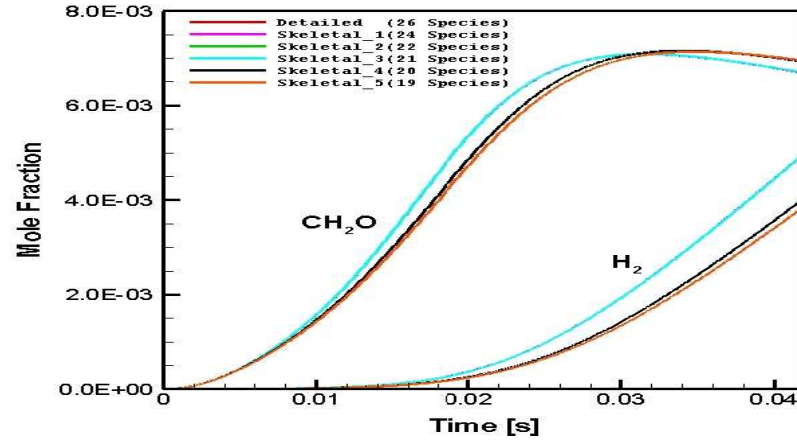
Figure 5.2 : Numerically predicted CH_2O and H_2 distribution in CPOX of methane as a function of time in the batch reactor: C/O=1.0, 1005.78 K
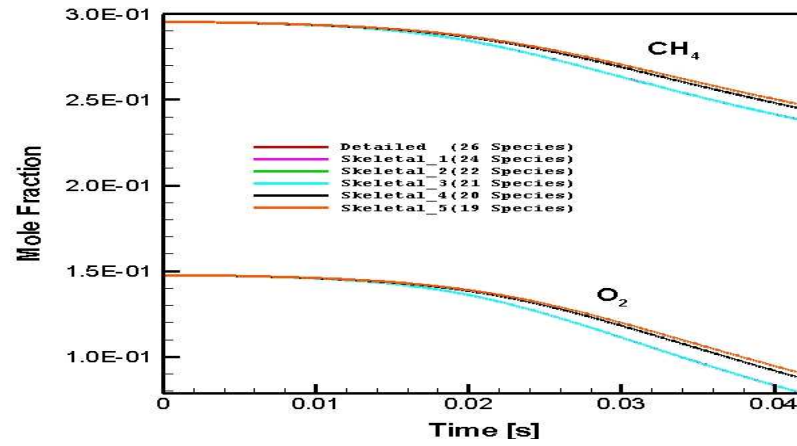
Figure 5.3 : Numerically predicted CH_4 and O_2 distribution in CPOX of methane as a function of time in the batch reactor: C/O=1.0, 1005.78 K
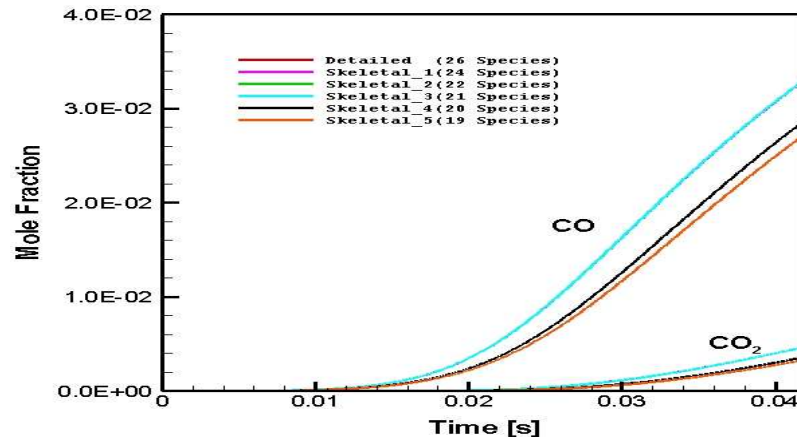
Figure 5.4 : Numerically predicted CO_2 and CO distribution in CPOX of methane as a function of time in the batch reactor: C/O=1.0, 1005.78 K

As it can be seen from the above graphics, skeletal 1 to skeletal 3 mechanisms give almost the same results with the detailed mechanism, but mole fraction profiles of skeletal 4 and skeletal 5 deviate from the detailed mechanism. The differences (or errors) from the detailed mechanism of skeletal 1 to skeletal 3 mechanisms are lower than 1%. However, the differences with skeletal 4 and skeletal 5 mechanisms increase. The meaning of error here is the deviation of the mole fraction results of the skeletal mechanisms from the detailed mechanism mole fraction results in a percentage interval. Error levels of mole fraction results of skeletal mechanisms are calculated through equation (5.1)

$$\text{Error} = \left(\frac{X_{det} - X_{skel}}{X_{det}} \right) \cdot 100\% \qquad (5.1)$$

where X_{det} represents mole fraction of the detailed mechanism, and X_{skel} represents mole fraction result of the skeletal mechanism.

Error levels of the skeletal mechanisms at 4.2E-02s are given in the below table.

Table 5.7 : Errors of the skeletal mechanisms for the predictions of important species distribution in the batch reactor for CPOX of methane: C/O=1.0, 1005.78 K

Mechanism	H_2 Error%	O_2 Error%	H_2O Error%	CO Error%	CO_2 Error%	CH_4 Error%	CH_2O Error%	C_2H_6 Error%	CH_3OH Error%
Skeletal_1	0.00	0.00	0.00	0.00	0.00	0.00	0.00	0.00	0.00
Skeletal_2	0.06	0.00	0.08	0.09	0.02	0.02	0.02	0.15	0.08
Skeletal_3	0.06	0.06	0.08	0.09	0.02	0.02	0.02	0.16	0.09
Skeletal_4	18.87	10.83	14.13	12.99	29.57	2.74	3.55	10.87	6.52
Skeletal_5	22.46	14.54	20.08	21.13	29.11	3.70	3.92	16.37	9.39

According to the error levels, skeletal-3 mechanism is chosen as the reduced mechanism for this case and it is shown with a red color in the below table.

The simulations aren't performed just for one exact time. The next simulation is performed for 0.2 seconds.

Predictions for the distribution of important species in the batch reactor of the detailed and skeletal mechanisms are shown in the following graphics.
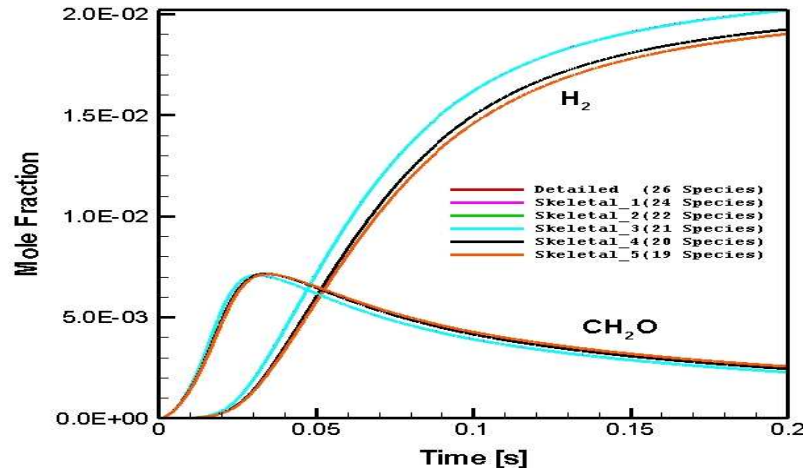
Figure 5.5 : Numerically predicted CH_2O and H_2 distribution in CPOX of methane as a function of time in the batch reactor: C/O=1.0, 1005.78 K, t=0.2s
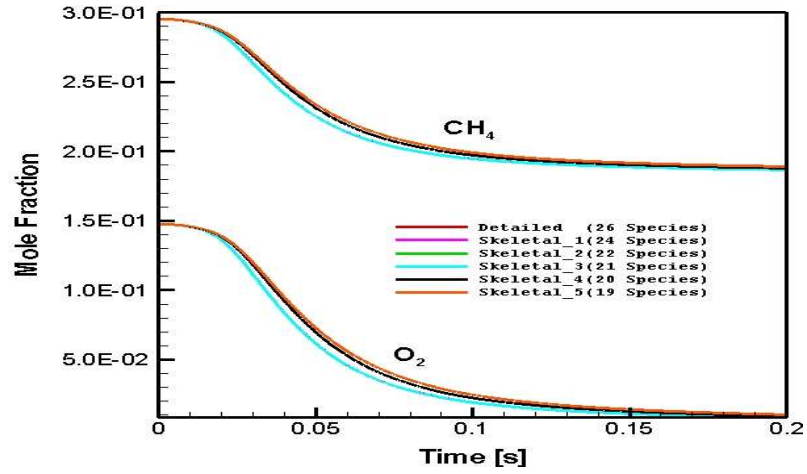
Figure 5.6 : Numerically predicted CH_4 and O_2 distribution in CPOX of methane as a function of time in the batch reactor: C/O=1.0, 1005.78 K, t=0.2s
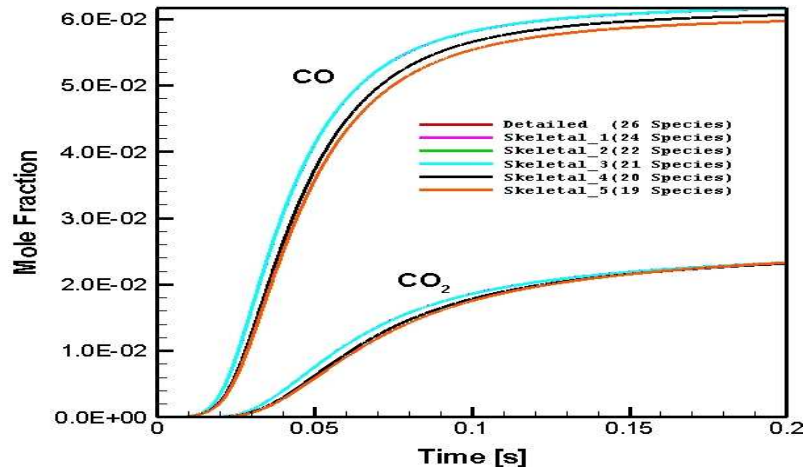
Figure 5.7 : Numerically predicted CO_2 and CO distribution in CPOX of methane as a function of time in the batch reactor: C/O=1.0, 1005.78 K, t=0.2s

It is seen again that skeletal-1 to skeletal-3 mechanisms give very consistent results. The differences from the detailed mechanisms are below 0.1 %. Skeletal 4 mechanism gives for all species an error level below 10 % except O_2. For O_2 the difference is about 15 %. Skeletal 5 mechanism can not predict O_2, CH_2O, CH_3OH mole fractions very accurately. The errors of all skeletal mechanisms at 0.2 time is given in the below table:

Table 5.8 : Errors of the skeletal mechanisms for the predictions of important species distribution in the batch reactor for CPOX of i-octane: C/O=1.6, 1005.78 K, t=0.2s

Mechanism	H_2 %Error	O_2 %Error	H_2O %Error	CO %Error	CO_2 %Error	CH_4 %Error	CH_2O %Error	C_2H_6 %Error	CH_3OH %Error
Skeletal_1	0.00	0.00	0.00	0.00	0.00	0.00	0.00	0.00	0.00
Skeletal_2	0.02	0.00	0.01	0.03	0.05	0.01	0.01	0.07	0.05
Skeletal_3	0.02	0.08	0.01	0.03	0.05	0.01	0.02	0.08	0.06
Skeletal_4	4.69	14.79	0.70	1.60	0.52	0.63	7.20	0.11	6.70
Skeletal_5	5.81	27.85	1.65	3.20	0.01	1.26	12.16	3.89	15.05

It is seen again that skeletal-3 mechanism gives very good results, and it is chosen as the reduced mechanism for the new condition. After these calculations, it is seen that the code gives consistent results for methane CPOX reaction mechanism. Finally, it is possible to delete up to 5 species and 24 reactions without any lose of information in the CPOX simulations of methane mechanism. So, it is decided to make further calculations with the detailed i-octane mechanism.

5.4.2 Results of The Batch Simulations With The LLNL I-Octane Mechanism

As the last simulation (methane detailed reaction mechanism) was performed through improved FORTRAN code that correlates with DETHCEM^{BATCH}, i-octane simulations will also be performed in the same code.

Applicability of the proposed reduction method for the CPOX study of i-octane will be investigated in this section. In more detail, fuel and oxygen consumption, major products (H_2, CO, H_2O and CO_2) and by-products (methane, ethylene, propylene and iso-butylene) occurrence will be examined. All these by-products play a significant role as coke and soot precursors, hence understanding the behavior of these by-products is crucial to understand coke formation in the catalyst. Accurate and fast prediction of fuel, oxygen, major products and by-products by the reduced mechanisms will be investigated through the simulations.

The parameters used at i-octane batch code simulations (not the mole fractions, but parameters) are always constant (except reactor temperature, C/O ratio and simulation time). As it is seen in table 5.9, the first simulation time is chosen as 4.2 E-02 s. And the reason of specifically selecting this time is the occurrence of the contact time specifically at this time. Because the first aim of this study is to validate the proposed method for rich conditions, C/O ratios are set for 1.2, 1.6 and 2.0. But, the conformity of the code for lean mixtures will be investigated, as well. C/O ratio for lean mixture is set as 0.8. The first simulation is performed for C/O=1.6 and 4.2E-02 seconds. The parameters and initial mole fractions used in the simulation for this case are shown in table (5.9) and table (5.10), respectively;

Table 5.9 : Initial parameters of i-octane simulation for C/O=1.6

Parameter	Value
Reactor Volume (m^3)	2.83 E-06
Diameter (m)	0.019
Radius (m)	9.50 E-03
Length (m)	1.00 E-02
Area (m^2)	2.83 E-04
Pressure (Pa)	101325
Reactor Temperature (K)	1005.78
C/O	1.6
Simulation Time (s)	4.2 E-02

Table 5.10 : Initial mole fractions of reactants for C/O=1.6

Species	Mole Fraction
IC_8H_{18}	5.71E-02
O_2	1.43E-01
N_2	8.00E-01

The results of the simulations are given respectively. The remaining reaction numbers and species numbers can be seen in the below table.

Table 5.11 : Remaining species numbers and reaction numbers for different skeletal mechanisms for CPOX of i-octane: C/O=1.6, 1005.78 K

Mechanism	Number of Remaining Species	Number of Reactions
Detailed	857	7191
Skeletal_1	587	5473
Skeletal_2	515	4827
Skeletal_3	434	4103
Skeletal _4	382	3599
Skeletal _5	338	3169
Skeletal _6	312	2903
Skeletal _7	287	2723

Predictions for the distribution of important species in the batch reactor of the detailed and skeletal mechanisms are shown in the following graphics.
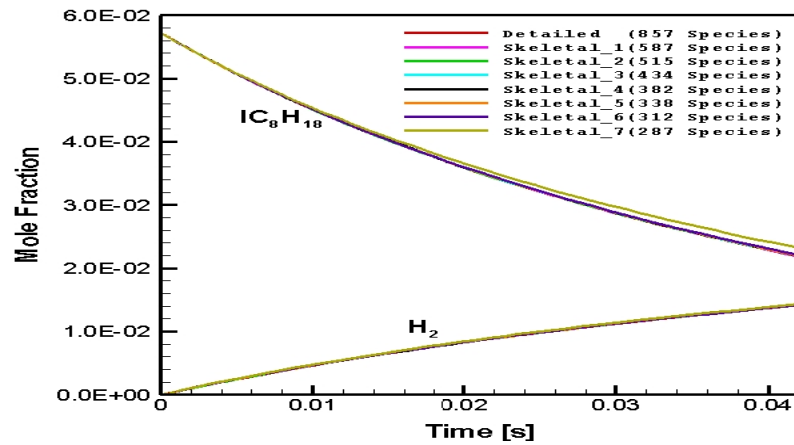
Figure 5.8 : Numerically predicted H_2 and IC_8H_{18} distribution in CPOX of i-octane as a function of time in the batch reactor: C/O=1.6, 1005.78 K
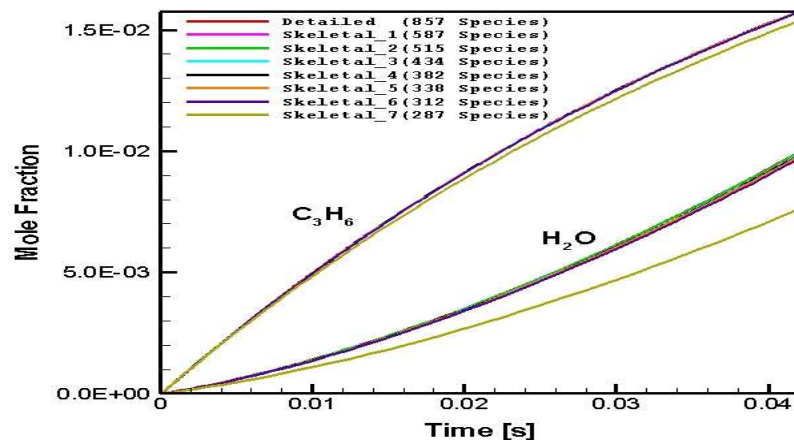
Figure 5.9 : Numerically predicted H_2O and C_3H_6 distribution in CPOX of i-octane as a function of time in the batch reactor: C/O=1.6, 1005.78 K
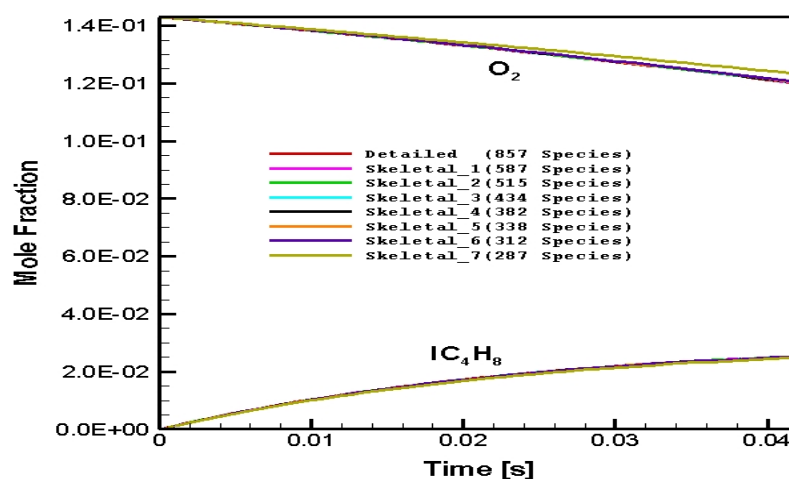
Figure 5.10 : Numerically predicted O_2 and IC_4H_8 distribution in CPOX of i-octane as a function of time in the batch reactor: C/O=1.6, 1005.78 K
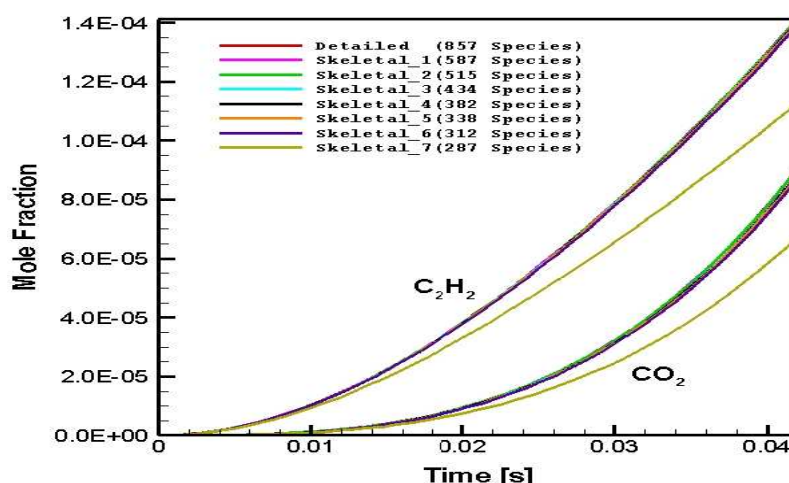
Figure 5.11 : Numerically predicted C_2H_2 and CO_2 distribution in CPOX of i-octane as a function of time in the batch reactor: C/O=1.6, 1005.78 K

In addition to the above main products and by-products, some of the main products, by-products and radical results can be found in the appendix section.

It is seen on the graphics that skeletal mechanisms give similar profiles for each observed species. But, it is not easy to compare the results just according to the mole fraction profiles on the graphics, or it can even be misleading sometimes. Because it can be just a rough estimation for the comparison of detailed and skeletal mechanisms. The main idea of observing the graphics is to see whether or not skeletal mechanisms give similar mole fraction profiles. In order to compare the detailed and skeletal mechanisms in more detail, it is better to investigate the error levels of each skeletal mechanism. The error levels of the skeletal mechanisms for the important reactants, products and by-products are shown in tables 5.12 and 5.13

(C/O = 1.6 and simulation time is 4.2 e-2 s). The best skeletal mechanism (maximum deleted species with minimum error) is shown with a red color in the tables.

Table 5.12 : (a) Errors of the skeletal mechanisms for the predictions of important species distribution in the batch reactor for CPOX of i-octane: C/O=1.6, 1005.78 K

| Mechanism	H_2 Error %	O_2 Error %	H_2O Error %	CO Error %	CO_2 Error %	CH_4 Error %	CH_2O Error %	C_2H_6 Error %
Skeletal_1	0.01	0.00	0.02	0.02	0.01	0.00	0.00	0.00
Skeletal _2	0.01	0.01	0.06	0.07	0.02	0.01	0.01	0.01
Skeletal _3	0.11	0.14	1.24	0.97	1.97	0.01	0.67	0.15
Skeletal _4	0.13	0.15	1.36	1.07	2.12	0.03	0.72	0.14
Skeletal _5	0.19	0.20	1.80	1.59	2.68	0.07	0.92	0.10
Skeletal _6	0.30	0.32	2.79	2.42	3.95	0.01	1.43	0.12
Skeletal _7	0.60	2.66	30.87	26.19	25.63	3.96	12.53	0.00

Table 5.13 : (b) Errors of the skeletal mechanisms for the predictions of important species distribution in the batch reactor for CPOX of i-octane: C/O=1.6, 1005.78 K

Mechanism	C_2H_4 Error%	C_2H_2 Error%	C_3H_6 Error%	IC_4H_8 Error%	IC_8H_{18} Error %	CH_3 Error%	OH Error%	HCCO Error%	CH_2CHO Error%
Skeletal _1	0.02	0.00	0.00	0.01	0.00	0.01	0.02	0.01	0.01
Skeletal _2	0.04	0.11	0.00	0.00	0.02	0.01	0.04	0.11	0.04
Skeletal _3	0.31	0.60	0.04	0.06	0.28	0.00	0.92	0.93	0.75
Skeletal _4	0.44	0.70	0.03	0.06	0.32	0.00	1.04	1.09	0.86
Skeletal _5	0.58	0.90	0.02	0.10	0.44	0.02	1.53	1.64	1.27
Skeletal _6	1.07	1.59	0.17	0.20	0.71	0.17	2.67	2.95	2.33
Skeletal _7	6.98	20.12	2.51	1.81	5.94	4.48	23.22	25.89	21.46

Error levels of skeletal 1, skeletal 2 and skeletal 3 mechanisms are lower than 2 %. Skeletal 4, skeletal 5 and skeletal 6 mechanisms give lower than 4 % error levels. Error levels of skeletal 7 mechanism increase sharply for some species such as CO_2 and H_2O.

CPU times of the detailed mechanism and all the skeletal mechanisms are shown in table 5.14.

Table 5.14 : CPU times of CPOX of i-octane simulations in batch reactor: C/O=1.6, 1005.78 K

Mechanism	CPU Time	Mechanism	CPU Time
Detailed	2,31	Skeletal _4	0,58
Skeletal_1	1,29	Skeletal _5	0,51
Skeletal _2	1,17	Skeletal _6	0,48
Skeletal _3	1,06	Skeletal _7	0,41

Finally, skeletal-6 is chosen as the reduced mechanism for C/O=1.6 and 4.2E-02 seconds. Because it gives consistent results without much loss of information and reduces the CPU times well. Remaining species versus error % graphs are also plotted for some species, and they can be seen below.
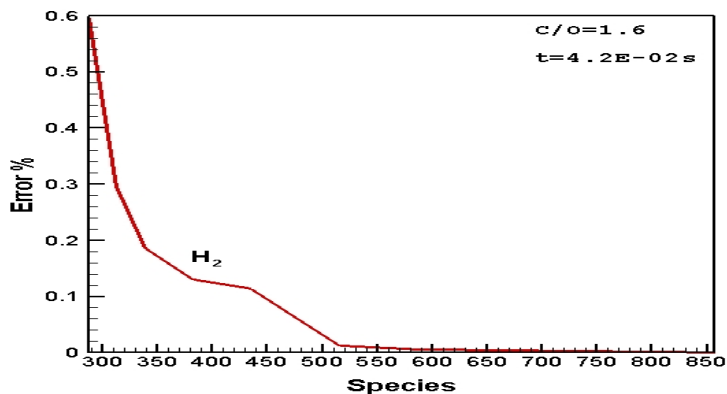
Figure 5.12 : Remaining Species – Error % of H_2 in CPOX of i-octane: C/O=1.6, 1005.78 K
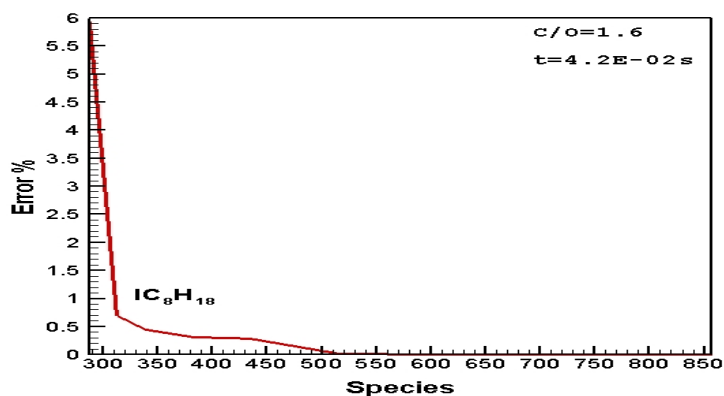
Figure 5.13 : Remaining Species – Error % of IC_8H_{18} in CPOX of i-octane: C/O=1.6, 1005.78 K
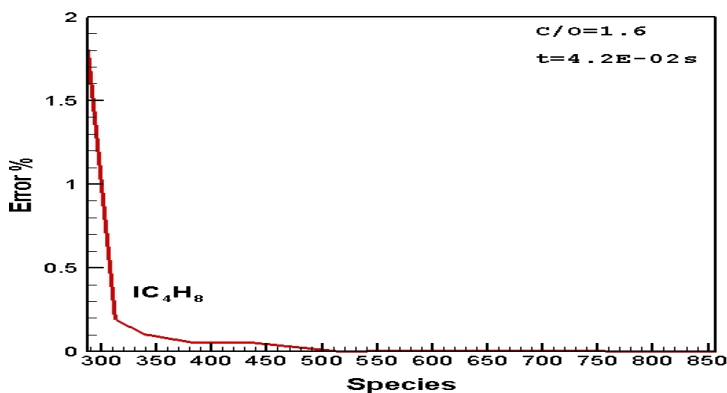
Figure 5.14 : Remaining Species –Error % of IC_4H_8 in CPOX of i-octane: C/O=1.6, 1005.78 K

Simulation is not performed just for one case; it is performed for different cases, as well. The next simulation is performed for C/O=2.0 and 4.2E-02s case. The parameters and initial mole fractions of this case are shown in the following tables,

Table 5.15 : Initial parameters of i-octane simulation for C/O=2.0

Parameter	Value
Reactor Volume (m^3)	2.83 E-06
Diameter (m)	0.019
Radius (m)	9.50 E-03
Length (m)	1.00 E-02
Area (m^2)	2.83 E-04
Pressure (Pa)	101325
Reactor Temperature (K)	998.26
C/O	2.0
Simulation Time (s)	4.2 E-02

Table 5.16 : Initial mole fractions of reactants for C/O=2.0

Species	Mole Fraction
IC_8H_{18}	6.67E-02
O_2	1.33E-01
N_2	8.00E-01

The results of the simulations are given respectively. The remaining reaction numbers and species numbers can be seen in the below table.

Table 5.17 : Remaining species numbers and reaction numbers for different skeletal mechanisms for CPOX of i-octane: C/O=2.0, 998.26 K

Mechanism	Number of Remaining Species	Number of Remaining Reactions
Detailed	857	7191
Skeletal_1	588	5475
Skeletal _2	514	4821
Skeletal _3	430	4049
Skeletal _4	380	3489
Skeletal _5	336	3155
Skeletal _6	320	2933
Skeletal _7	286	2701

Predictions for the distribution of important species in the batch reactor of the detailed and skeletal mechanisms are shown in the following graphics.
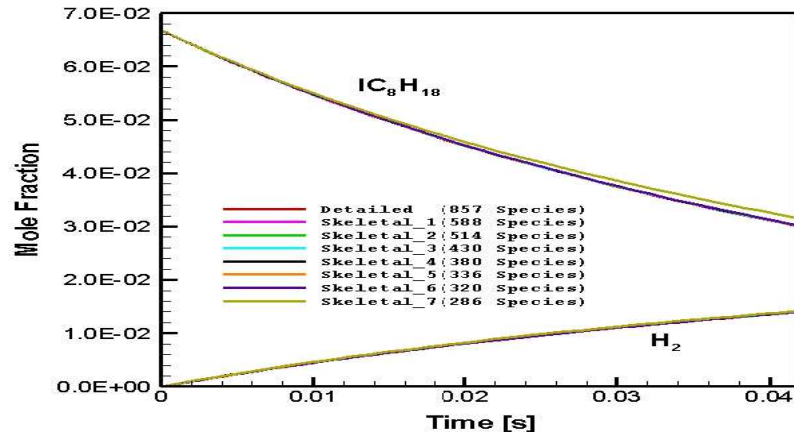
Figure 5.15 : Numerical prediction of H_2 and IC_8H_{18} distribution in CPOX of i-octane as a function of time in the batch reactor: C/O=2.0, 998.26 K
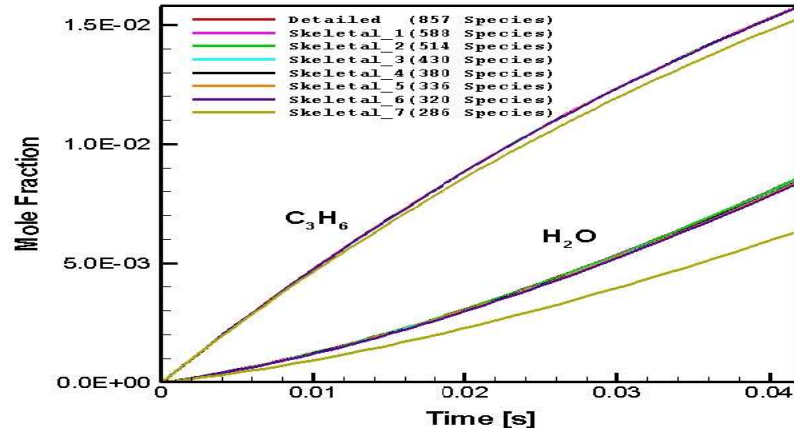
Figure 5.16 : Numerical prediction of H_2O and C_3H_6 distribution in CPOX of i-octane as a function of time in the batch reactor: C/O=2.0, 998.26 K
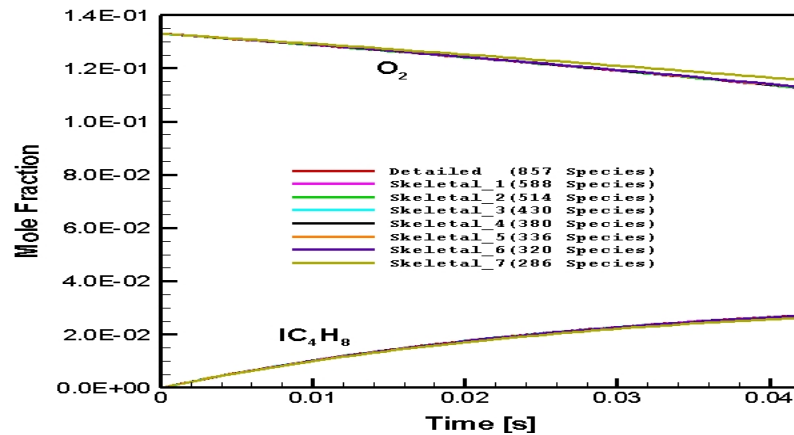
Figure 5.17 : Numerical prediction of O2 and IC_4H_8 distribution in CPOX of i-octane as a function of time in the batch reactor: C/O=2.0, 998.26 K
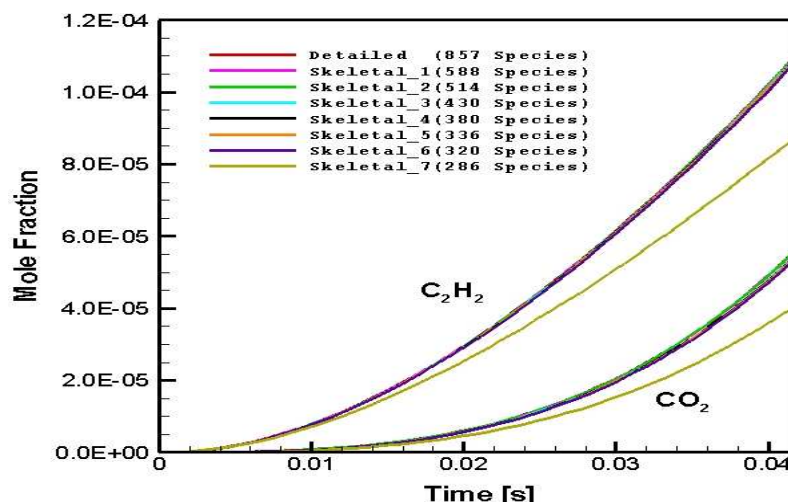
Figure 5.18 : Numerical prediction of C_2H_2 and CO_2 distribution in CPOX of i-octane as a function of time in the batch reactor: C/O=2.0, 998.26 K

As it is seen on the graphics, all skeletal mechanisms give similar mole fraction profiles for C/O=2.0 case. In order to examine the results in detail, error levels are calculated again. Error levels of the skeletal mechanisms for C/O=2.0 and 4.2E-02 seconds can be seen in table 5.18 and table 5.19. The best skeletal mechanism is shown with a red color in the tables.

In addition to the above main products and by-products, some of the main products, by-products and radical results (CH_3, OH, HCCO, CH_2CHO) are shown in the appendix section, as well. But, error levels of all considered species are shown in table 5.18 and table 5.19. And as it is seen from the graphs and error levels, the method gives consistent results for radicals, as well.

Table 5.18 : (a) Errors of the skeletal mechanisms for the predictions of important species distribution in the batch reactor for CPOX of i-octane: C/O=2.0, 998.26 K

Mechanism	H_2 Error %	O_2 Error %	H_2O Error %	CO Error %	CO_2 Error %	CH_4 Error %	CH_2O Error %	C_2H_6 Error %
Skeletal_1	0.00	0.00	0.02	0.02	0.01	0.00	0.00	0.00
Skeletal_2	0.02	0.01	0.07	0.09	0.06	0.01	0.03	0.02
Skeletal_3	0.12	0.14	1.37	1.01	2.58	0.00	0.75	0.13
Skeletal_4	0.14	0.15	1.49	1.12	2.72	0.01	0.80	0.13
Skeletal_5	0.19	0.20	1.96	1.66	3.30	0.07	1.00	0.06
Skeletal_6	0.26	0.27	2.67	2.22	4.04	0.13	1.34	0.09
Skeletal_7	0.01	2.63	34.95	28.19	27.10	4.03	13.44	3.72

Table 5.19 : (b) Errors of the skeletal mechanisms for the predictions of important species distribution in the batch reactor for CPOX of i-octane: C/O=2.0, 998.26 K

Mechanism	C_2H_4 Error%	C_2H_2 Error%	C_3H_6 Error%	IC_4H_8 Error%	IC_8H_{18} Error%	CH_3 Error%	OH Error%	HCCO Error%	CH_2CHO Error%
Skeletal_1	0.02	0.00	0.00	0.01	0.00	0.00	0.03	0.01	0.01
Skeletal_2	0.06	0.16	0.01	0.00	0.02	0.01	0.05	0.06	0.04
Skeletal _3	0.32	0.67	0.06	0.09	0.24	0.02	1.01	0.98	0.75
Skeletal _4	0.47	0.74	0.05	0.10	0.26	0.02	1.13	1.13	0.86
Skeletal _5	0.62	0.97	0.05	0.14	0.36	0.01	1.63	1.69	1.27
Skeletal _6	1.01	1.54	0.15	0.24	0.51	0.10	2.38	2.54	1.94
Skeletal _7	7.13	20.46	3.21	2.52	4.99	4.75	25.24	26.41	22.40

The error levels of skeletal 1, skeletal 2 and skeletal 3 are again lower than 2 %. Skeletal 4, skeletal 5 and skeletal 6 give lower than 4 % error levels. The error levels of skeletal 7 mechanism increase sharply again for some species.

CPU times of the detailed mechanism and all the skeletal mechanisms are shown in table 5.20.

Table 5.20 : CPU times of CPOX of i-octane simulations in batch reactor: C/O=2.0, 998.26 K

Mechanism	CPU Time
Detailed	2,26
Skeletal_1	1,27
Skeletal_2	1,16
Skeletal_3	1,04
Skeletal_4	0,58
Skeletal_5	0,52
Skeletal_6	0,46
Skeletal_7	0,42

Finally, skeletal 6 is chosen again as the reduced mechanism. Because it gives consistent results without much loss of information and reduces the CPU times well. Remaining species versus error % graphs are plotted for some species again, and they can be seen below.
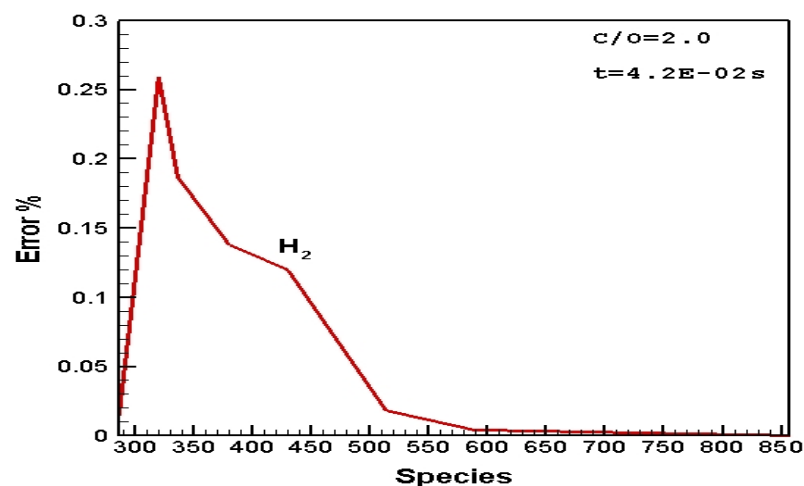
Figure 5.19 : Remaining Species – Error % of H_2 in CPOX of i-octane: C/O=2.0, 998.26 K
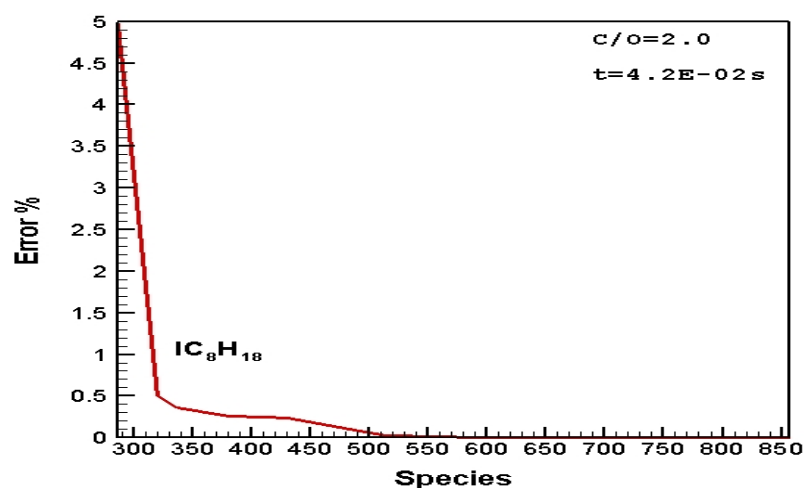
Figure 5.20 : Remaining Species – Error % of IC_8H_{18} in CPOX of i-octane: C/O=2.0, 998.26 K
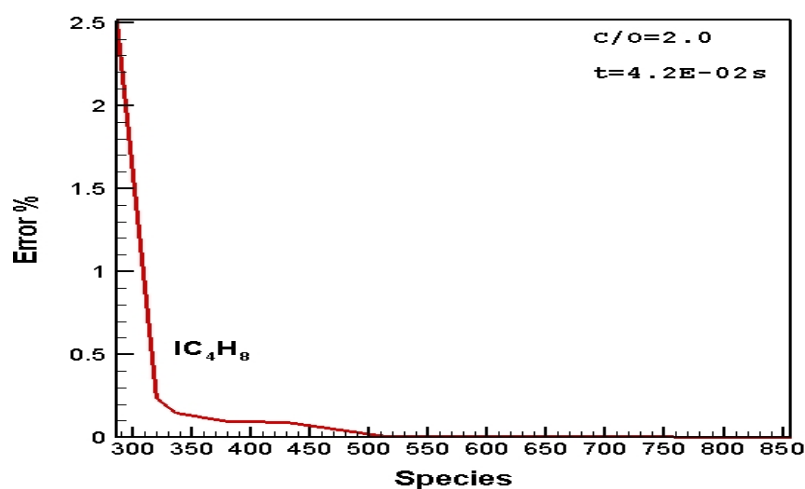
Figure 5.21 : Remaining Species –Error % of IC_4H_8 in CPOX of i-octane: C/O=2.0, 998.26 K

The next simulation is performed for C/O=1.2 case. Simulation conditions of this case is shown in the table 5.21 and table 5.22,

Table 5.21 : Initial parameters of i-octane simulation for C/O=1.2 and 4.2E-02 s

Parameter	Value
Reactor Volume (m^3)	2.83 E-06
Diameter (m)	0.019
Radius (m)	9.50 E-03
Length (m)	1.00 E-02
Area (m^2)	2.83 E-04
Pressure (Pa)	101325
Reactor Temperature (K)	1017.86
C/O	1.2
Simulation Time (s)	4.2 E-02

Table 5.22 : Initial mole fractions of reactants for C/O=1.2

Species	Mole Fraction
IC_8H_{18}	4.62E-02
O_2	1.54E-01
N_2	8.00E-01

The remaining reaction and species numbers can be seen in table 5.23.

Table 5.23 : Remaining species numbers and reaction numbers for different skeletal mechanisms for CPOX of i-octane: C/O=1.2, 1017.86 K

Mechanism	Number of Remaining Species	Number of Remaining Reactions
Detailed	857	7191
Skeletal_1	591	5505
Skeletal_2	521	4907
Skeletal_3	436	4149
Skeletal_4	389	3659
Skeletal_5	343	3191
Skeletal_6	320	3073
Skeletal_7	293	2729

Predictions for the distribution of important species in the batch reactor of the detailed and skeletal mechanisms are shown in the following graphics.
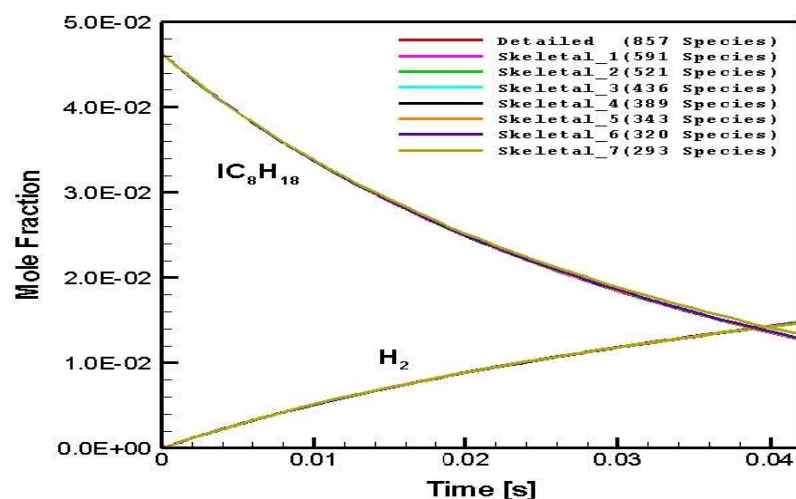
Figure 5.22 : Numerically predicted H_2 and IC_8H_{18} distribution in CPOX of i-octane as a function of time in the batch reactor: C/O=1.2, 1017.86 K
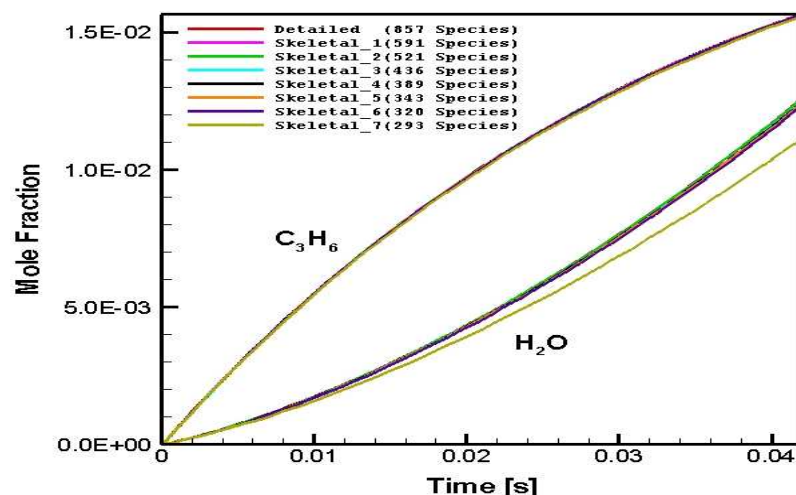
Figure 5.23 : Numerically predicted H_2O and C_3H_6 distribution in CPOX of i-octane as a function of time in the batch reactor: C/O=1.2, 1017.86 K
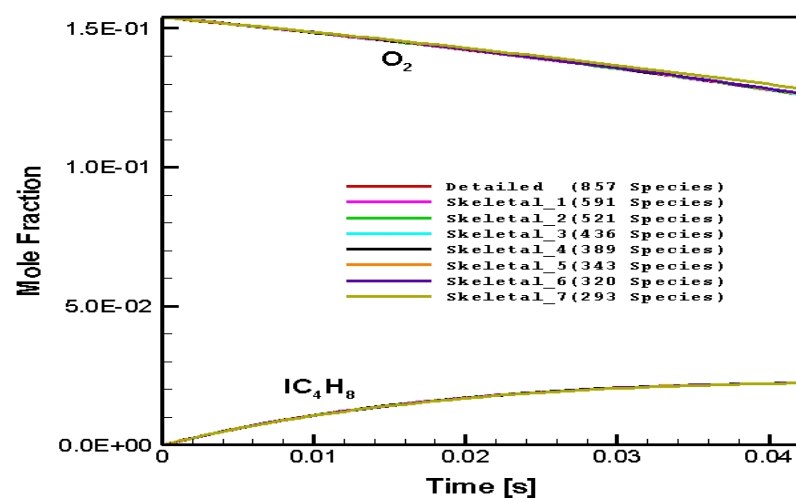
Figure 5.24 : Numerically predicted O_2 and IC_4H_8 distribution in CPOX of i-octane as a function of time in the batch reactor: C/O=1.2, 1017.86 K

71
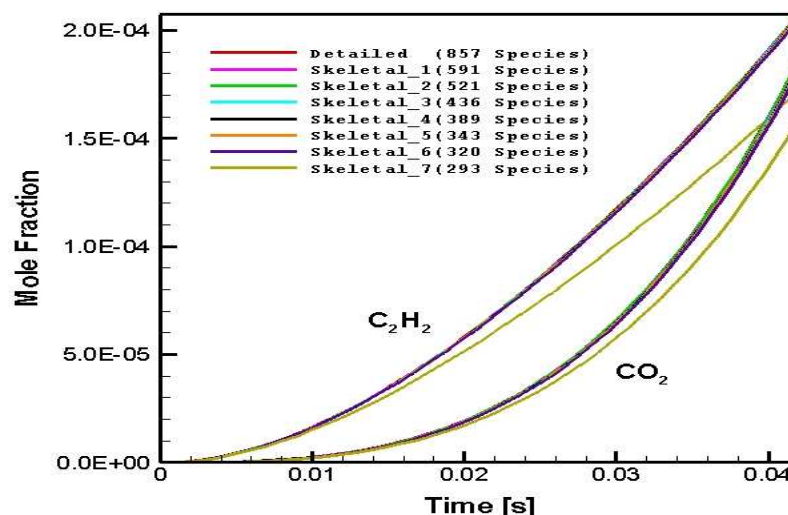
Figure 5.25 : Numerically predicted O_2 and IC_4H_8 distribution in CPOX of i-octane as a function of time in the batch reactor: C/O=1.2, 1017.86 K

As it is seen on the graphics, all skeletal mechanisms give similar mole fraction profiles for C/O=1.2 case. In order to examine the results in detail, error levels are calculated again. Error levels of skeletal mechanisms for C/O=1.2 can be seen in table 5.24 and table 5.25. The best skeletal mechanism is shown with a red color in the tables. In addition to the main products and by-products some of the main products, by-product and radical results (CH_3, OH, HCCO, CH_2CHO) are shown in the appendix section, as well. Error levels of all of them are shown in table 5.24 and table 5.25. And as it is seen from the graphs and error levels, the method gives consistent results for radicals, as well.

Table 5.24 : (a) Errors of the skeletal mechanisms for the predictions of important species distribution in the batch reactor for CPOX of i-octane: C/O=1.2, 1017.86 K

Mechanism	H_2 Error%	O_2 Error%	H_2O Error%	CO Error%	CO_2 Error%	CH_4 Error%	CH_2O Error%	C_2H_6 Error%
Skeletal_1	0.10	0.14	1.03	0.87	1.38	0.03	0.55	0.15
Skeletal_2	0.11	0.15	1.11	0.95	1.49	0.04	0.58	0.16
Skeletal_3	0.11	0.15	1.11	0.93	1.48	0.04	0.57	0.16
Skeletal_4	0.14	0.20	1.44	1.34	1.84	0.04	0.76	0.20
Skeletal_5	0.15	0.20	1.48	1.35	1.86	0.04	0.76	0.20
Skeletal_6	0.27	0.29	2.05	1.91	2.73	0.12	0.87	0.21
Skeletal_7	0.47	1.69	12.69	12.65	14.77	2.31	6.49	1.20

Table 5.25 : (b) Errors of the skeletal mechanisms for the predictions of important species distribution in the batch reactor for CPOX of i-octane: C/O=1.2, 1017.86 K

Mechanism	C_2H_4 Error%	C_2H_2 Error%	C_3H_6 Error%	IC_4H_8 Error%	IC_8H_{18} Error%	CH_3 Error%	OH Error%	HCCO Error%	CH_2CHO Error%
Detailed	0.00	0.00	0.00	0.00	0.00	0.00	0.00	0.00	0.00
Skeletal_1	0.27	0.49	0.00	0.02	0.36	0.01	0.02	0.01	0.00
Skeletal_2	0.36	0.56	0.02	0.02	0.40	0.03	0.00	0.19	0.00
Skeletal_3	0.36	0.55	0.02	0.02	0.40	0.03	0.80	0.89	0.78
Skeletal_4	0.44	0.72	0.06	0.02	0.52	0.05	0.86	0.92	0.81
Skeletal_5	0.44	0.75	0.06	0.02	0.53	0.02	1.30	1.34	1.18
Skeletal_6	0.53	1.19	0.76	0.04	0.79	0.08	1.84	2.17	1.70
Skeletal_7	4.07	17.01	0.38	0.29	4.51	3.10	13.31	16.33	12.68

The error levels of skeletal 1, skeletal 2, skeletal 3, skeletal 4, skeletal 5 and skeletal 6 are lower than 3%. Error levels of skeletal 7 mechanism increase sharply again for some species.

CPU times of detailed mechanism and all skeletal mechanisms are shown in table 5.26.

Table 5.26 : CPU times of CPOX of i-octane simulations in batch reactor: C/O=1.2, 1017.86 K

Mechanism	CPU Time
Detailed	2,39
Skeletal_1	1,3
Skeletal_2	1,16
Skeletal_3	1,03
Skeletal_4	0,56
Skeletal_5	0,52
Skeletal_6	0,49
Skeletal_7	0,43

Skeletal 6 mechanism is chosen again as the reduced mechanism. Because it gives consistent results without much loss of information and reduces the CPU times well. Remaining species versus error % graphs are plotted for some species again, and they can be seen below.
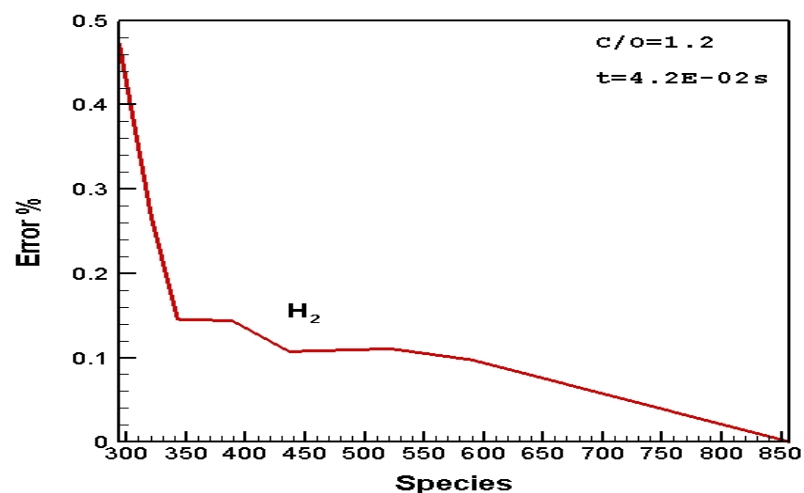
Figure 5.26 : Remaining Species – Error % of H_2 in CPOX of i-octane: C/O=1.2, 1017.86 K
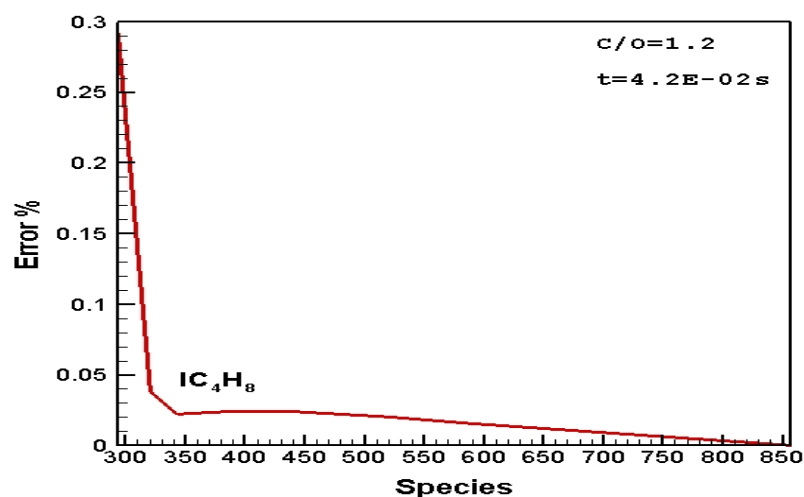
Figure 5.27 : Remaining Species – Error % of IC_4H_8 in CPOX of i-octane: C/O=1.2, 1017.86 K
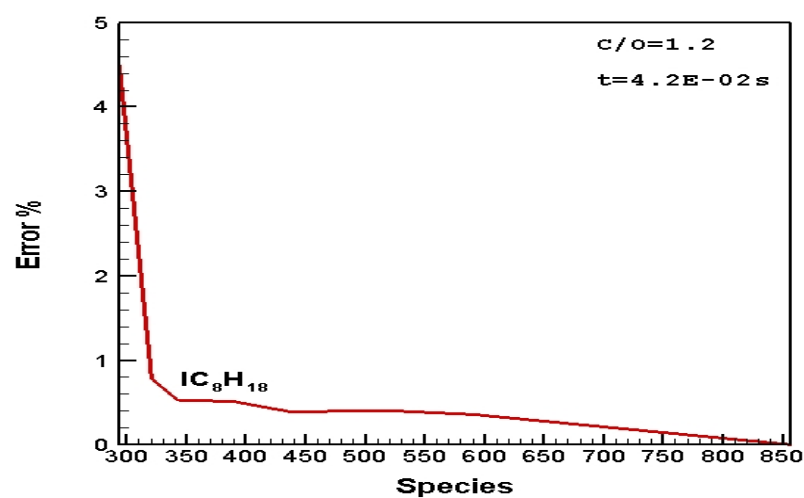
Figure 5.28 : Remaining Species –Error % of IC_4H_8 in CPOX of i-octane: C/O=1.2, 1017.86 K

The last simulation is performed for C/O=0.8 case for 4.2E-02 seconds. Simulation conditions of this case are shown in the table 5.27 and table 5.28.

Table 5.27 : Initial parameters of i-octane simulation for C/O=0.8 and 4.2E-02 s

Parameter	Value
Reactor Volume (m^3)	2.83 E-06
Diameter (m)	0.019
Radius (m)	9.50 E-03
Length (m)	1.00 E-02
Area (m^2)	2.83 E-04
Pressure (Pa)	101325
Reactor Temperature (K)	1374.85
C/O	0.8
Simulation Time (s)	4.2 E-02

Table 5.28 : Initial mole fractions of reactants for C/O=0.8

Species	Mole Fraction
IC_8H_{18}	3.33E-02
O_2	1.67E-01
N_2	8.00E-01

The remaining reaction and species numbers can be seen in table 5.29.

Table 5.29 : Remaining species numbers and reaction numbers for different skeletal mechanisms for CPOX of i-octane: C/O=0.8, 1374.85 K

Mechanism	Number of Remaining Species	Number of Reactions
Detailed	857	7191
Skeletal_1	608	5703
Skeletal_2	540	5121
Skeletal_3	441	4113
Skeletal_4	381	3665
Skeletal_5	332	3315
Skeletal_6	315	3127
Skeletal_7	270	2463

Predictions for the distribution of important species in the batch reactor of the detailed and skeletal mechanisms are shown in the following graphics.
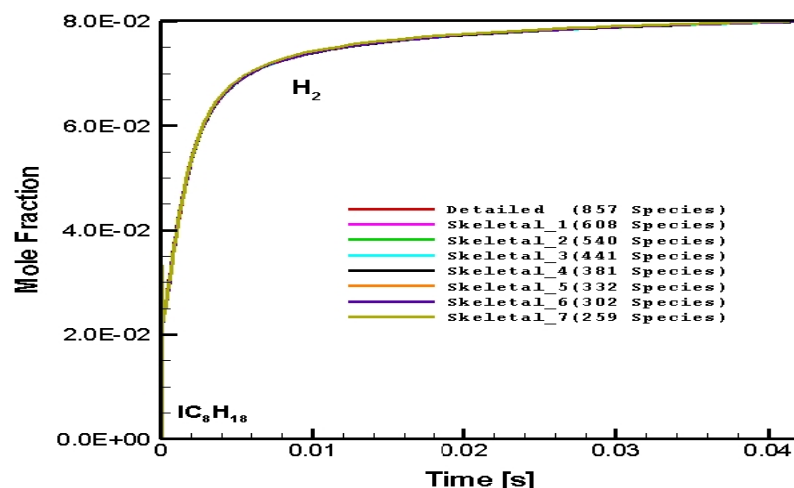
Figure 5.29 : Numerically of H_2 and IC_8H_{18} distribution in CPOX of i-octane as a function of time in the batch reactor: C/O=0.8, 1374.85 K
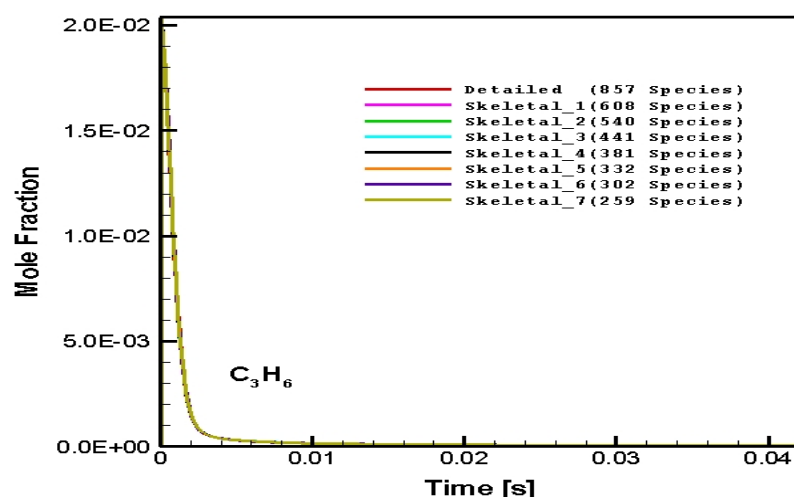
Figure 5.30 : Numerically predicted C_3H_6 distribution in CPOX of i-octane as a function of time in the batch reactor: C/O=0.8, 1374.85 K
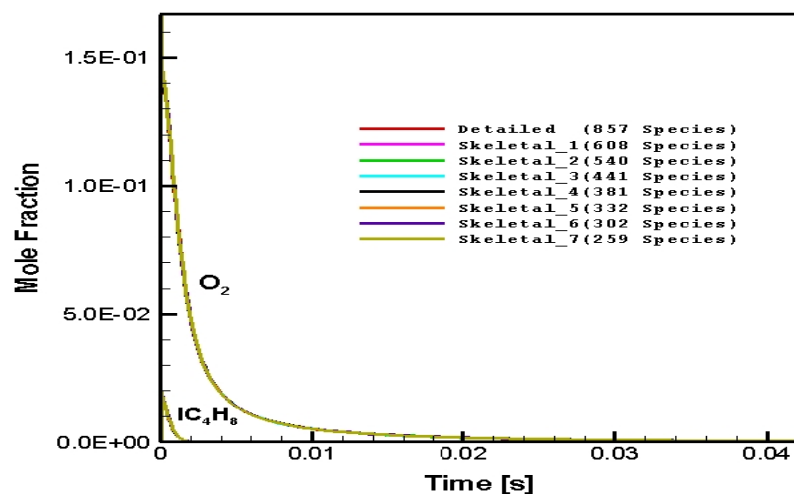
Figure 5.31 : Numerically predicted O2 and IC_4H_8 distribution in CPOX of i-octane as a function of time in the batch reactor: C/O=0.8, 1374.85 K
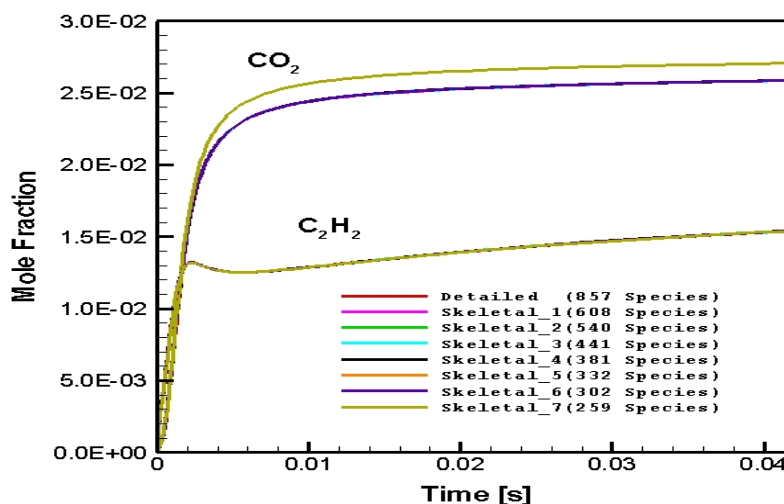
Figure 5.32 : Numerically predicted C_2H_2 and CO_2 distribution in CPOX of i-octane as a function of time in the batch reactor: C/O=0.8, 1374.85 K

As it is seen on the graphics, all skeletal mechanisms gives similar mole fraction profiles for C/O=0.8 case. Error levels of skeletal mechanisms for C/O=0.8 can be seen in table 5.30 and table 5.31. The best skeletal mechanism is shown with a red color in the tables. In addition to the above main products and by-products, some of the main products, by-products and radical results (CH_3, OH, HCCO, CH_2CHO) are shown in the appendix section, as well. As it is seen from the graphs and error levels the method gives consistent results for the lean conditions, as well.

Table 5.30 : (a) Errors of the skeletal mechanisms for the predictions of important species distribution in the batch reactor for CPOX of i-octane: C/O=0.8, 1374.85 K

Mechanism	H_2 Error%	O_2 Error%	H_2O Error%	CO Error%	CO_2 Error%	CH_4 Error%	CH_2O Error%	C_2H_6 Error%
Skeletal_1	0.00	0.03	0.01	0.00	0.00	0.04	0.00	0.01
Skeletal_2	0.00	0.05	0.01	0.00	0.01	0.05	0.00	0.04
Skeletal_3	0.00	0.05	0.01	0.00	0.01	0.05	0.00	0.04
Skeletal_4	0.00	0.05	0.01	0.00	0.01	0.05	0.00	0.03
Skeletal_5	0.01	0.05	0.01	0.00	0.01	0.04	0.00	0.02
Skeletal_6	0.01	0.05	0.01	0.00	0.01	0.04	0.00	0.02
Skeletal_7	0.00	0.04	0.01	0.00	0.01	0.04	0.00	0.02

Table 5.31 : (b) Errors of the skeletal mechanisms for the predictions of important species distribution in the batch reactor for CPOX of i-octane: C/O=0.8, 1374.85 K

Mechanism	C_2H_4 Error%	C_2H_2 Error%	C_3H_6 Error%	IC_4H_8 Error%	CH_3 Error%	OH Error%	HCCO Error%	CH_2CHO Error%
Skeletal_1	0.04	0.49	0.03	13.24	0.00	0.00	0.00	0.00
Skeletal_2	0.05	0.56	0.04	13.22	0.02	0.05	0.11	0.08

Table 5.31 : (Continued) (b) Errors of the skeletal mechanisms for the predictions of important species distribution in the batch reactor for CPOX of i-octane: C/O=0.8, 1374.85 K

Mechanism	C_2H_4 Error%	C_2H_2 Error%	C_3H_6 Error%	IC_4H_8 Error%	CH_3 Error%	OH Error%	HCCO Error%	CH_2CHO Error%
Skeletal_3	0.05	0.55	0.04	13.24	0.01	0.05	0.10	0.07
Skeletal_4	0.05	0.72	0.04	13.24	0.00	0.05	0.08	0.05
Skeletal_5	0.04	0.75	0.03	13.67	0.01	0.05	0.09	0.06
Skeletal_6	0.04	1.07	0.03	13.67	0.01	0.05	0.09	0.07
Skeletal_7	0.04	10.14	0.04	13.67	0.41	1.56	6.85	4.60

The error levels of skeletal 1, skeletal 2, skeletal 3, skeletal 4, skeletal 5 and skeletal 6 are lower than 1% except IC_4H_8 species. The error level of IC_4H_8 is at about 13% for all skeletal mechanisms. The error level of IC_8H_{18} cannot be defined because at this time (4.2E-02) the mole fraction of IC_8H_{18} goes to zero, in other words, full conversion of i-octane is reached. The error levels of skeletal 7 mechanism increase sharply again for some species (C_2H_2). Finally, CPU times of detailed mechanism and all skeletal mechanisms are shown in table 5.33.

Table 5.32 : CPU times of CPOX of i-octane simulations in batch reactor: C/O=0.8, 1374.85 K

Mechanism	CPU Time
Detailed	29,30
Skeletal_1	21,06
Skeletal_2	19,23
Skeletal_3	16,01
Skeletal_4	14,05
Skeletal_5	2,28
Skeletal_6	2,18
Skeletal_7	1,54

Skeletal 6 is chosen again as the reduced mechanism for C/O=0.8 for 4.2E-02 seconds. Because it gives consistent results without much loss of information and reduces the CPU times well. Remaining species versus error % graphs are plotted for some species again, and they can be seen below.
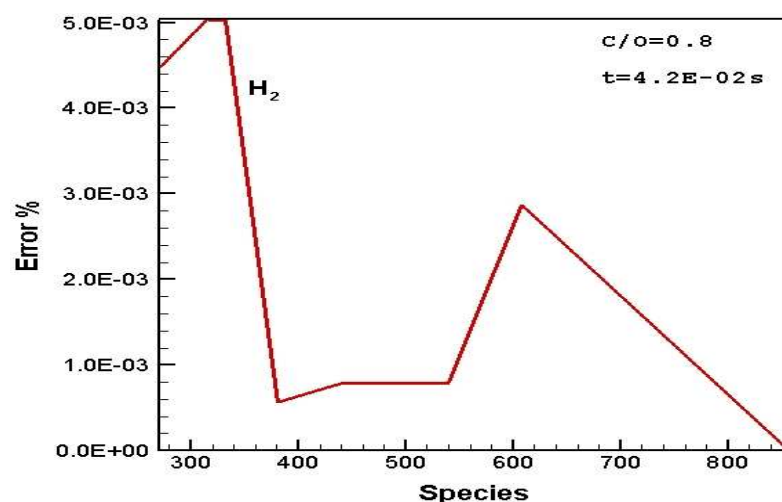
Figure 5.33 : Remaining Species – Error % of H_2 in CPOX of i-octane: C/O=0.8, 1374.85 K
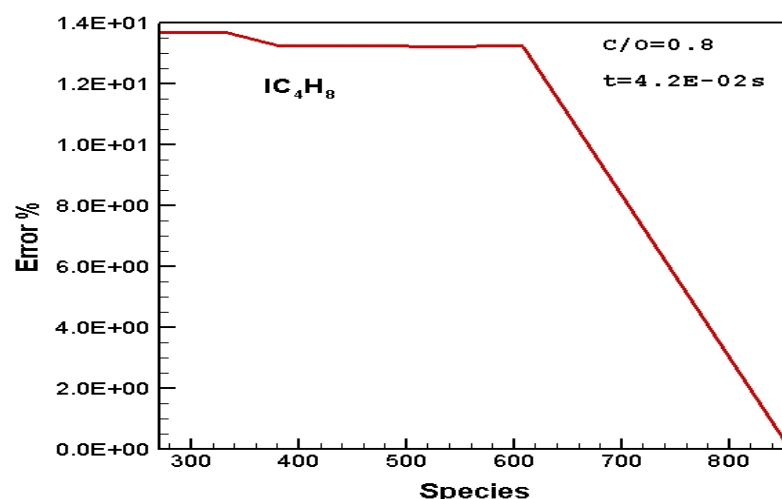
Figure 5.34 : Remaining Species – Error % of IC_4H_8 in CPOX of i-octane: C/O=0.8, 1374.85 K

It is seen for 4.2E-02 seconds that newly improved reduction method based on necessity analysis gives consistent results up to 63-64 % species and 63-64 % reactions deleting for all observed working conditions including rich and lean conditions. But, in order to validate the method well, next simulation time is chosen as 1.0 second. In such a long time, in comparison to previous simulation time, inconsistent results can deviate much from the detailed mechanism. Next simulation time is chosen as 1.0 seconds from this point of view. Graphs, error levels and CPU times of C/O=1.6 simulation will be shown, respectively.

The parameters and initial mole fractions used for C/O=1.6 for 1.0 seconds simulation are shown in table 5.33 and table 5.34.

Table 5.33 : Initial parameters of i-octane simulation for C/O=1.6 and 1.0 second

Parameter	Value
Reactor Volume (m^3)	2.83 E-06
Diameter (m)	0.019
Radius (m)	9.50 E-03
Length (m)	1.00 E-02
Area (m^2)	2.83 E-04
Pressure (Pa)	101325
Reactor Temperature (K)	1005.78
C/O	1.6
Simulation Time (s)	1.0

Table 5.34 : Initial mole fractions of reactants for C/O=1.6

Species	Mole Fraction
IC_8H_{18}	5.71E-02
O_2	1.43E-01
N_2	8.00E-01

The remaining reaction and species numbers can be seen in table 5.35.

Table 5.35 : Remaining species numbers and reaction numbers for different skeletal mechanisms for CPOX of i-octane: C/O=1.6, 1005.78 K, t=1.0 s

Mechanism	Number of RemainingSpecies	Number of Reactions
Detailed	857	7191
Skeletal_1	653	5945
Skeletal_2	573	5377
Skeletal_3	483	4535
Skeletal_4	439	4163
Skeletal_5	337	3183
Skeletal_6	314	2989
Skeletal_7	286	2629

Predictions for the distribution of important species in the batch reactor of the detailed and skeletal mechanisms are shown in the following graphics.
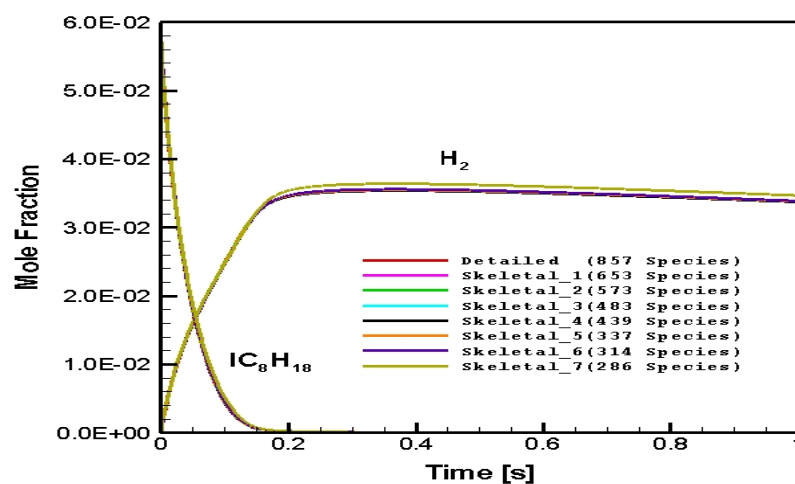
Figure 5.35 : Numerically predicted H_2 and IC_8H_{18} distribution in CPOX of i-octane as a function of time in the batch reactor: C/O=1.6, 1005.78 K, t=1.0s
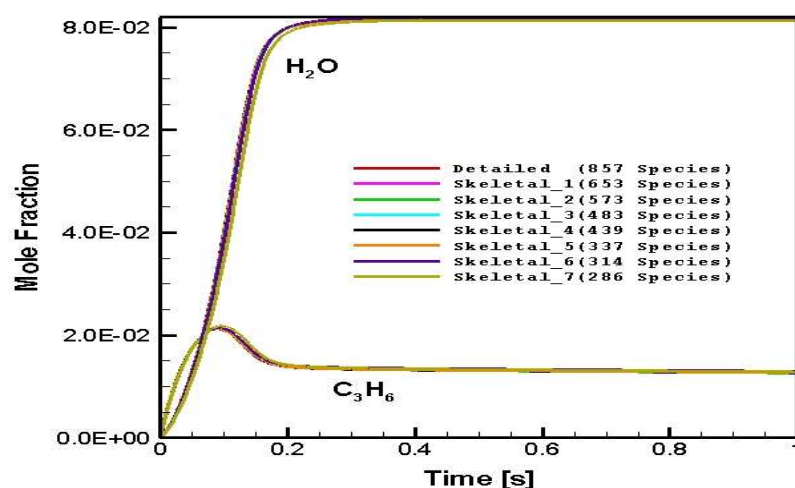
Figure 5.36 : Numerically predicted H_2O and C_3H_6 distribution in CPOX of i-octane as a function of time in the batch reactor: C/O=1.6, 1005.78 K, t=1.0s
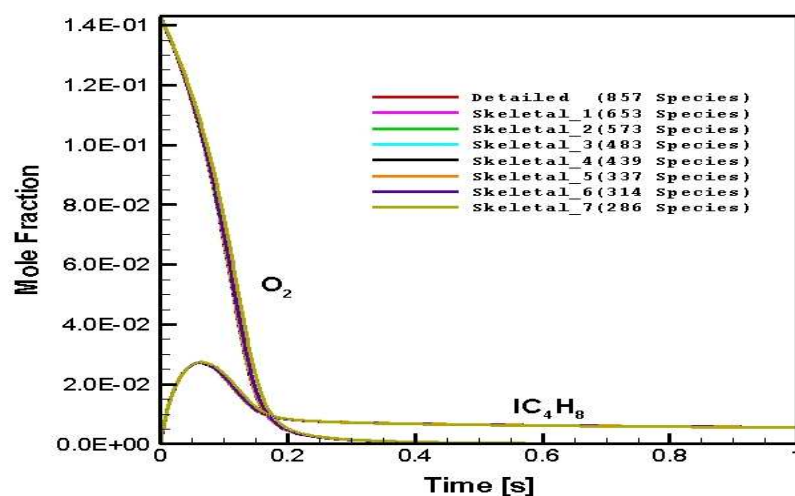
Figure 5.37 : Numerically predicted O2 and IC_4H_8 distribution in CPOX of i-octane as a function of time in the batch reactor: C/O=1.6, 1005.78 K, t=1.0s
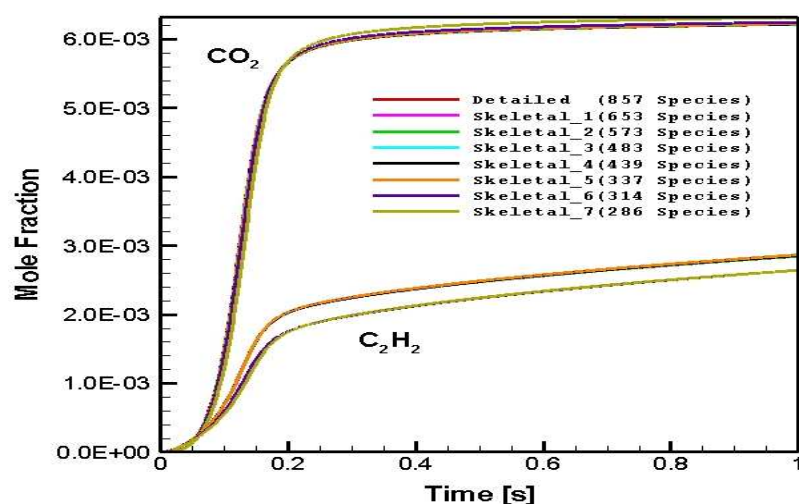
Figure 5.38 : Numerically predicted C_2H_2 and CO_2 distribution in CPOX of i-octane as a function of time in the batch reactor: C/O=1.6, 1005.78 K, t=1.0s

As it is seen on the graphics, all skeletal mechanisms gives similar mole fraction profiles for C/O=1.6 and 1.0s of simulation time case. In addition to above main products and by-products, some of the main products, by-products radical results (CH_3, OH, HCCO, CH_2CHO) are shown in the appendix section, as well. Error levels of species related to skeletal mechanisms can be seen in table 5.36 and table 5.37. The best skeletal mechanism is shown with a red color in the tables.

Table 5.36 : (a) Errors of the skeletal mechanisms for the predictions of important species distribution in the batch reactor for CPOX of i-octane: C/O=1.6, 1005.78 K, t=1.0s

Mechanism	H_2 Error%	O_2 Error%	H_2O Error%	CO Error%	CO_2 Error%	CH_4 Error%	CH_2O Error%	C_2H_6 Error%
Skeletal_1	0.03	0.06	0.01	0.00	0.02	0.00	0.01	0.01
Skeletal_2	0.03	0.06	0.01	0.00	0.02	0.00	0.01	0.02
Skeletal_3	0.13	5.86	0.13	0.08	0.15	0.22	1.24	0.17
Skeletal_4	0.14	5.63	0.13	0.09	0.07	0.23	1.15	0.16
Skeletal_5	0.18	6.97	0.18	0.10	0.14	0.16	3.00	0.00
Skeletal_6	0.31	14.1	0.10	0.22	0.48	0.27	6.87	1.26
Skeletal_7	2.67	0.71	0.57	0.68	1.61	0.00	3.32	2.01

Table 5.37 : (b) Errors of the skeletal mechanisms for the predictions of important species distribution in the batch reactor for CPOX of i-octane: C/O=1.6, 1005.78 K, t=1.0s

Mechanism	C2H4 Error%	C2H2 Error%	C3H6 Error%	IC4H8 Error%	IC8H18 Error%	CH3 Error%	OH Error%	HCCO Error%	CH2CHO Error%
Skeletal_1	0.02	0.02	0.01	0.02	0.06	0.03	0.01	0.06	0.03
Skeletal_2									

Table 5.37 : (Continued) (b) Errors of the skeletal mechanisms for the predictions of important species distribution in the batch reactor for CPOX of i-octane: C/O=1.6, 1005.78 K, t=1.0s

Mechanism	C2H4 Error%	C2H2 Error%	C3H6 Error%	IC4H8 Error%	IC8H18 Error%	CH3 Error%	OH Error%	HCCO Error%	CH2CHO Error%
Skeletal_3	0.15	0.37	0.18	0.92	0.61	1.64	0.05	4.26	2.92
Skeletal_4	0.15	0.35	0.20	0.93	0.57	1.59	0.02	4.16	2.85
Skeletal_5	0.29	0.76	0.44	0.86	1.05	1.71	0.43	4.53	3.24
Skeletal_6	1.98	7.08	2.48	0.22	2.28	0.93	0.53	1.21	0.19
Skeletal_7	3.23	7.11	1.62	1.17	8.60	1.62	0.57	3.65	0.60

Error levels of skeletal mechanisms from skeletal 1 to skeletal 5 are lower than 7%. Skeletal 6 gives unacceptable errors for O_2. Skeletal 7 gives less error than skeletal 6 for O_2, but it gives more errors for other species than other skeletal mechanisms.

Finally, CPU times of detailed mechanism and all skeletal mechanisms are shown in table 5.38.

Table 5.38 : CPU times of CPOX of i-octane simulations in Batch reactor: C/O=1.6, 1005.78 K, t=1.0 s

Mechanism	CPU Time
Detailed	20,23
Skeletal_1	12,59
Skeletal_2	10,45
Skeletal_3	8,27
Skeletal_4	7,1
Skeletal_5	5,38
Skeletal_6	4,55
Skeletal_7	4,25

Skeletal 6 is chosen as the reduced mechanism. Because it gives consistent results without much loss of information and reduces the CPU times well.

Remaining species versus error % graphs are plotted again, and they can be seen in the below table. Because of the limited number of graphs in order, the other graphs are shown in the appendix again.
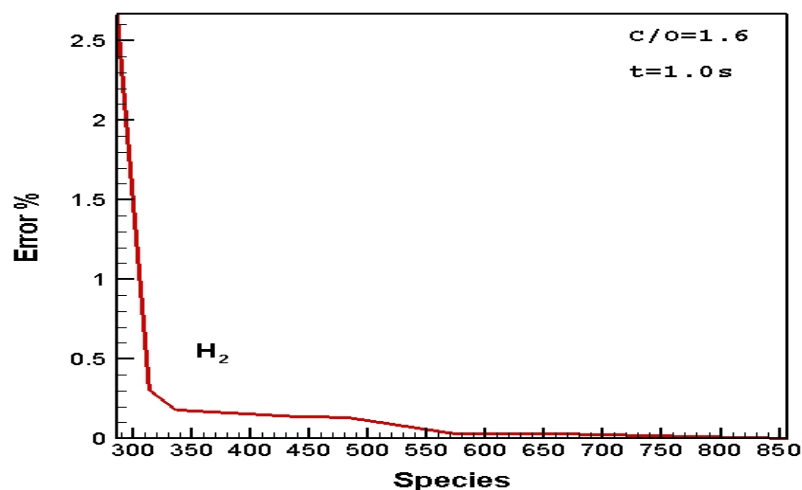
Figure 5.39 : Remaining Species – Error % of H_2 in CPOX of i-octane: C/O=1.6, 1005.78 K, t=1.0s
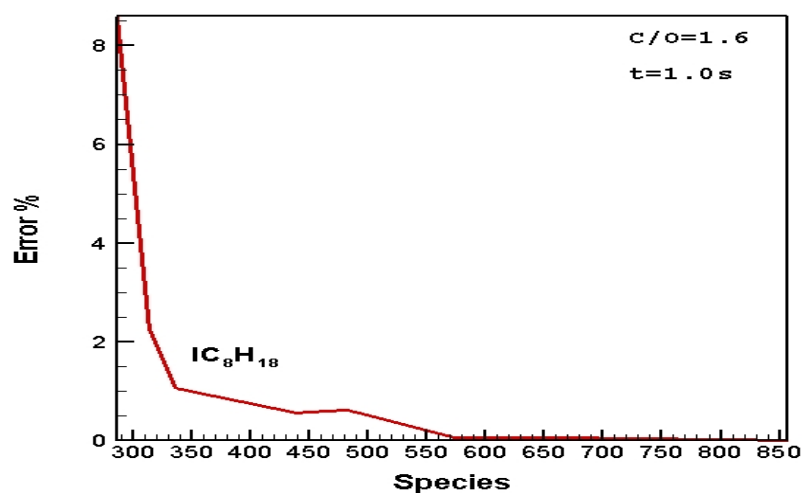
Figure 5.40 : Remaining Species – Error % of IC_8H_{18} in CPOX of i-octane: C/O=1.6, 1005.78 K, t=1.0s
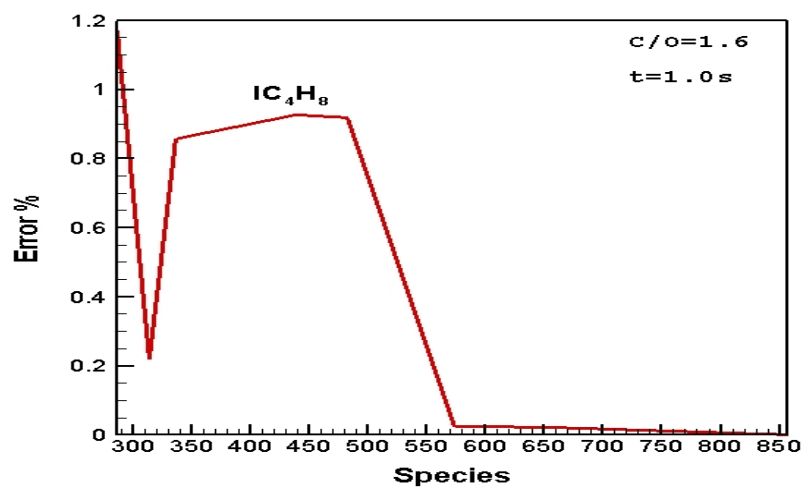
Figure 5.41 : Remaining Species – Error % of IC_4H_8 in CPOX of i-octane: C/O=1.6, 1005.78 K, t=1.0s

In a conclusion of i-octane results for different C/O ratios, full conversion of i-octane is obtained in fuel lean mixtures which results in increasing H_2O and CO_2 selectivity. It is the result of full conversion of i-octane (IC_8H_{18}).

The amount of oxygen is too little for full conversion at fuel rich conditions. 56 % conversion of i-octane is obtained at C/O=2.0 condition.

Methane dominates by-products at fuel lean conditions that is followed by acetylene (C_2H_2) and ethylene (C_2H_4). Propylene (C_3H_6) and iso-butylene (IC_4H_8) does not play significant role at this condition (they are produced in the beginning of the CPOX process, but further consumed again through the following reactions).

Iso-butylene and propylene selectivities increases under fuel rich conditions. Methane has also high selectivity under fuel rich conditions. In contrast, acetylene and ethylene selectivities decreases with the increasing C/O ratios. Their selectivities are high under fuel lean conditions.

Finally, it is seen that the reduction method allows making the above investigations of CPOX of i-octane process consistent with the detailed mechanism results up to % 61-62 species and % 58-60 reactions deleting not only for small time scales but also for long time scales such as 1.0 seconds.

5.4.3 Comparison of The Batch Simulations of Necessity Analysis Method And Necessity Analysis With Simultaneously Combined Sensitivity And Reaction Flow Analysis Through Each Reaction Method

In this chapter the differences of necessity analysis method and necessity analysis with simultaneously combined reaction flow and sensitivity analysis through each reaction method for the prediction of the important species distribution in the batch reactor for CPOX of iso-octane is introduced. Important species distribution comparisons of these two method will be performed for two different conditions respectively; one is for C/O=1.6 case and the other is for C/O=1.2 case. Reactant, main product and by-product distribution predictions will be considered during the comparison. Necessity analysis with simultaneously combined sensitivity and reaction flow analysis through each reaction method is declared as the improved method in the graphs and at graph explanations. Most of the comparison graphs are shown in the appendix section because of the space limitation.
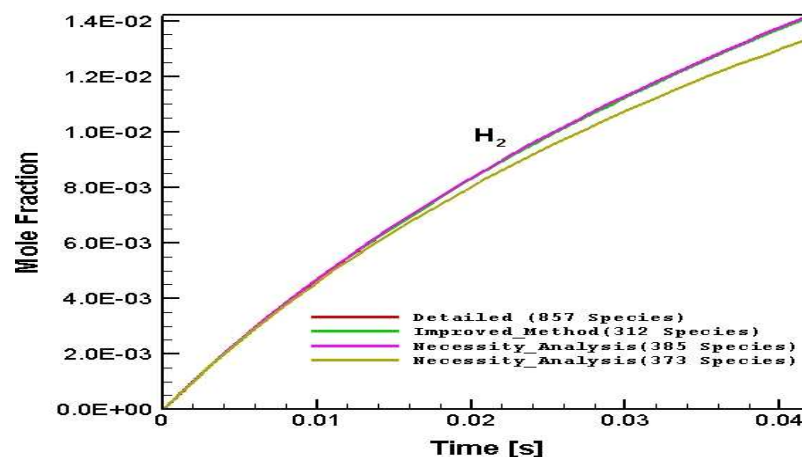
Figure 5.42 : Comparison of the necessity analysis method and improved method for numerically predicted H_2 distribution in CPOX of i-octane as a function of time in the batch reactor: C/O=1.6, 1005.78 K
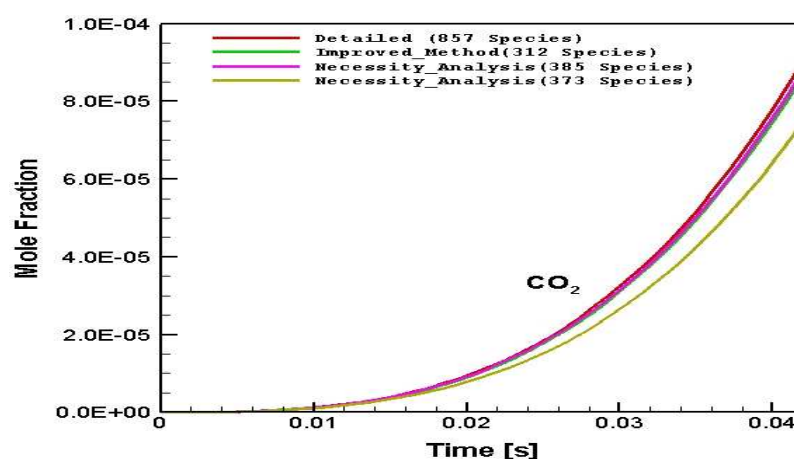
Figure 5.43 : Comparison of the necessity analysis method and improved method for numerically predicted CO_2 distribution in CPOX of i-octane as a function of time in the batch reactor: C/O=1.6, 1005.78
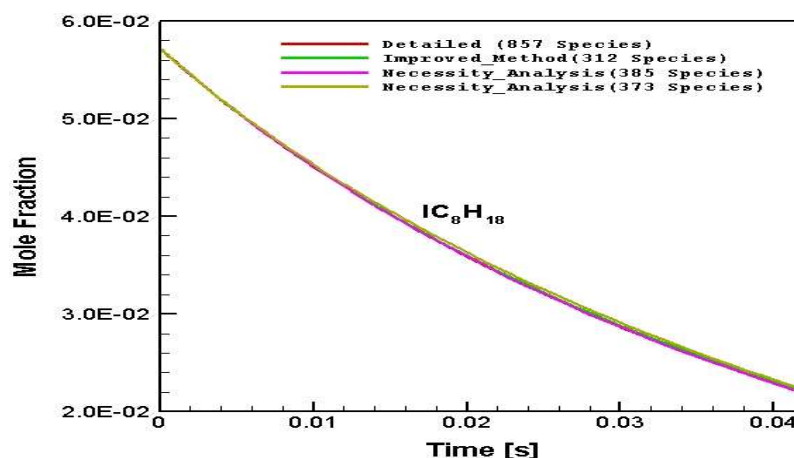
Figure 5.44 : Comparison of the necessity analysis method and improved method for numerically predicted IC_8H_{18} distribution in CPOX of i-octane as a function of time in the batch reactor: C/O=1.6, 1005.78
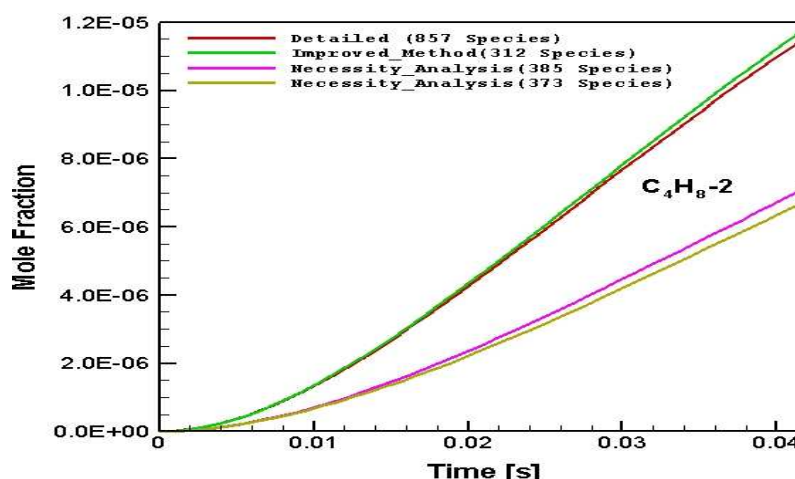
**Figure 5.45 :** Comparison of the necessity analysis method and improved method for numerically predicted C_4H_8-2 distribution in CPOX of i-octane as a function of time in the batch reactor: C/O=1.6, 1005.78

Necessity analysis method results with 385 species gives similar prediction results with the detailed mechanism except C_4H_8-2 by-product result for C/O=1.6 case. However necessity analysis method results with 373 species gives unsatisfactory distribution prediction results especially for by-products such as C_4H_8-2,C_4H_8-1 ,C_3H_8 and for some radicals such as HCCO. Improved method results with 312 species (necessity analysis with simultaneously combined sensitivity and reaction flow analysis through each reaction method) which was selected as the reduced mechanism for C/O=1.6 case gives similar results with the detailed mechanism for all considered species results. It must also be pointed out that both methods predict mole fraction profiles correctly for all cases.

Next comparison is considered for C/O=1.2 case.
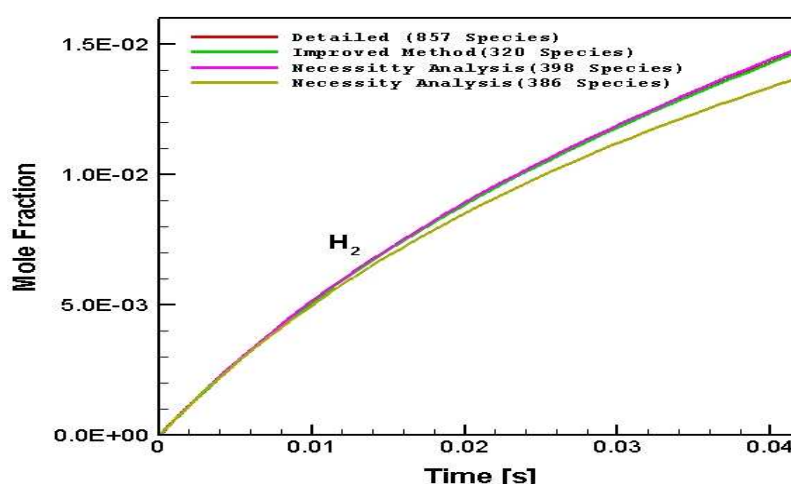
Figure 5.46 : Comparison of the necessity analysis method and improved method for numerically predicted H_2 distribution in CPOX of i-octane as a function of time in the batch reactor: C/O=1.2, 1017.86
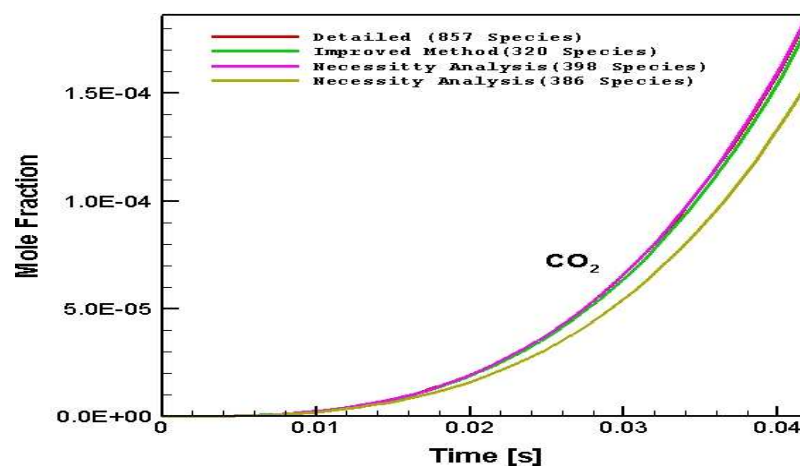
Figure 5.47 : Comparison of the necessity analysis method and improved method for numerically predicted CO_2 distribution in CPOX of i-octane as a function of time in the batch reactor: C/O=1.2, 1017.86)
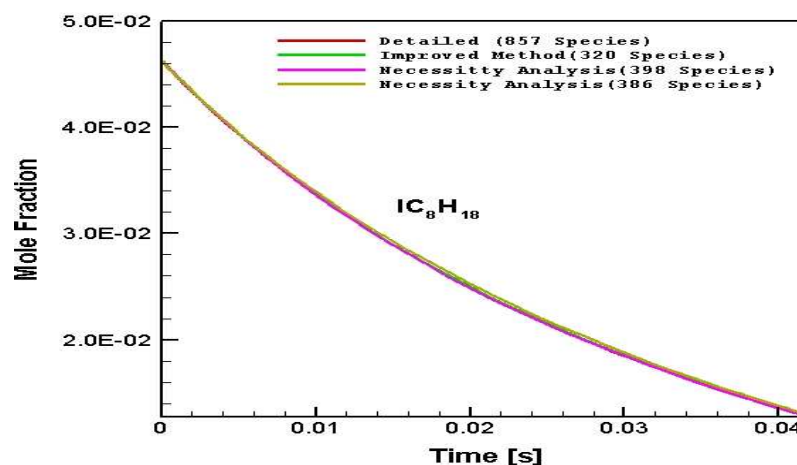
Figure 5.48 : Comparison of the necessity analysis method and improved method for numerically predicted IC_8H_{18} distribution in CPOX of i-octane as a function of time in the batch reactor: C/O=1.2, 1017.86)
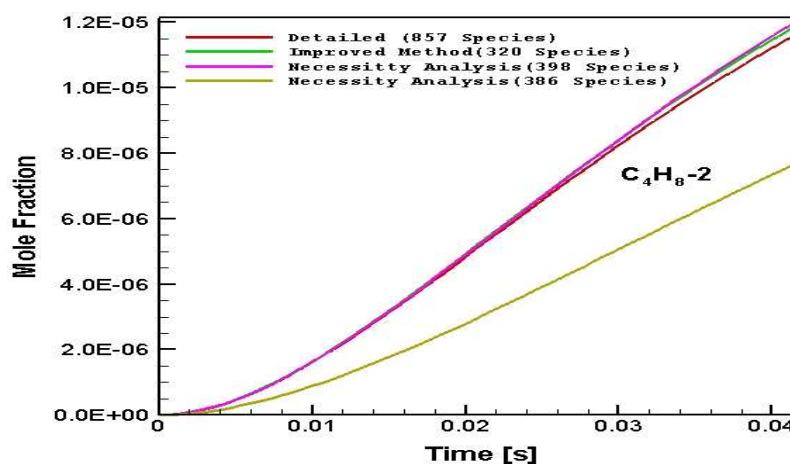
Figure 5.49 : Comparison of the necessity analysis method and improved method for numerically predicted C_4H_8-2 distribution in CPOX of i-octane as a function of time in the batch reactor: C/O=1.2, 1017.86)

Necessity analysis method results with 398 species gives similar results with the detailed mechanism except C_4H_8-2 by-product result for C/O=1.2 case. However necessity analysis method results with 386 species gives unsatisfactory distribution prediction results especially for by-products such as C_4H_8-2,C_4H_8-1 ,C_3H_8 and for some radicals such as HCCO. Improved method results with 320 species (necessity analysis with simultaneously combined sensitivity and reaction flow analysis through each reaction method) which was selected as the reduced mechanism for C/O=1.2 case gives similar results with the detailed mechanism for all considered species results. It must also be pointed out that both methods predict the mole fraction profiles correctly for all cases.

After these comparisons, it is seen that necessity analysis method allows deleting up to 56 % of the species from the detailed mechanism without loss of information for C/O=1.6 and 4.2E-02 s case, where the improved method which is called as necessity analysis with simultaneously combined sensitivity and reaction flow analysis through each reaction method allows deleting up to 64 % of the species for the same case. Necessity analysis method allows deleting up to 53 % of the species from the detailed mechanism without loss of information for C/O=1.2 and 4.2E-02 s case, where the improved method method allows deleting up to 63 % of the species for the same case. After these observations, it can be declared that necessity analysis with simultaneously combined sensitivity and reaction flow analysis through each reaction method allows deleting more species and more reactions than necessity analysis for the same conditions.

5.4.4 Results of The Plug Simulations With The Detailed LLNL Iso-Octane Mechanism

The next step of this study is to investigate the applicability of the reduced mechanisms for the noncatalytic study of gas composition after the reforming in plug flow simulations. To investigate the behavior of unconverted fuel in the fuel rich region downstream the catalyst, simulation of an exhaust gas composition, from CPOX reforming of i-octane, consisting of syngas, total oxidation products and two hydrocarbon species (table 5.41) with i-octane is used for different C/O ratios at the plug flow simulations. In more detail, thermal cracking of remaining IC_8H_{18} because of the high temperatures (at temperatures higher than 973 K) which leads to the

potential production of soot precursors and give raise to a starting deposition of carbon on the catalytic surface, and hydrogenation of ethylene (C_2H_4) into ethane (C_2H_6) which decreases the amount of hydrogen produced during CPOX process in the catalytic reactor is investigated in plug flow simulations. DETCHEM^{PLUG} is used for this purpose. To start making the simulations with PLUG code, different skeletal mechanisms and the reduced mechanism are selected from the BATCH code simulation results of C/O=1.6 for 4.2E-02 seconds. These selected skeletal mechanisms are skeletal 5 and skeletal 7 mechanisms. The main idea of choosing skeletal 5 is that it gives very small errors for large amount of species deleting, reduced mechanism is the optimal mechanism, and skeletal 7 will be investigated if it gives consistent results in plug simulations, because though skeletal 7 gives inconsistent results in batch code simulations, it may give consistent results in Plug simulations. It must also be pointed out that skeletal mechanism 6 is declared as "reduced mechanism" in graphs for the important species distribution prediction in the reactor.

Plug simulations are also performed for different conditions such as C/O=1.0, C/O=1.3, C/O=1.6 and C/O=2.0. The results are investigated at four different temperatures in an exact position of the channel, and through the channel for one exact temperature. The remaining species and reaction numbers of skeletal mechanisms that are used in plug simulations is shown in the below table,

Table 5.39 : Number of the species and reactions of the skeletal mechanisms and reduced mechanism used in plug simulations

Mechanism	Number of Remaining Species	Number of Reactions
Detailed	857	7191
Skeletal_5	338	3169
Reduced	312	2903
Skeletal_7	287	2723

5.4.4.1 Simulation Results of Species Distribution Predictions For One Exact Temperature Along The Channel

The first simulation is performed through the channel for one exact temperature. And these results will be shown for each case respectively.

The first simulation is performed for C/O=1.6 case. The parameters and mole fractions used in this simulation are shown in table 5.41 and table 5.42, respectively.

Table 5.40 : Initial parameters of i-octane simulations in plug code for C/O=1.6

Parameter	Value
Reactor Volume (m^3)	8.01 E-05
Radius (m)	1.00 E-02
Length (m)	2.55 E-01
Area (m^2)	3.14 E-04
Flow (m^3/s)	1.00E-04
Reactor Temperature (K)	1108
Initial flow speed (m/s)	3.18E-01
C/O	1.6
Simulation Time (s)	8.01E-01

Table 5.41 : Initial mole fractions of species for C/O=1.6

Species	Mole Fraction
IC_8H_{18}	7.682E-03
H_2	2.120E-01
CO_2	1.414E-02
H_2O	1.336E-02
CO	1.681E-01
C_2H_4	4.387E-04
N_2	5.843E-01

Predictions for the distribution of important species in the reactor of the detailed, skeletal and reduced mechanisms are shown in the following graphics. The error levels of plug simulations will not be shown for this case. They are going to be shown for one exact length in the channel for different temperatures.
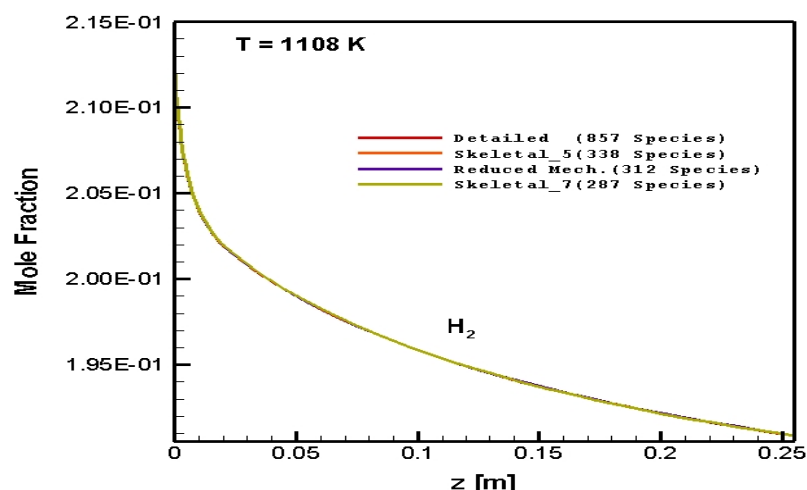
Figure 5.50 : Numerically predicted H_2 distribution as a function of axial position along the reactor: C/O=1.6, 1108 K
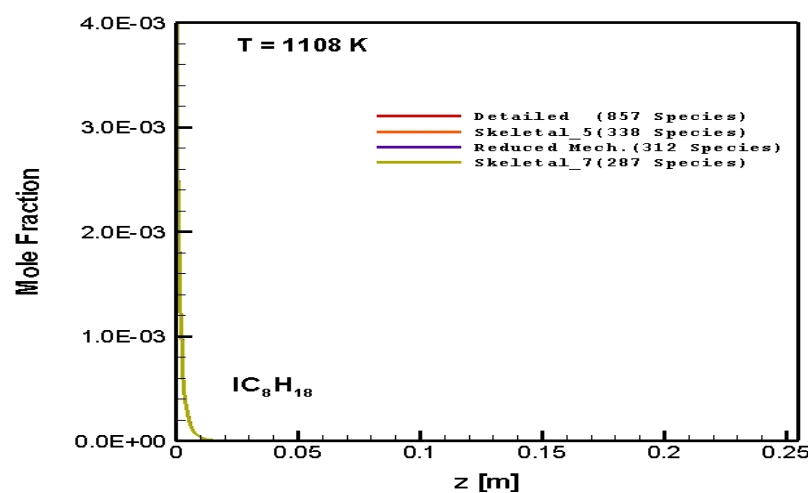
Figure 5.51 : Numerically predicted IC_8H_{18} distribution as a function of axial position along the reactor: C/O=1.6, 1108 K
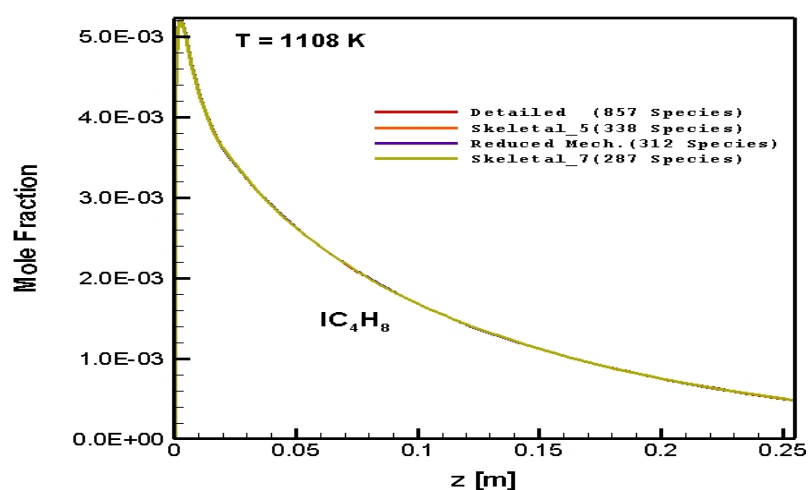
Figure 5.52 : Numerically predicted IC_4H_8 distribution as a function of axial position along the reactor: C/O=1.6, 1108 K

Figure 5.53 : Numerically predicted CH$_4$ distribution as a function of axial position along the reactor: C/O=1.6, 1108 K

Figure 5.54 : Numerically predicted C$_3$H$_6$ distribution as a function of axial position along the reactor: C/O=1.6, 1108 K

As it is seen in from the figures that i-octane is completely converted in the beginning of 0.01-0.05 m in the flow reactor while other hydrocarbon species like methane, ethylene, propylene and acetylene are produced within 0.05 m. Lengthwise the reactor, propylene is decreased again, consumed either via further thermal cracking and hydrogenation processes or the formation of aromatics or polyaromatics finally resulting in carbon deposition. Conversion of hydrogen reaches 10% at this high temperature and fuel rich condition whereas CO is slightly converted (1-2 %). Simulations of exhaust gases after catalyst for C/O=1.6 case prove that skeletal mechanisms and reduced mechanism give similar distribution prediction for each considered species. Skeletal 5 mechanism and reduced mechanism give consistent results again, as they give consistent results in gas phase (batch) simulations. Even

though skeletal 7 mechanism gives inconsistent results for some species in gas-phase (batch) simulations, it gives consistent results for plug calculations for C/O=1.6 case.

The next simulation of exhaust gases after catalyst is performed for C/O=2.0 case. The parameters and mole fractions used for this calculation is shown in table 5.43 and table 5.44.

Table 5.42 : Initial parameters of i-octane simulations in plug code for C/O=2.0

Parameter	Value
Reactor Volume (m^3)	8.01 E-05
Radius (m)	1.00 E-02
Length (m)	2.55 E-01
Area (m^2)	3.14 E-04
Flow (m^3/s)	1.00E-04
Reactor Temperature (K)	1103
Initial flow speed (m/s)	3.18E-01
C/O	2.0
Simulation Time (s)	8.01E-01

Table 5.43 : Initial mole fractions of reactants for C/O=2.0

Species	Mole Fraction
IC_8H_{18}	3.154E-03
H_2	1.947E-01
CO_2	1.909E-02
H_2O	2.126E-02
CO	1.652E-01
C_2H_4	2.354E-04
N_2	5.963E-01

Predictions for the distribution of important species in the reactor of the detailed, skeletal and reduced mechanisms are shown in the following graphics.
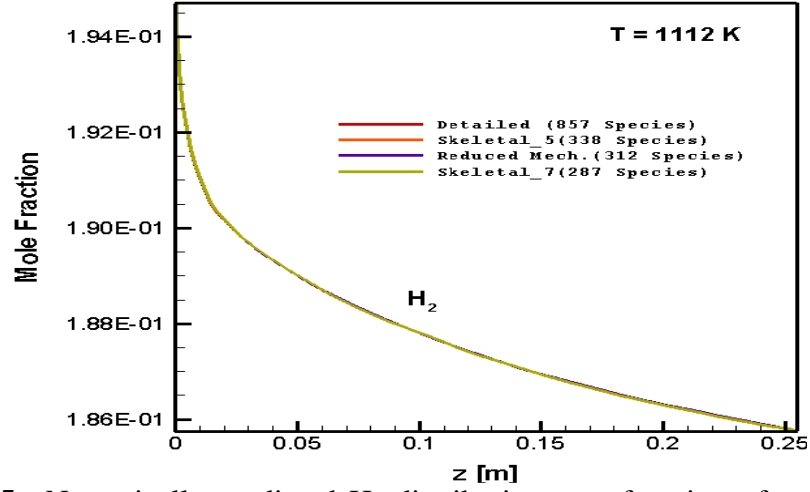
Figure 5.55 : Numerically predicted H_2 distribution as a function of axial position along the reactor: C/O=2.0, 1112 K
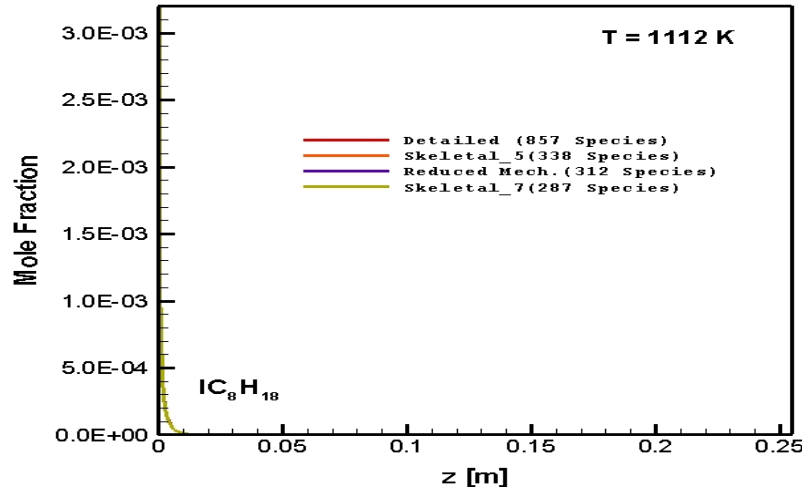
Figure 5.56 : Numerically predicted IC_8H_{18} distribution as a function of axial position along the reactor: C/O=2.0, 1112 K
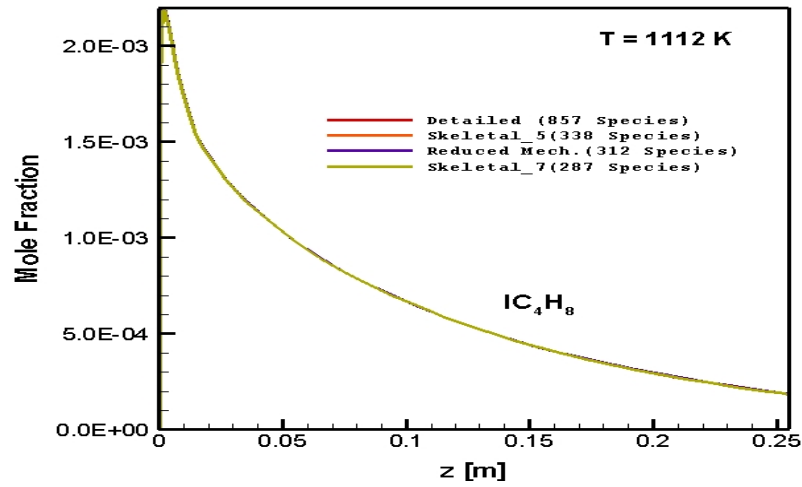
Figure 5.57 : Numerically predicted IC_4H_8 distribution as a function of axial position along the reactor: C/O=2.0, 1112 K

95
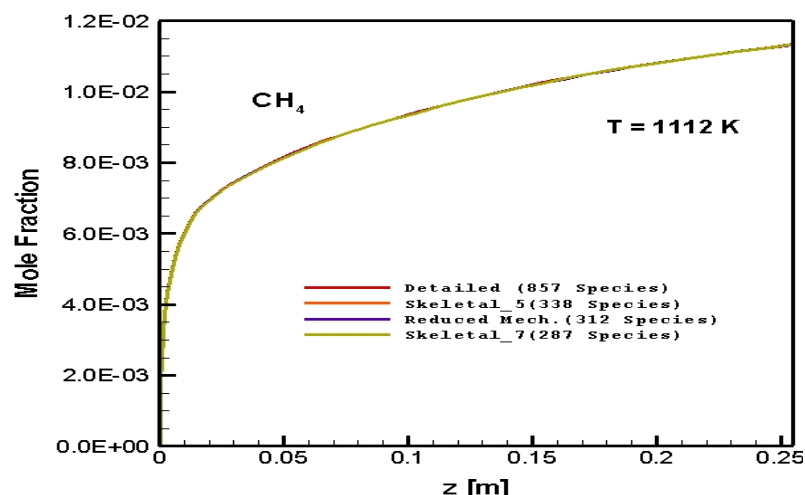
Figure 5.58 : Numerically predicted CH_4 distribution as a function of axial position along the reactor: C/O=2.0, 1112 K
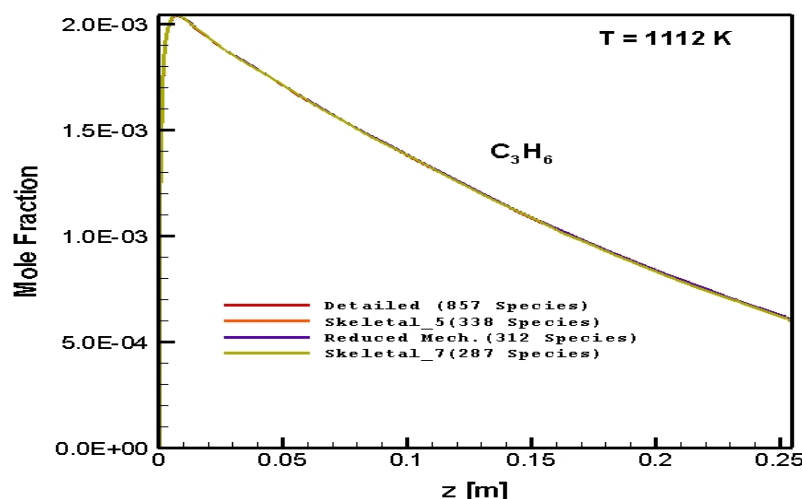
Figure 5.59 : Numerically predicted C_3H_6 distribution as a function of axial position along the reactor: C/O=2.0, 1112 K

As it is seen in the figures that i-octane is completely converted in the beginning of 0.01-0.05 m in the flow reactor again while other hydrocarbon species like methane, ethylene, propylene and acetylene are produced within 0.05 m. Lengthwise the reactor, propylene is decreased again, consumed either via further thermal cracking and hydrogenation processes or the formation of aromatics or polyaromatics finally resulting in carbon deposition. Conversion of hydrogen reaches 5% at this high temperature and fuel rich condition whereas CO is slightly converted (less than 1%). Simulations of exhaust gases after catalyst for C/O=2.0 case prove that skeletal mechanisms and reduced mechanism give similar distribution prediction for each considered species. Skeletal 5 mechanism and reduced mechanism give consistent results again, as they give consistent results in gas phase (batch) simulations. Even

though skeletal 7 mechanism gives inconsistent results for some species in gas-phase (batch) simulations, it gives consistent results for plug calculations C/O=2.0 case.

The next simulation of exhaust gases after catalyst is performed for C/O=1.3 case. The parameters and mole fractions used for this calculation is shown in table 5.46 and table 5.47.

Table 5.44 : Initial parameters of i-octane simulations in plug code for C/O=1.3

Parameter	Value
Reactor Volume (m^3)	8.01 E-05
Radius (m)	1.00 E-02
Length (m)	2.55 E-01
Area (m^2)	3.14 E-04
Flow (m^3/s)	1.00E-04
Reactor Temperature (K)	1107
Initial flow speed (m/s)	3.18E-01
C/O	1.3
Simulation Time (s)	8.01E-01

Table 5.45 : Initial mole fractions of reactants for C/O=1.3

Species	Mole Fraction
IC_8H_{18}	2.773E-03
H_2	2.294E-01
CO_2	1.175E-02
H_2O	8.749E-03
CO	1.821E-01
C_2H_4	4.852E-04
N_2	5.648E-01

Predictions for the distribution of important species in the reactor of the detailed, skeletal and reduced mechanisms are shown in the following graphics.
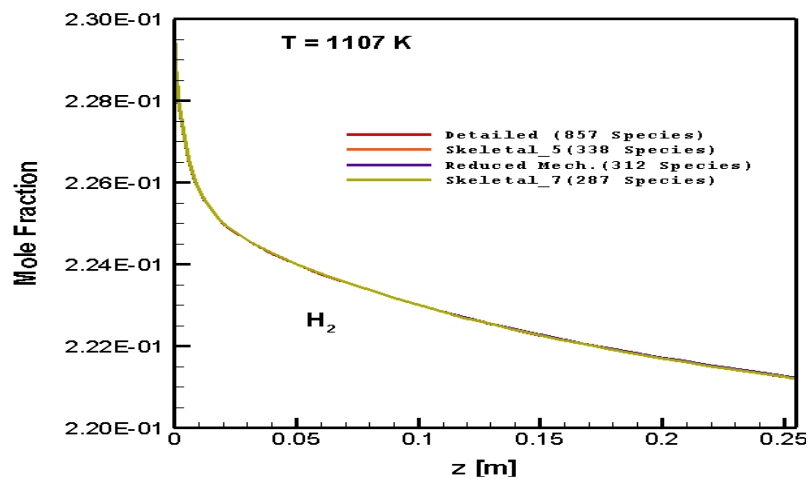
Figure 5.60 : Numerically predicted H_2 distribution as a function of axial position along the reactor: C/O=1.3, 1107 K
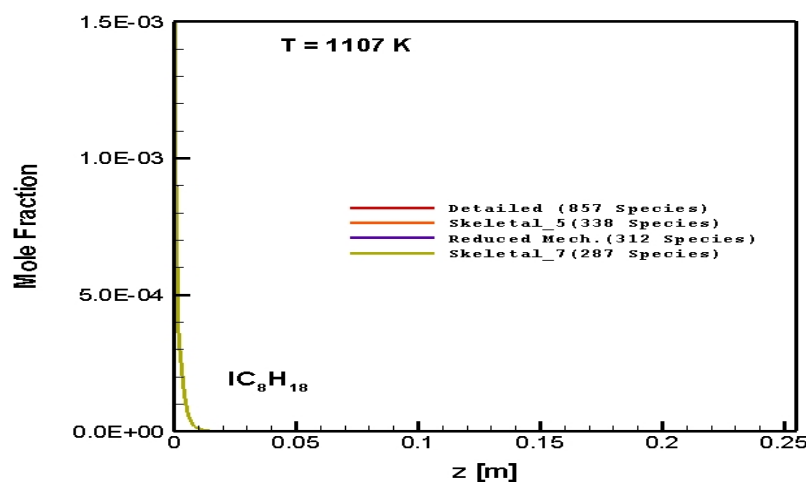
Figure 5.61 : Numerically predicted IC_8H_{18} distribution as a function of axial position along the reactor: C/O=1.3, 1107 K
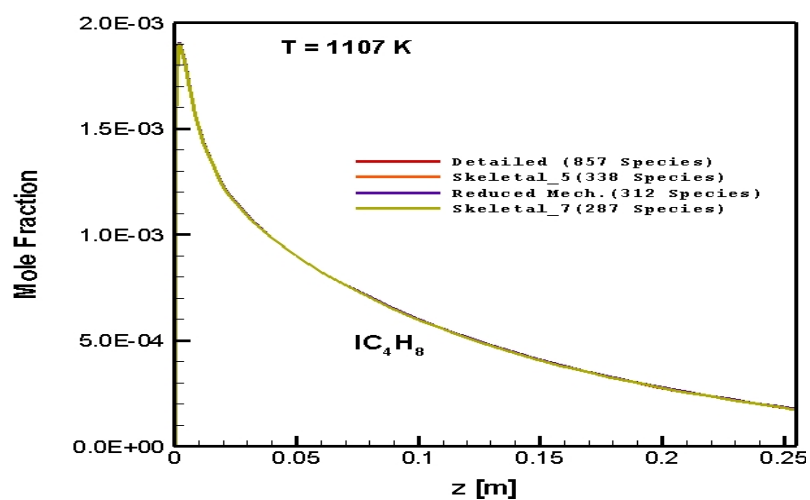
Figure 5.62 : Numerically predicted IC_4H_8 distribution as a function of axial position along the reactor: C/O=1.3, 1107 K
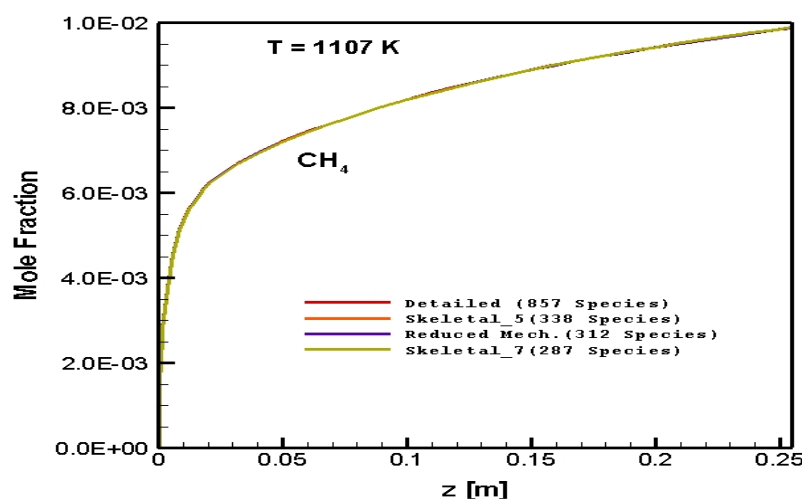
Figure 5.63 : Numerically predicted CH$_4$ distribution as a function of axial position along the reactor: C/O=1.3, 1107 K
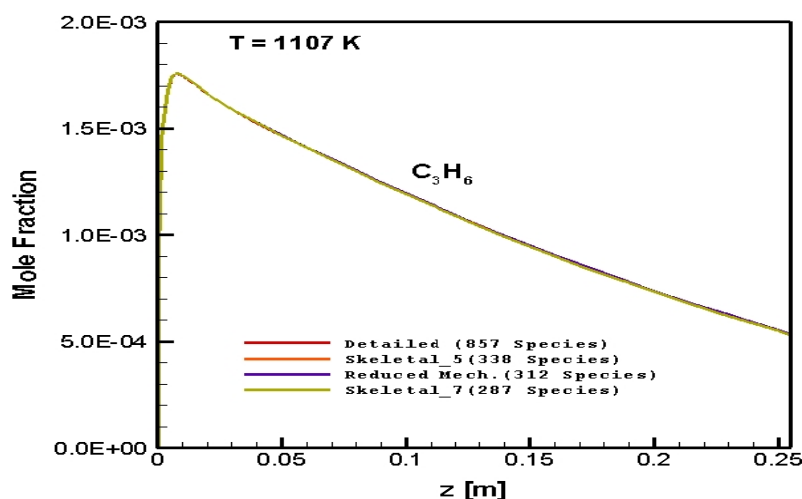
Figure 5.64 : Numerically predicted C$_3$H$_6$ distribution as a function of axial position along the reactor: C/O=1.3, 1107 K

As it is seen in the figures that i-octane is completely converted in the beginning of 0.01-0.05 m in the flow reactor while other hydrocarbon species like methane, ethylene, propylene and acetylene are produced within 0.05 m. Lengthwise the reactor, propylene is decreased again, consumed either via further thermal cracking and hydrogenation processes or the formation of aromatics or polyaromatics finally resulting in carbon deposition. Conversion of hydrogen reaches 4-5% at this high temperature and fuel rich condition whereas CO is slightly converted (less than 1 %). Simulations of exhaust gases after catalyst for C/O=1.3 case prove that skeletal mechanisms and reduced mechanism give similar distribution prediction for each considered species. Skeletal 5 mechanism and reduced mechanism give consistent

results again, as they give consistent results in gas phase (batch) simulations. Even though skeletal 7 mechanism gives inconsistent results for some species in gas-phase (batch) simulations, it gives consistent results for plug calculations C/O=1.3 case.

The last simulation for one exact temperature through the channel is performed for C/O=1.0 case. The parameters and mole fractions used for this calculation is given in table 5.48 and table 5.49.

Table 5.46 : parameters of i-octane simulations in plug code for C/O=1.0

Parameter	Value
Reactor Volume (m^3)	8.01 E-05
Radius (m)	1.00 E-02
Length (m)	2.55 E-01
Area (m^2)	3.14 E-04
Flow (m^3/s)	1.00E-04
Reactor Temperature (K)	1112
Initial flow speed (m/s)	3.18E-01
C/O	1.0
Simulation Time (s)	8.01E-01

Table 5.47 : Initial mole fractions of reactants for C/O=1.0

Species	Mole Fraction
IC_8H_{18}	6.255E-05
H_2	2.316E-01
CO_2	1.100E-02
H_2O	1.471E-02
CO	2.014E-01
C_2H_4	1.679E-05
N_2	5.412E-01

Predictions for the distribution of important species in the reactor of the detailed, skeletal and reduced mechanisms are shown in the following graphics.
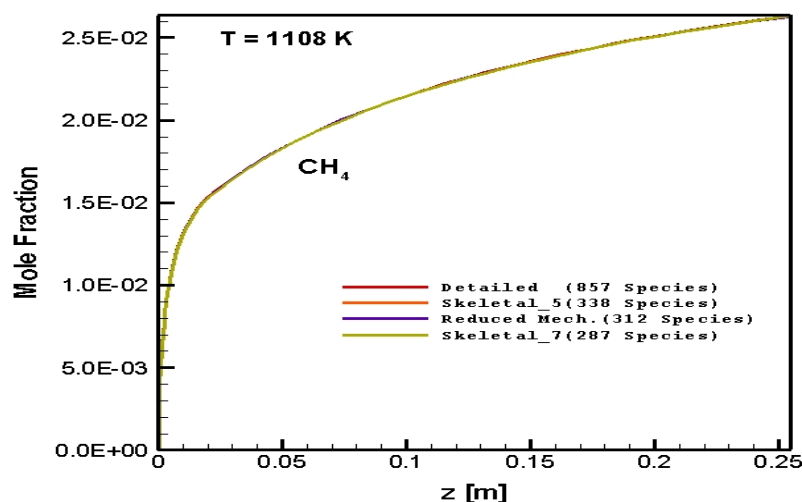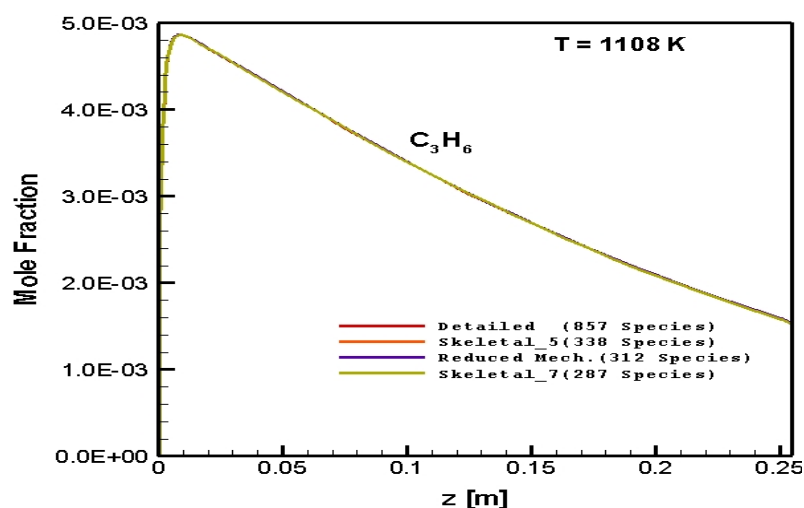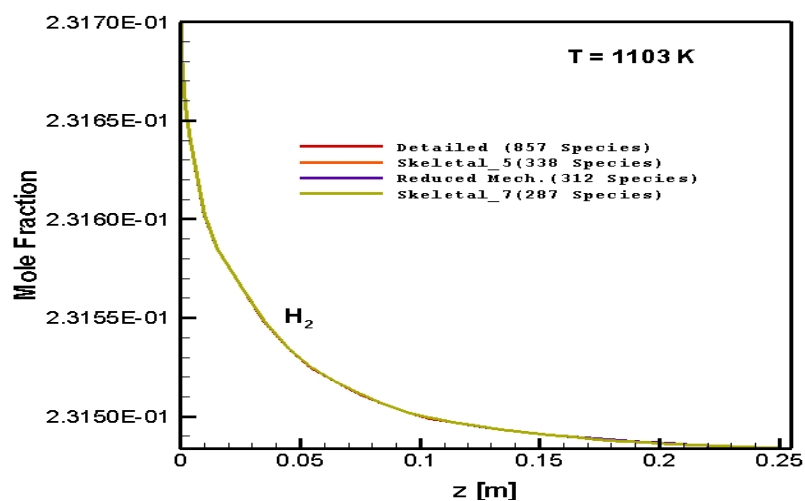
Figure 5.65 : Numerically predicted H_2 distribution as a function of axial position along the reactor: C/O=1.0, 1103 K
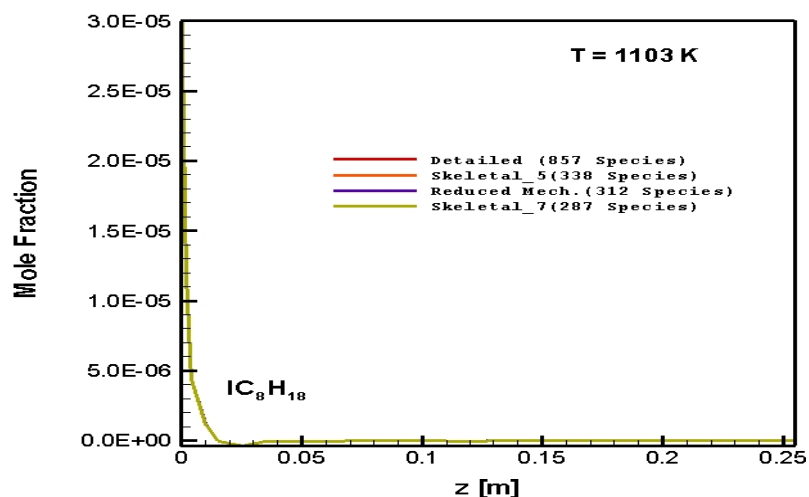
Figure 5.66 : Numerically predicted IC_8H_{18} Numerically predicted H_2 distribution as a function of axial position along the reactor: C/O=1.0, 1103 K
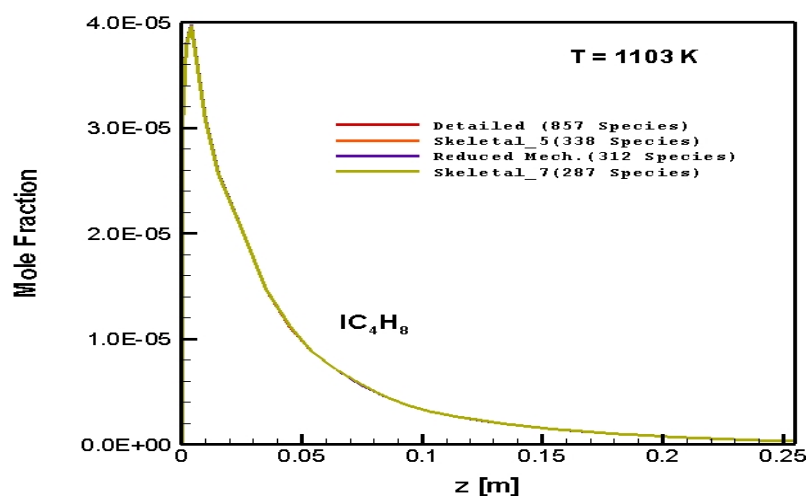
Figure 5.67 : Numerically predicted IC_4H_8 distribution as a function of axial position along the reactor: C/O=1.0, 1103 K
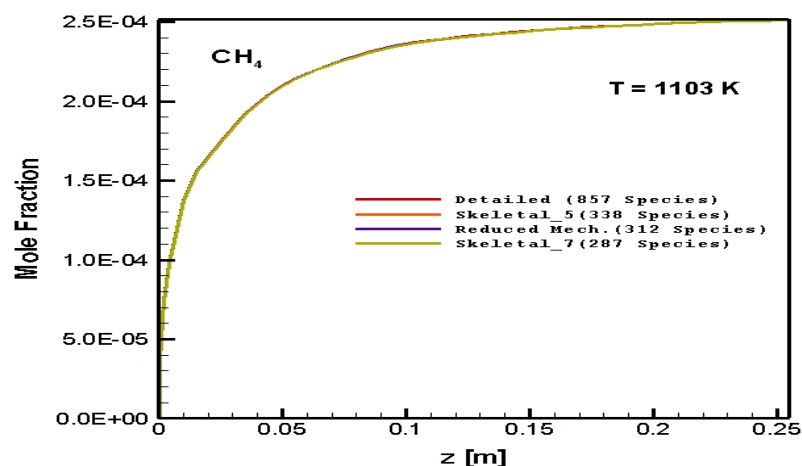
Figure 5.68 : Numerically predicted CH_4 distribution as a function of axial position along the reactor: C/O=1.0, 1103 K
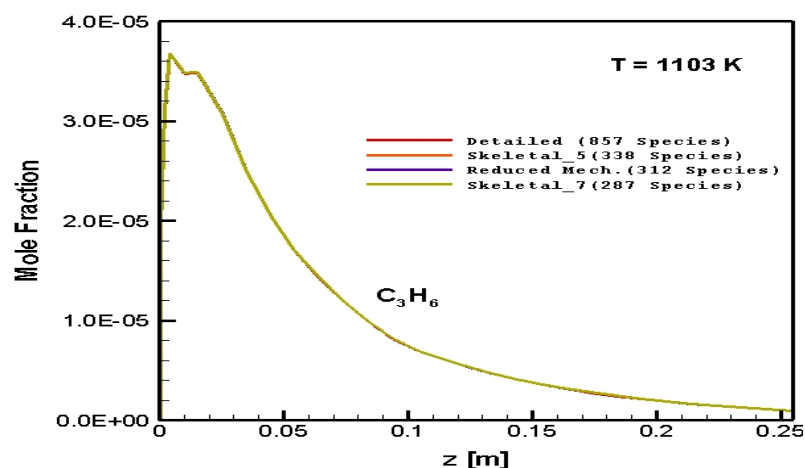
Figure 5.69 : Numerically predicted C_3H_6 distribution as a function of axial position along the reactor: C/O=1.0, 1103 K

As it is seen in the figures that i-octane is completely converted in the beginning of 0.01-0.05 m in the flow reactor while other hydrocarbon species like methane, ethylene, propylene and acetylene are produced within 0.05 m. Lengthwise the reactor, propylene is decreased again, consumed either via further thermal cracking and hydrogenation processes or the formation of aromatics or polyaromatics finally resulting in carbon deposition. Conversion of hydrogen is less than 1 % at this high temperature and fuel rich condition whereas CO conversion is less than 0.1 %. Simulations of exhaust gases after catalyst for C/O=1.0 case prove that skeletal mechanisms and reduced mechanism give similar distribution prediction for each considered species. Skeletal 5 mechanism and reduced mechanism give consistent results again, as they give consistent results in gas phase (batch) simulations. Even though skeletal 7 mechanism gives inconsistent results for some species in gas-phase (batch) simulations, it gives consistent results for plug calculations C/O=1.0 case.

5.4.4.2 Simulation Results of Species Mole Fractions For One Exact Position In The Channel For Different Temperatures

The next simulations are performed for one exact position in the channel for different temperatures for exhaust gases after catalyst. Predictions for the distribution of important species in the reactor are shown in the following graphics. Apart from the mole fractions of one exact temperature through the reactor, error levels will also be shown in this case. Even though skeletal 7 mechanism also gives consistent results in plug calculations at one exact temperature through the reactor, reduced mechanism of the gas phase simulation results of C/O=1.6 and t=4.2E-02s is chosen for the simulations of one exact position in the channel for different temperatures. Different C/O ratios are used again for the calculations (C/O=1.6, C/O=2.0, C/O=1.3, C/O=1.0)
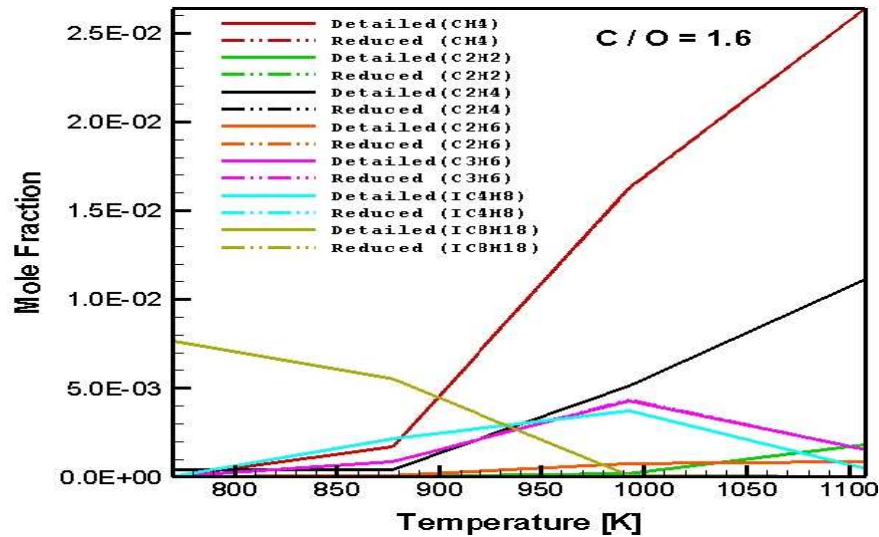
Figure 5.70 : Numerically predicted distribution of some important species as a function of gas temperature at one exact position in the channel (20 mm): C/O=1.6

Reduced mechanism gives very consistent results for one exact position in the channel for different temperatures for C/O=1.6 case. Mole fraction profiles are very similar, detailed mechanism and skeletal mechanism mole fraction profiles can not be seperated on the graphs. The error levels will be shown on the below tables (from table 5.50 to table 5.53).

Table 5.48 : Errors of the reduced mechanism for the predictions of important species distribution after catalyst: C/O=1.6, 770 K

Mechanism	CH4 Error%	C2H6 Error%	C2H4 Error%	C2H2 Error%	C3H6 Error%	IC4H8 Error%	IC8H18 Error%
Reduced	4.69E-02	4.71E-02	4.14E-04	5.76E-02	4.70E-02	4.58E-02	2.22E-04

Table 5.49 : Errors of the reduced mechanism for the predictions of important species distribution after catalyst: C/O=1.6, 877 K

Mechanism	CH4 Error%	C2H6 Error%	C2H4 Error%	C2H2 Error%	C3H6 Error%	IC4H8 Error%	IC8H18 Error%
Reduced	9.50E-02	2.14E-03	3.46E-03	2.60E-02	1.42E-02	1.20E-02	4.18E-03

Table 5.50 : Errors of the reduced mechanism for the predictions of important species distribution after catalyst: C/O=1.6, 993 K

Mechanism	CH4 Error%	C2H6 Error%	C2H4 Error%	C2H2 Error%	C3H6 Error%	IC4H8 Error%	IC8H18 Error%
Reduced	3.54E-01	5.45E-01	1.27E-01	1.21E+00	2.20E-01	1.34E-02	3.22E-01

Table 5.51 : Errors of the reduced mechanism for the predictions of important species distribution after catalyst: C/O=1.6, 1108 K

Mechanism	CH4 Error%	C2H6 Error%	C2H4 Error%	C2H2 Error%	C3H6 Error%	IC4H8 Error%	IC8H18 Error%
Reduced	3.86E-02	5.30E-03	1.52E-02	2.56E-01	1.35E-01	1.06E-01	1.03E-01

It is seen in tables that error levels of plug simulations of one exact position in the channel for different temperatures for C/O=1.6 case are below than 1%. So it can be easily mentioned that reduced mechanism gives very consistent results for considered cases.

The next simulation of one exact position in the channel for different temperatures is performed for C/O=2.0. Predictions for the distribution of important species in the reactor are shown in the following graphics.
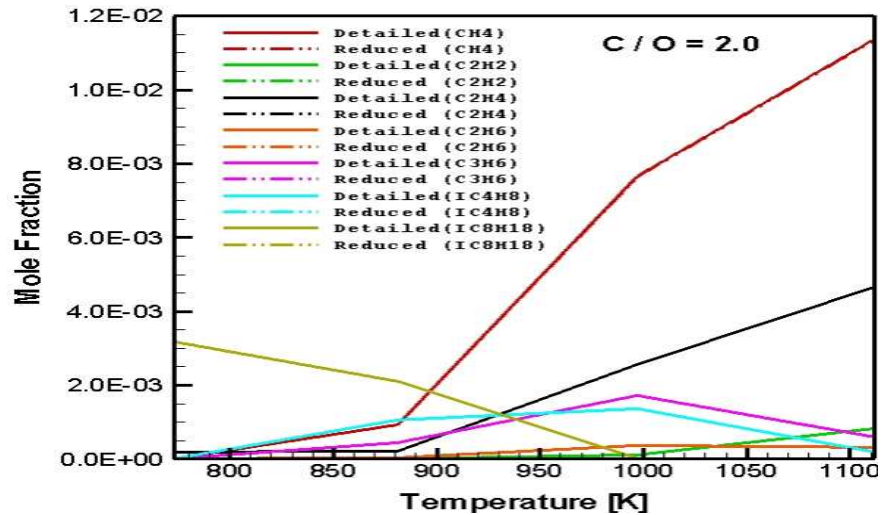
Figure 5.71 : Numerically predicted distribution of some important species as a function of gas temperature at one exact position in the channel (20 mm): C/O=2.0

Reduced mechanism gives very consistent results again for one exact position in the channel for different temperatures for C/O=2.0 case. Mole fraction profiles are very similar, detailed mechanism and skeletal mechanism mole fraction profiles cannot be seperated again on the graphs. The error levels will be shown on the below tables (from table 5.54 to table 5.57).

Table 5.52 : Errors of the reduced mechanism for the predictions of important species distribution after catalyst: C/O=2.0, 773 K

Mechanism	CH4 Error%	C2H6 Error%	C2H4 Error%	C2H2 Error%	C3H6 Error%	IC4H8 Error%	IC8H18 Error%
Reduced	3.23E-02	3.21E-02	3.54E-04	4.23E-02	3.23E-02	3.13E-02	2.20E-04

Table 5.53 : Errors of the reduced mechanism for the predictions of important species distribution after catalyst: C/O=2.0, 881 K

Mechanism	CH4 Error%	C2H6 Error%	C2H4 Error%	C2H2 Error%	C3H6 Error%	IC4H8 Error%	IC8H18 Error%
Reduced	1.46E-01	5.96E-03	2.02E-03	2.34E-02	1.38E-02	1.25E-02	4.83E-03

Table 5.54 : Errors of the reduced mechanism for the predictions of important species distribution after catalyst: C/O=2.0, 997 K

Mechanism	CH4 Error%	C2H6 Error%	C2H4 Error%	C2H2 Error%	C3H6 Error%	IC4H8 Error%	IC8H18 Error%
Reduced	2.98E-01	5.99E-01	1.36E-01	1.30E+00	2.84E-01	6.39E-03	5.95E-01

Table 5.55 : Errors of the reduced mechanism for the predictions of important species distribution after catalyst: C/O=2.0, 1112 K

Mechanism	CH4 Error%	C2H6 Error%	C2H4 Error%	C2H2 Error%	C3H6 Error%	IC4H8 Error%	IC8H18 Error%
Reduced	5.36E-02	6.14E-02	3.54E-02	2.20E-01	2.85E-01	3.03E-01	4.19E-02

It is seen in tables that error levels of plug simulations of one exact position in the channel for different temperatures for C/O=2.0 case are below than 1% again. So it can be easily mentioned that reduced mechanism gives very consistent results.

The next simulation of one exact position in the channel for different temperatures is performed for C/O=1.3 case. Predictions for the distribution of important species in the reactor are shown in the following graphics.
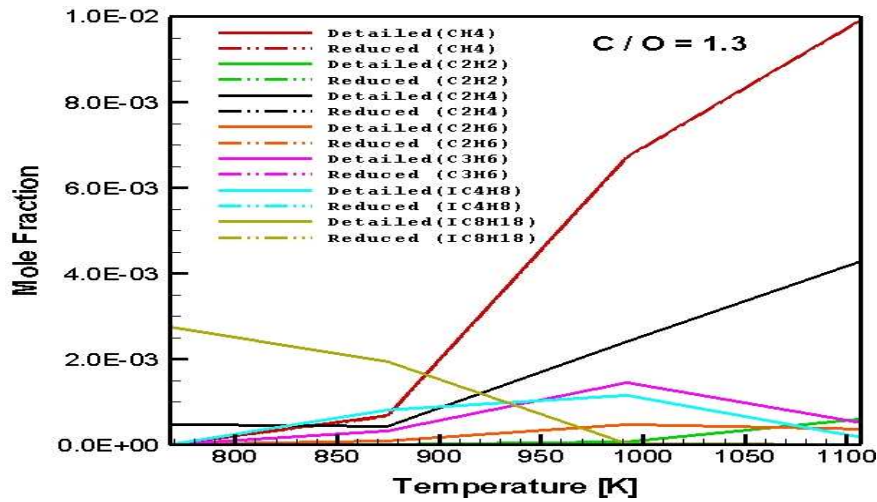
Figure 5.72 : Numerically predicted distribution of some important species as a function of gas temperature at one exact position in the channel (20 mm): C/O=1.3

Reduced mechanism gives very consistent results again for one exact position in the channel for different temperatures for C/O=1.3 case. Mole fraction profiles are very similar, detailed mechanism and reduced mechanism mole fraction profiles cannot be seperated again on the graphs. The error levels will be shown on the below tables (from table 5.58 to table 5.61).

Table 5.56 : Errors of the reduced mechanism for the predictions of important species distribution after catalyst: C/O=1.3, 768 K

Mechanism	CH4 Error%	C2H6 Error%	C2H4 Error%	C2H2 Error%	C3H6 Error%	IC4H8 Error%	IC8H18 Error%
Reduced	4.09E-02	4.04E-02	3.02E-04	4.15E-02	4.10E-02	4.00E-02	1.43E-04

Table 5.57 : Errors of the reduced mechanism for the predictions of important species distribution after catalyst: C/O=1.3, 875 K

Mechanism	CH4 Error%	C2H6 Error%	C2H4 Error%	C2H2 Error%	C3H6 Error%	IC4H8 Error%	IC8H18 Error%
Reduced	1.19E-01	7.83E-03	5.43E-04	2.24E-02	1.27E-02	1.14E-02	4.08E-03

Table 5.58 : Errors of the reduced mechanism for the predictions of important species distribution after catalyst: C/O=1.3, 992 K

Mechanism	CH4 Error%	C2H6 Error%	C2H4 Error%	C2H2 Error%	C3H6 Error%	IC4H8 Error%	IC8H18 Error%
Reduced	3.34E-01	6.05E-01	1.51E-01	1.44E+00	2.83E-01	7.45E-03	8.46E-01

Table 5.59 : Errors of the reduced mechanism for the predictions of important species distribution after catalyst: C/O=1.3, 1107 K

Mechanism	CH4 Error%	C2H6 Error%	C2H4 Error%	C2H2 Error%	C3H6 Error%	IC4H8 Error%	IC8H18 Error%
Reduced	7.77E-02	9.65E-02	4.05E-02	2.59E-01	4.09E-01	4.61E-01	3.94E+00

It is seen in tables that error levels of plug simulations of one exact position in the channel for different temperatures for C/O=1.3 case are below than 1% again. So it can be easily mentioned that reduced mechanism gives very consistent results.

The next simulation of one exact position in the channel for different temperatures is performed for C/O=1.0 case. Predictions for the distribution of important species in the reactor are shown in the following graphics.
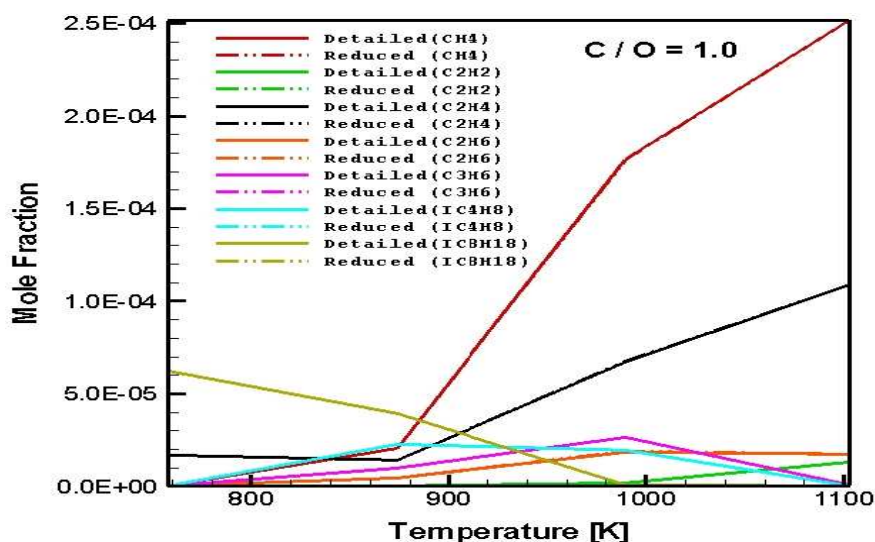
Figure 5.73 : Numerically predicted distribution of some important species as a function of gas temperature at one exact position in the channel (20 mm): C/O=1.0

Reduced mechanism gives very consistent results again for one exact position in the channel for different temperatures for C/O=1.0 case. Mole fraction profiles are very similar, detailed mechanism and reduced mechanism mole fraction profiles can not be seperated again on the graphs. The error levels will be shown on the below tables (from table 4.53 to table 4.56).

Table 5.60 : Errors of the reduced mechanism for the predictions of important species distribution after catalyst: C/O=1.0, 758 K

Mechanism	CH4 Error%	C2H6 Error%	C2H4 Error%	C2H2 Error%	C3H6 Error%	IC4H8 Error%	IC8H18 Error%
Reduced	3.28E-04	5.64E-03	4.92E-03	1.68E-04	7.22E-05	7.49E-05	0.00E+00

Table 5.61 : Errors of the reduced mechanism for the predictions of important species distribution after catalyst: C/O=1.0, 874 K

Mechanism	CH4 Error%	C2H6 Error%	C2H4 Error%	C2H2 Error%	C3H6 Error%	IC4H8 Error%	IC8H18 Error%
Reduced	2.09E-01	1.23E-01	7.56E-03	2.36E-02	1.28E-02	1.49E-02	6.10E-03

Table 5.62 : Errors of the reduced mechanism for the predictions of important species distribution after catalyst: C/O=1.0, 990 K

Mechanism	CH4 Error%	C2H6 Error%	C2H4 Error%	C2H2 Error%	C3H6 Error%	IC4H8 Error%	IC8H18 Error%
Reduced	0.00E+00	0.00E+00	0.00E+00	0.00E+00	0.00E+00	0.00E+00	0.00E+00

Table 5.63 : Errors of the reduced mechanism for the predictions of important species distribution after catalyst: C/O=1.0, 1103 K

| Mechanism	CH4 Error%	C2H6 Error%	C2H4 Error%	C2H2 Error%	C3H6 Error%	IC4H8 Error%	IC8H18 Error%
Reduced	3.49E-02	6.69E-04	1.35E-02	2.01E-01	3.26E-01	3.72E-01	6.27E-01

It is seen in tables that error levels of plug simulations of one exact position in the channel for different temperatures for C/O=1.3 case are below than 1% again. So it can be easily mentioned that reduced mechanism gives very consistent results.

Finally, experimental results and detailed and reduced mechanism predictions for the distribution of important species in the reactor are shown for C/O=1.6 in the following graph. Experimental procedure and experimental results are given by Deutschmann et al. [49].
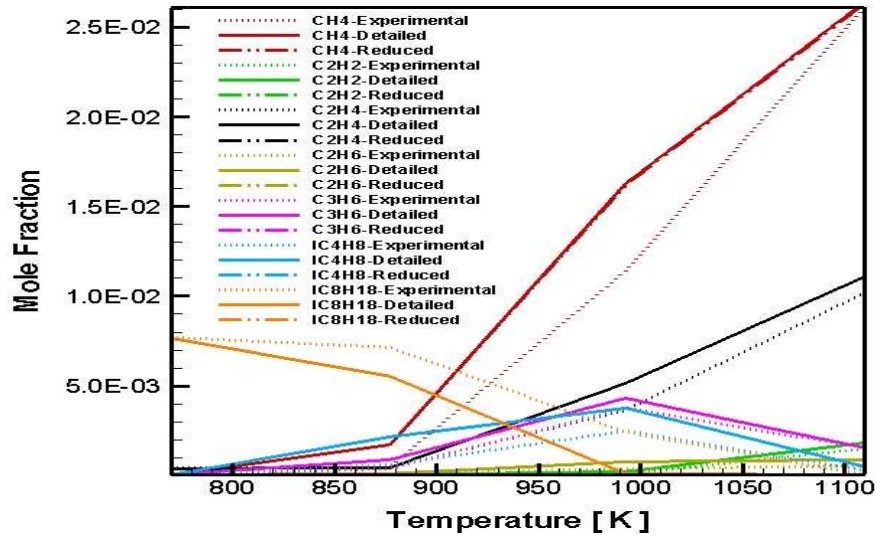
Figure 5.74 : Numerically predicted and experimentally measured distribution of some important species as a function of gas temperature at one exact position in the channel (20 mm): C/O=1.6

6. CONCLUSIONS

The main purpose of this study was coupling mechanism reduction procedures with DETCHEM software and development of i-octane reduced mechanism for fast and accurate prediction of soot precursors in CPOX reformer at fuel rich operating conditions. Necessity analysis was used as the starting reduction method for this purpose. The method has been improved for this study and the validity of the proposed new method which is called as necessity analysis with simultaneously combined sensitivity and reaction flow analysis through each reaction method is investigated. It is shown that proposed method allows deleting up to 64 % of species and 60 % of reactions of the detailed mechanism without loss of information. And it allows fast and accurate prediction of soot precursors in CPO reformer at fuel rich as well as fuel lean operating conditions.

REFERENCES

[1] **Thomas, C. E., James B. D., Lomax F. D., Kuhn Jr. I. F.,** Int. J. Hydrogen Energy 25 (2000) 551-567.

[2] **Ahmed, S., Krumpelt M.,** Int. J. Hydrogen Energy 26 (2001) 291-301.

[3] **Curran, H. J., Gafurri, P., Pitz, W.J., Westbrook, C.K.,** A Comprehensive Modeling Study of iso-Octane Oxidation, *Combust & Flame* 129:253-280. Flowers, D., Aceves, S., Smith, R., Torres, J., Girard, J., and Dibble, R. (2000) HCCI in a CFR

[4] **Hartmann, M., Maier, L., Minh, H. D., Deutschmann O.,** 2010: Catalytic Partial Oxidation of i-Octane over Rhodium Catalysts: An Experimental Modeling and Simulation Study. Combustion and Flame, in Press. http://dx.doi.org/10.1016/j.combustflame.2010.03.005

[5] **Minh, H. D., Bock, H. G., Tischer, S., Deutschmann O.,** Fast solution for large-scale for large-scale 2-D convection-diffusion, reacting flows. Computational Science and its Applications - ICCSA 2008. Lecture Notes in Computer Science 507, Gervasi, B.Murgante (eds.), p.1121-1130, Springer, 2008.

[6] **Deutschmann, O., Tischer, S., Kleditzsch, S., Janardhanan, V. M., Correa, C., Chatterjee, D., Mladenov, N., Minh, H. D.,** DETCHEM^{TM} Software package, 2.2 ed., www.detchem.com, Karlsruhe 2008.

[7] **Aceves, S. M., Martinez-Frias, J., Flower, D., Smith, J. R., Dibble, R. W., and Chen, J.-Y.,** A Computer Generated Reduced Iso-Octane Chemical Kinetic Mechanism Applied to Simulation of HCCI Combustion, *SAE Paper* 2002-01-2870.

[8] **Momirlana, M., Veziroglu, T.N.,** The properties of hydrogen as fuel tomorrow in sustainable energy system for a cleaner planet, International Journal of Hydrogen Energy 30 (2005) 795 – 802

[9] **Thring, R.H.,** Alternative fuels for spark ignition engines. SAE Transaction paper 831685, (SP-559), Vol. 92, Section 4, (1983)

[10] **Jamal, Y., Wyszynski, M. L.,** 1994: On board generation of hydrogen-rich gaseous fuels-a review, Int. J. Hydrogen Energy, Vol. 19, No. 7. pp. 557-572, International Association for Hydrogen Energy, Elsevier Ltd

[11] **Lenz, B., Aicher, T.,** Catalytic autothermal reforming of Jet fuel, Journal of Power Sources 149 (2005) 44–52

[12] **Halabi, M. H., de Croon, M.H.J.M., van der Schaaf, J., Cobden, P.D., Schouten J.C.,** 2007: Modeling and analysis of autothermal reforming of methane to hydrogen in a fixed bed reformer, Chemical Engineering Journal 137 (2008) 568–578

[13] **Kim, D. H., Ryu, J. W., Choi, E. H., Gong, G. T., Lee, H., Lee, B. G., Moon, D. J.,** Production of synthesis gas by autothermal reforming of iso-

octane and toluene over metal modified Ni-based catalyst, Catalysis Today 136 (2008) 266–272

[14] **Deutschmann, O.,** Computational Fluid Dynamics Simulation of Catalytic Reactors. Chapter 6.6 in Handbook of Heterogeneous Catalysis, 2nd Ed., G. Ertl, H. Knözinger, F. Schüth, J. Weitkamp (eds.), p. 1811-1828, Wiley-VCH, 2008

[15] **Degenstein, N. J., Subramanian, R., Schmidt, L. D.,** Appl. Catal. A. 305 (2006) 146.

[16] **Gould, B. D., Chen, X. Y., Schwank, J. W.,** J. Catal. 250 (2007) 209.

[17] **Kee, R. J., Rupley, F. M., Miller, J. A., Coltrin, M. E., Grcar, J. F., Meeks, E., Moffat, H. K., Lutz, A. E., Dixon-Lewis, G., Smooke, M. D., Warnatz, J., Evans, G. H., Larson, R. S., Mitchell, R. E., Petzold, L. R., Reynolds, W. C., Caracotsios, M., Stewart, W. E., Glarborg, P., Wang, C., Adigun, O.,** *CHEMKIN*, 3.6 ed., Reaction Design, Inc., www.chemkin.com, San Diego, 2000.

[18] **Schmidt, L. D., Deutschmann, O., Goralski, C.T., Jr.,** Modeling the Partial Oxidation of Methane to Syngas at Millisecond Contact Times, Natural Gas Conversion V, Studies in Surface Science and Catalysis, Vol. 119 A., A. Parmaliana et al. (Editors), 1998 Elsevier Science B.V.

[19] **Quiceno, R., Ramirez, J., P., Warnatz, J., Deutschmann, O.,** 2006: Modeling the high-temperature catalytic partial oxidation of methane over platinum gauze: Detailed gas-phase and surface chemistries coupled with 3D flow field simulations, Applied Catalysis A: General 303 (2006) 166-176

[20] **Hartmann, M., Kaltschmitt, T., Deutschmann, O.,** 2009: Catalytic partial oxidation of higher hydrocarbon fuel components on Rh/Al2O3 coated honeycomb monoliths, Catalysis Today 147S (2009) S204–S209

[21] **Warnatz J., Maas U., Dibble, R.W.,** Combustion: Physical and chemical fundamentals, modeling and simulation, experiments, pollutant formation, p.63-104, Springer-Verlag Berlin Heidelberg, 1996

[22] **Kenneth K. Kuo**, Principles of Combustion, Second edition, p. 116-182, John Wiley & Sons, Inc.

[23] **Tomlin, A.S., Turanyi, T., Pilling, M.J.,** Mathematical Tools For Construction, Investigation, and Reduction of Combustion Mechanisms, in Low-Temperature Combustion and Autoignition, Comprehensive Chemical Kinetics, pp.293-437, Elsevier

[24] **Chevalier, C., Warnatz, J., Melenk, H.,** Ber. Bunsenges. Phys. Chem. 1990, 94,1362.

[25] **Susnow, R. G., Dean, A. M., Green, W. H., Peczak, P., Broadbelt, L.,** J. J. Phys. Chem. A, 1997, 101, 3731

[26] **Warth, V., Battin-Leclerc, F., Fournet, P. A., Glaude, P. A., Come, G. M., Scacchi, G.** Computers and Chemistry, 2000, 24, 541.

[27] **Kojima, S.** Detailed Modeling of n-Butane Autoignition Chemistry, Combustion and Flame, 99, 87-136

[28] **Soyhan, S. H.,** Chemical Kinetic Modeling of Autoignition Under Conditions Relevant To Knock In Spark Ignition Engines, Ph.D. Thesis (503950023012), September 2000

[29] **Nowak, U., Warnatz J.,** "Sensitivity Analysis in Aliphatic Hydrocarbon Combustion", in A.L. Kuhl et al., eds., Dynamics of Reactive Systems, Vol. 1, Part I, AIAA, 1998, p.87

[30] **Warnatz J., 1984:** Critical Survey of Elementary Reaction Rate Coefficients In The C/H/O System. In: Gardiner WC jr. (ed) Combustion Chemistry. Springer-Verlag, New York

[31] **Soyhan, S. H., Mauss F.,** Kinetic Analysis of A Detailed Chemical Mechanism For HCCI Engines, *5. Mediterranean Combustion Symposium,* September 9-13, 2007.

[32] **Soyhan, S. H., Amnéus, P., Løvås, T., Nilsson, D., Maigaard P., Mauss, F., Sorusbay C.,** Automatic Reduction of Detailed Chemical Reaction Mechanisms for Autoignition Under SI Engine Conditions, 2000-01-1895, SAE

[33] **Soyhan, S. H., Mauss, F., Sorusbay C.,** Chemical Kinetic Modelling of Combustion In Internal Combustion Engines Using Reduced Chemistry, Combustion Science and Technology, 174:11, 73-91, DOI: 10.1080/713712950

[34] **Lu, T., Law, K. C.,** A directed relation graph method for mechanism reduction, Proceedings of the Combustion Institute 30 (2005) 1333–1341

[35] **Lu, T., Law, K. C.,** Linear time reduction of large kinetic mechanisms with directed relation graph: n-Heptane and iso-octane, Combustion and Flame 144 (2006) 24–36

[36] **Xin, Y., Song Z., Tan, Y. Z., Wang, Y. Z.,** The directed relation graph method for mechanism reduction in the oxidative coupling of methane, Catalysis Today 131 (2008) 483-488

[37] **Lu, T., Law, K. C.,** On the applicability of directed relation graphs to the reduction of reaction mechanisms, Combustion and Flame 146 (2006) 472-483

[38] **Desjardins, P. P., Pitsch, H., An efficient error-propagation-based reduction method for large chemical kinetic mechanisms, Combustion and Flame 154 (2008) 67-81**

[39] **Lu, T., Law, K. C.,** Strategies for Mechanism Reduction for Large Hydrocarbons: n-Heptane, Combustion and Flame 154 (2008) 153-163

[40] **Niemeyer, E. K., Sung, J. C., Raju, P. M.,** Skeletal mechanism generation for surrogate fuels using directed relation graph with error propagation

and sensitivity analysis, Combustion and Flame 157 (2010) 1760–1770

[41] **He, K., Androulakis, P. I., Ierapetritou, G. M.,** On-the-fly reduction of kinetic mechanisms using element flux analysis, Chemical Engineering Science 65 (2010) 1173-1184

[42] **Revel, J., Boettner, J. C., Cathonnet, M., Bachman, J. S.,** Derivation of a global chemical kinetic mechanism for methane ignition and combustion

[43] **Pope, S. B.,** Computational efficient implementation of combustion chemistry using in situ adaptive tabulation, Combustion Theory and Modeling, 1741-3559, Volume 1, Issue 1, 1997, Pages 41-63

[44] **Lu, T., Law, K. C.,** A criterion based on computational singular perturbation for the identification of quasi steady state species: A reduced mechanism for methane oxidation with NO chemistry, Combustion and Flame 154 (2008) 761-774

[45] **Maas U., Pope, S. B.,** Simplifying Chemical Kinetics: Intrinsic Low-Dimensional Manifolds in Composition Space, Combustion and Flame 88: 293-264 (1992)

[46] **Maas U., Pope, S. B.,** Laminar Flame Calculations Using Simplified Chemical Kinetics Based On Intrinsic Low-Dimensional Manifolds, Twenty-Fifth Symposium (International) on Combustion/The Combustion Institute, 1994/pp. 1349-1356

[47] **Maas U., Pope, S. B.,** Implementation of Simplified Chemical Kinetics Based On Intrinsic Low-Dimensional Manifolds, Twenty-Fourth Symposium (International) on Combustion/The Combustion Institute, 1992/pp. 103-112

[48] **Glassmaker J. N.,** Intrinsic Low-Dimensional Manifold Method For Rational Simplification of Chemical Kinetics, University of Notre Dame, *<http://www.nd.edu/~powers/nick.glassmaker.pdf>*

[49] **Kaltschmitt T., Maier L., Hartmann M., Hauck C., Deutschmann O.,** Significance of Gas phase reactions on catalytic reforming of isooctane - Manuscript

APPENDICES

APPENDIX A : – Numerically predicted species distribution in CPOX of i-octane as a function of time in the catalyst

– Comparison of the necessity analysis method and improved method for numerically predicted species distribution in CPOX of i-octane as a function of time in the catalyst

– Numerically predicted species distribution as a function of axial position along the reactor

APPENDIX B : – The list of the species of detailed LLNL i-octane reaction mechanism

– The list of the reduced mechanism species for the description of catalytic partial oxidation of i-octane for different cases

APPENDIX A
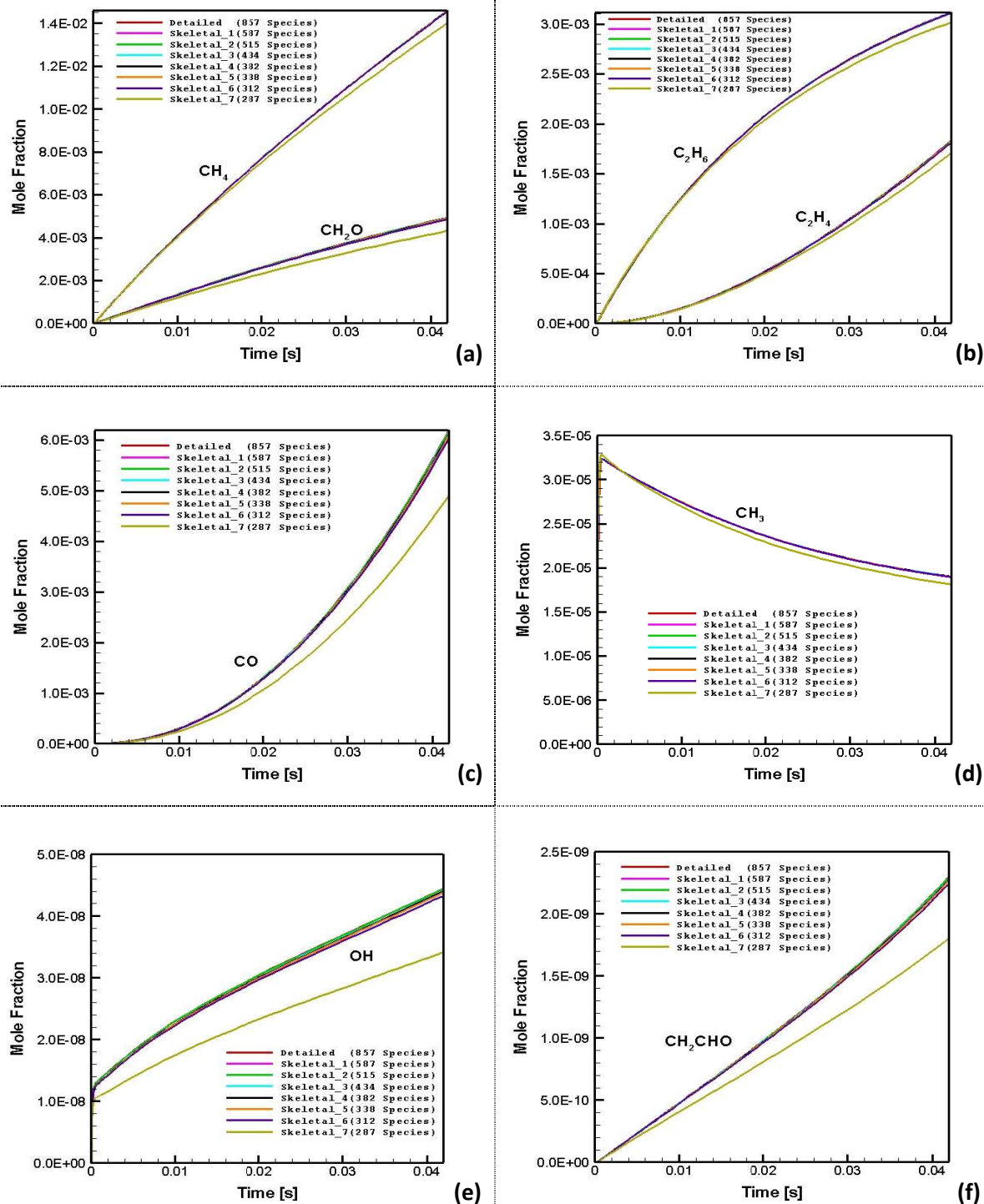
Figure A.1 : Numerically predicted species distribution in CPOX of i-octane as a function of time in the batch reactor: C/O=1.6, 1005.78 K : (a) CH_4 and CH_2O. (b) C_2H_6 and C_2H_4. (c) CO. (d) CH_3. (e) OH. (f) CH_2CHO
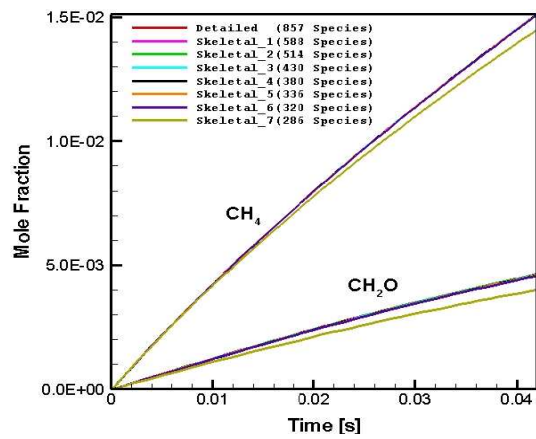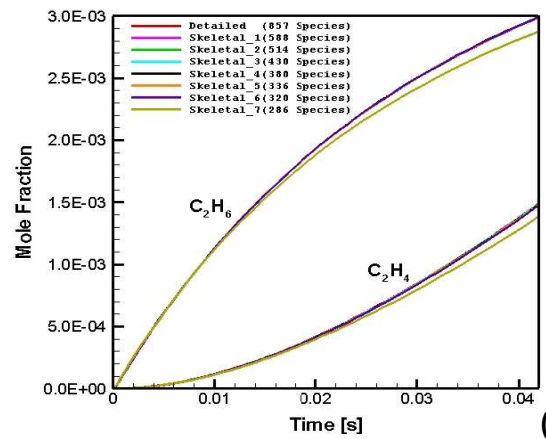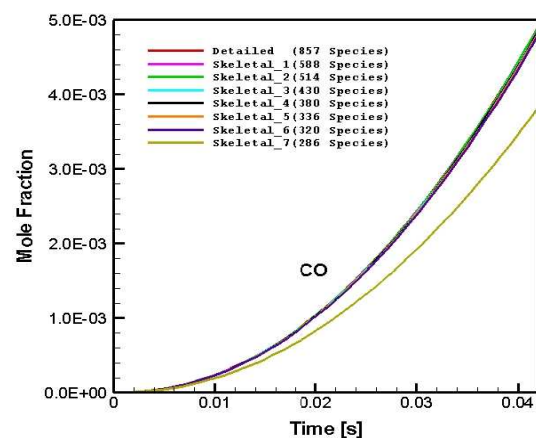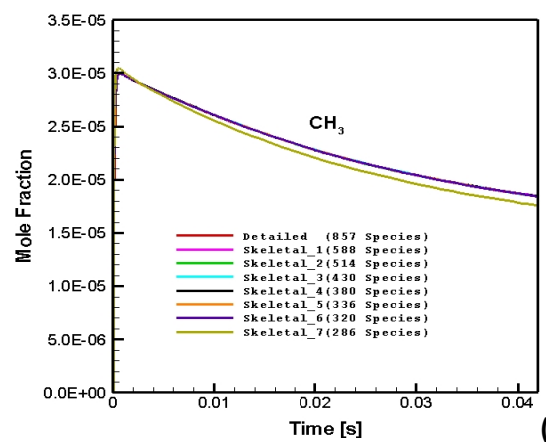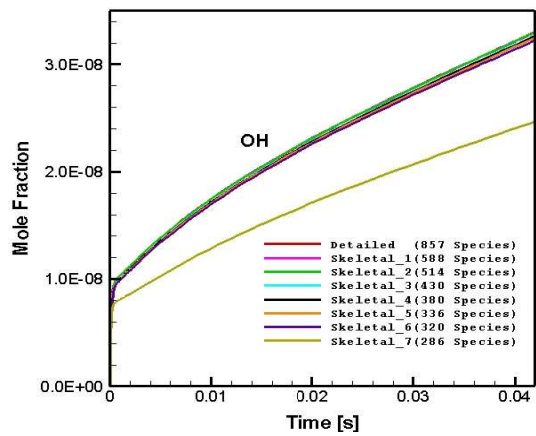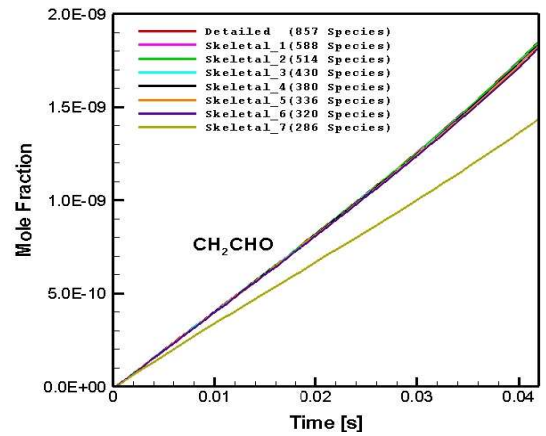
Figure A.2 : Numerically predicted species distribution in CPOX of i-octane as a function of time in the batch reactor: C/O=2.0, 998.26 K: (a) CH_4 and CH_2O. (b) C_2H_6 and C_2H_4. (c) CO. (d) CH_3. (e) OH. (f) CH_2CHO
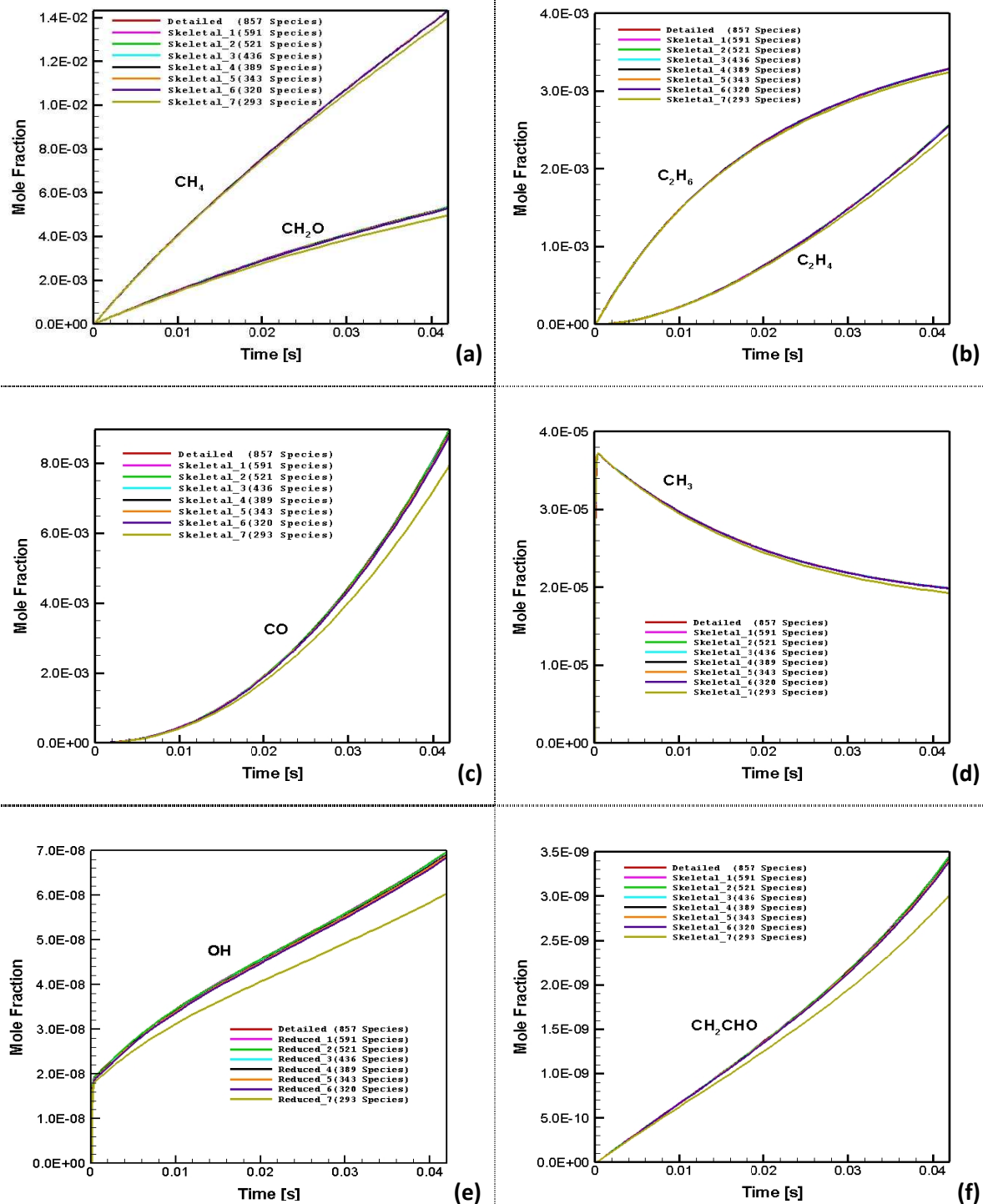
Figure A.3 : Numerically predicted species distribution in CPOX of i-octane as a function of time in the batch reactor: C/O=1.2, 1017.86 K: (a) CH_4 and CH_2O. (b) C_2H_6 and C_2H_4. (c) CO. (d) CH_3. (e) OH. (f) CH_2CHO
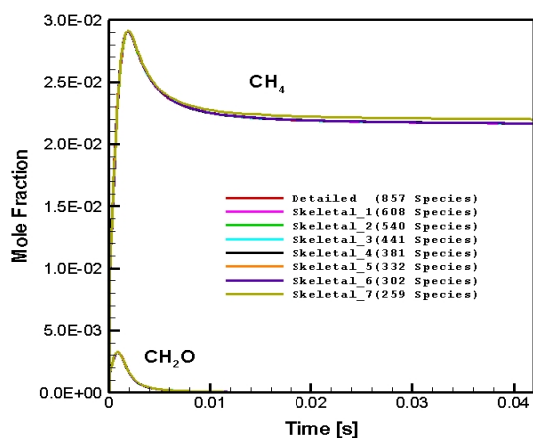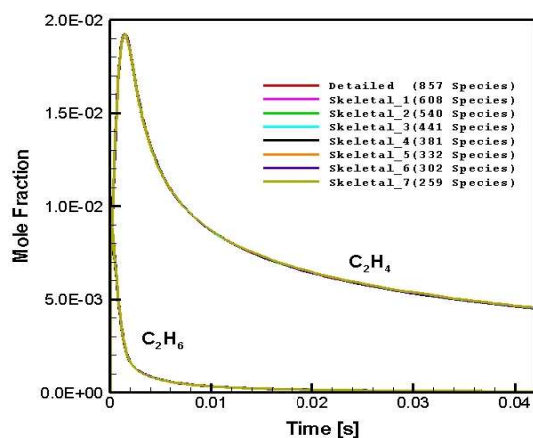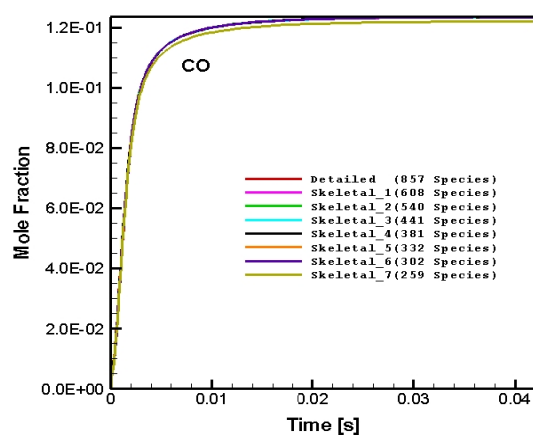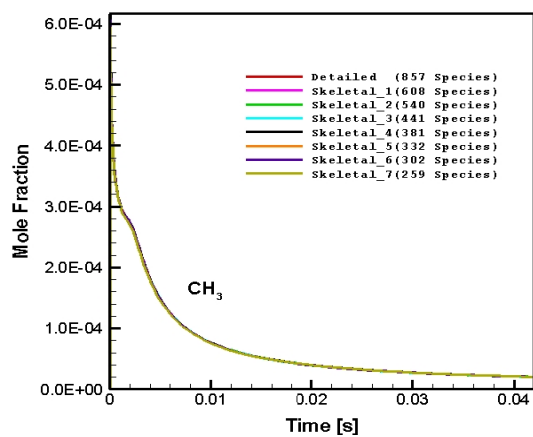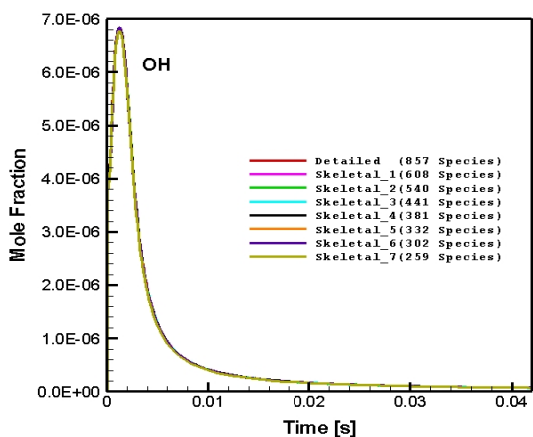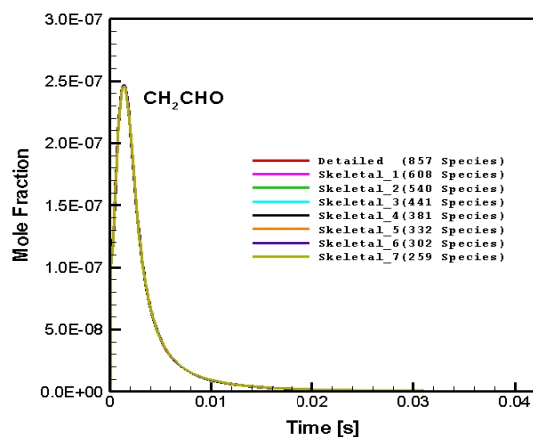
Figure A.4 : Numerically predicted species distribution in CPOX of i-octane as a function of time in the batch reactor: C/O=0.8, 1374.85 K: (a) CH$_4$ and CH$_2$O. (b) C$_2$H$_6$ and C$_2$H$_4$. (c) CO. (d) CH$_3$. (e) OH. (f) CH$_2$CHO
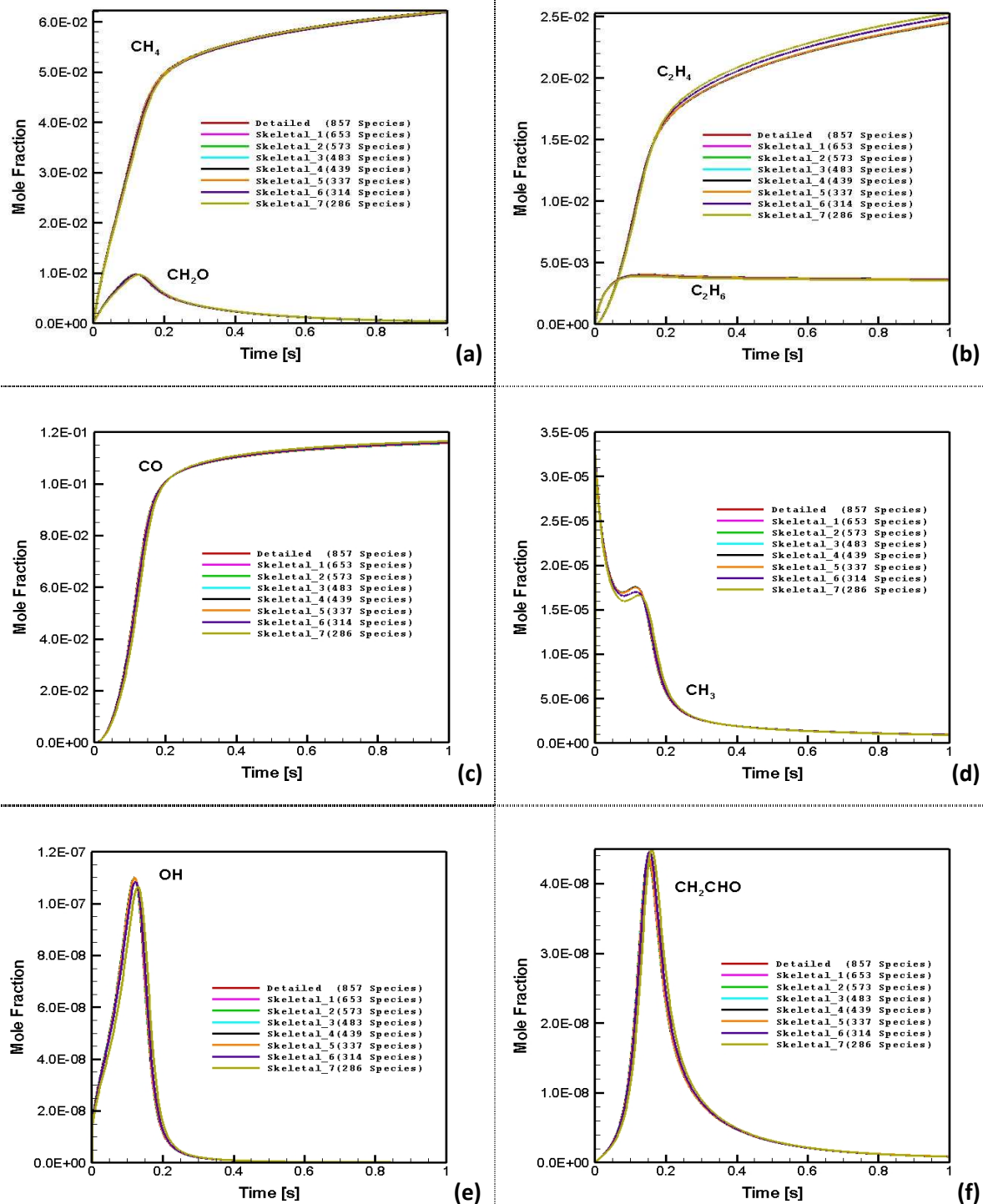
Figure A.5 : Numerically predicted species distribution in CPOX of i-octane as a function of time in the batch reactor: C/O=1.6, 1005.78 K, t=1.0s: (a) CH$_4$ and CH$_2$O. (b) C$_2$H$_6$ and C$_2$H$_4$. (c) CO. (d) CH$_3$. (e) OH. (f) CH$_2$CHO
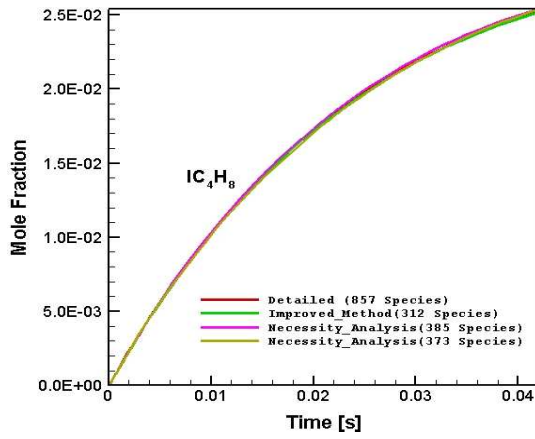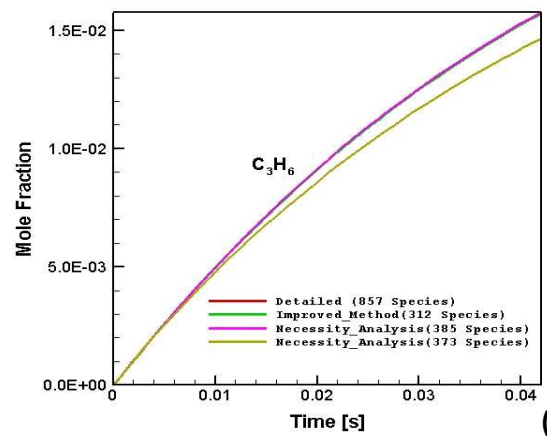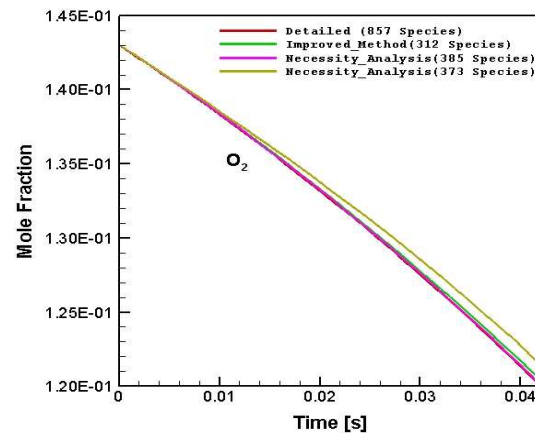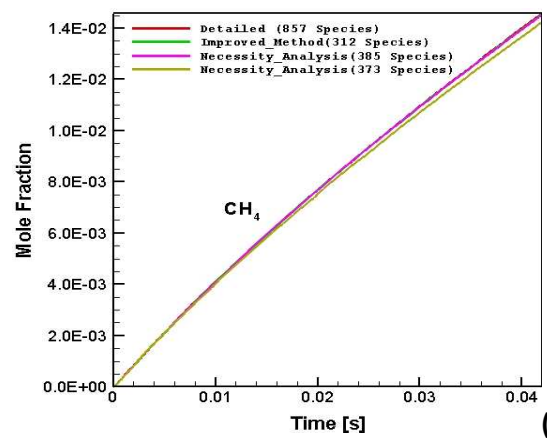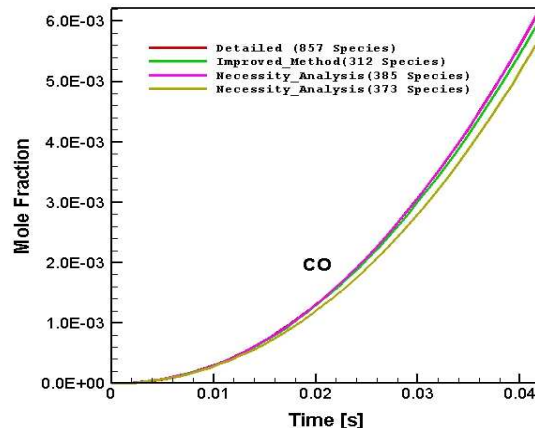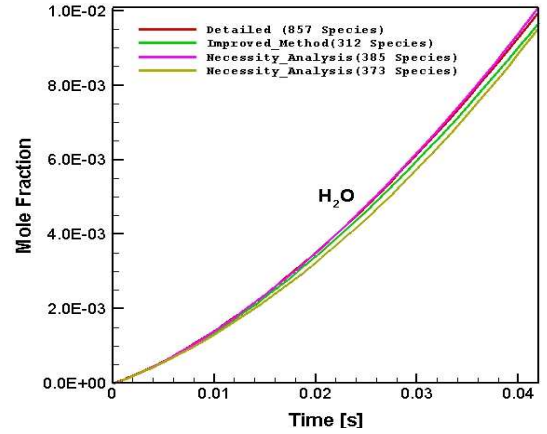
Figure A.6 : Comparison of the necessity analysis method and improved method for numerically predicted species distribution in CPOX of i-octane as a function of time in the batch reactor: C/O=1.6, 1005.78 K: (a) IC_4H_8. (b) C_3H_6. (c) O_2. (d) CH_4. (e) CO. (f) H_2O
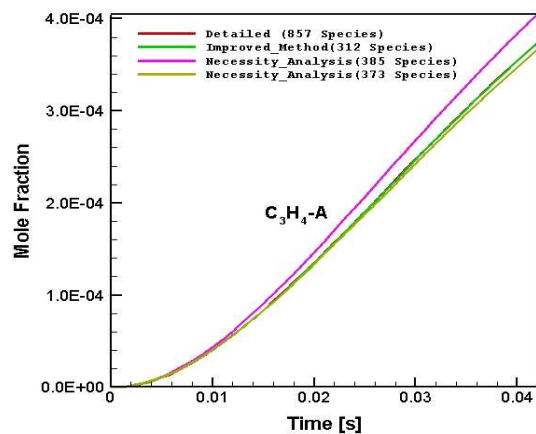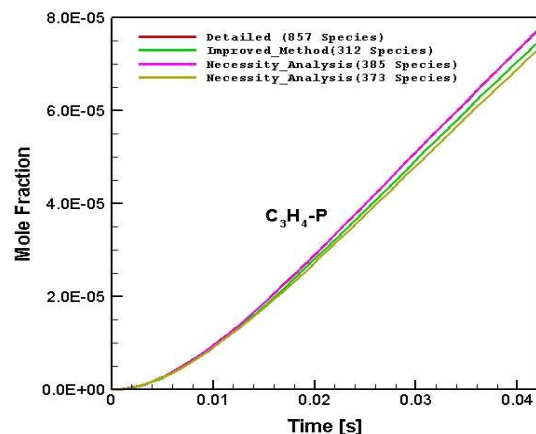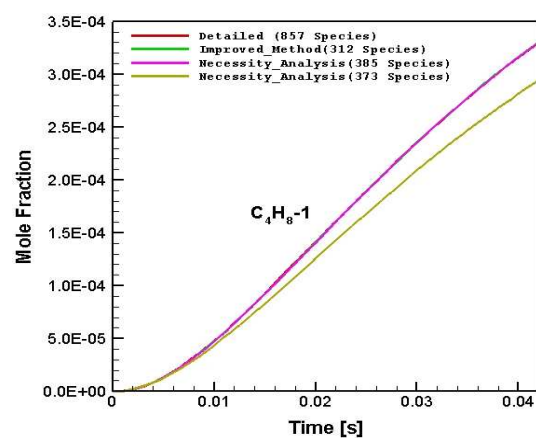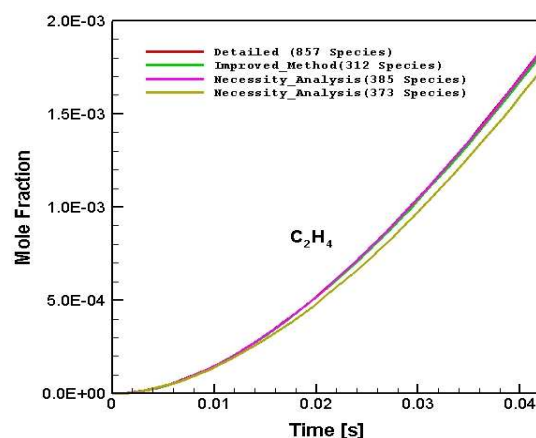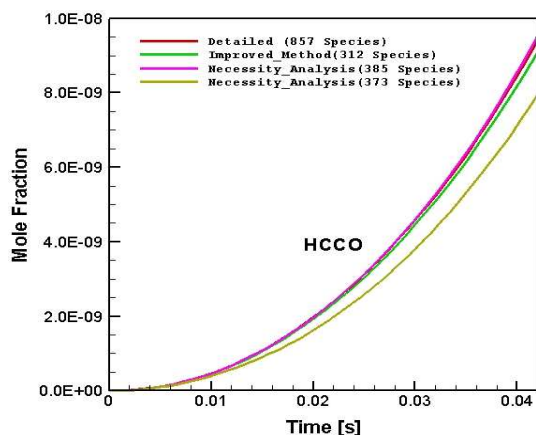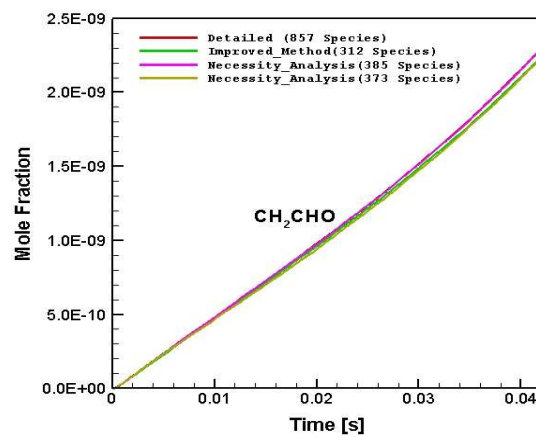
Figure A.7 : Comparison of the necessity analysis method and improved method for numerically predicted species distribution in CPOX of i-octane as a function of time in the batch reactor: C/O=1.6, 1005.78 K: (a) C_3H_4-A. (b) C_3H_4-P. (c) C_4H_8-1. (d) C_2H_4. (e) HCCO. (f) CH_2CHO
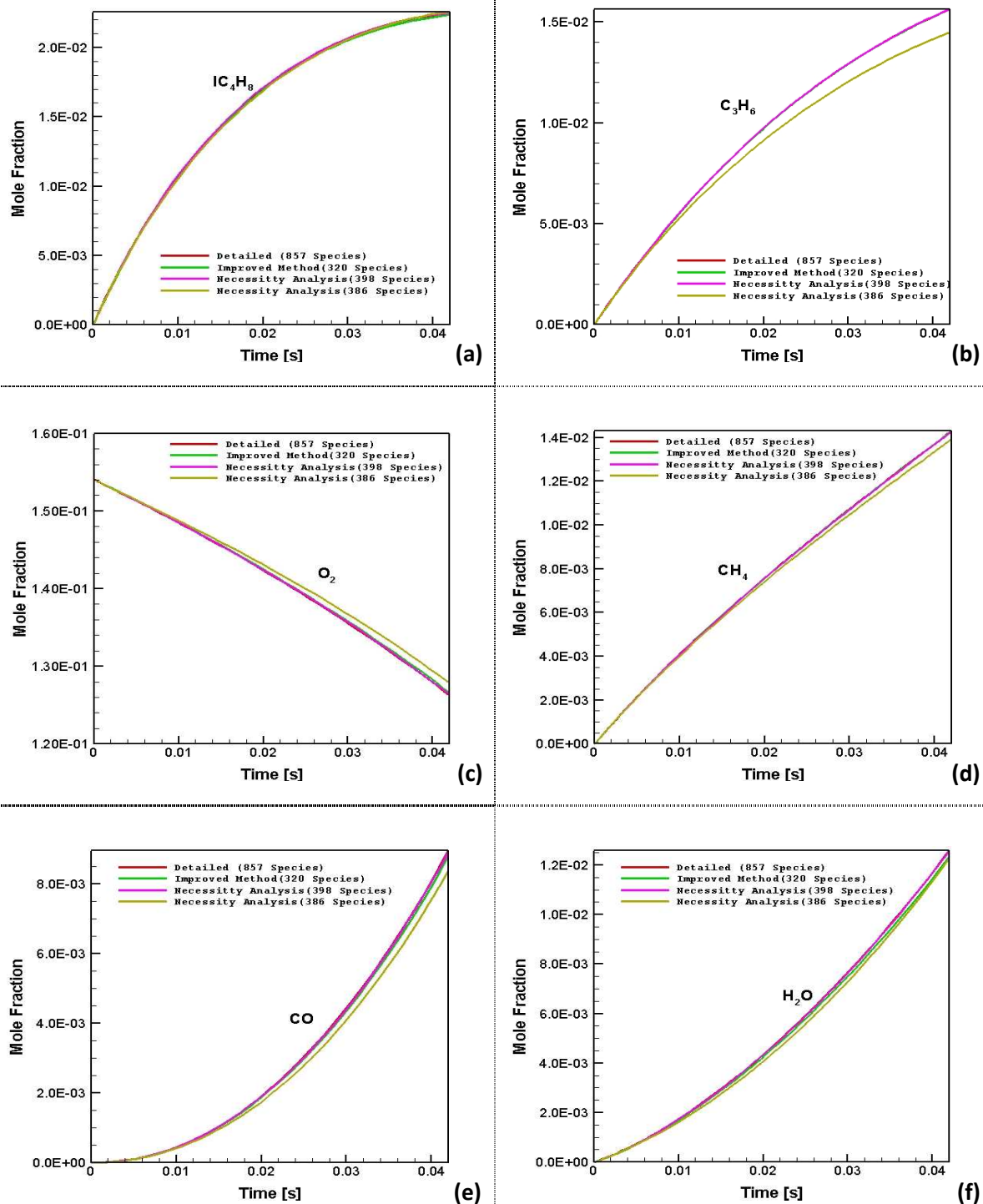
Figure A.8 : Comparison of the necessity analysis method and improved method for numerically predicted species distribution in CPOX of i-octane as a function of time in the batch reactor: C/O=1.2, 1017.86: (a) IC_4H_8. (b) C_3H_6. (c) O_2. (d) CH_4. (e) CO. (f) H_2O
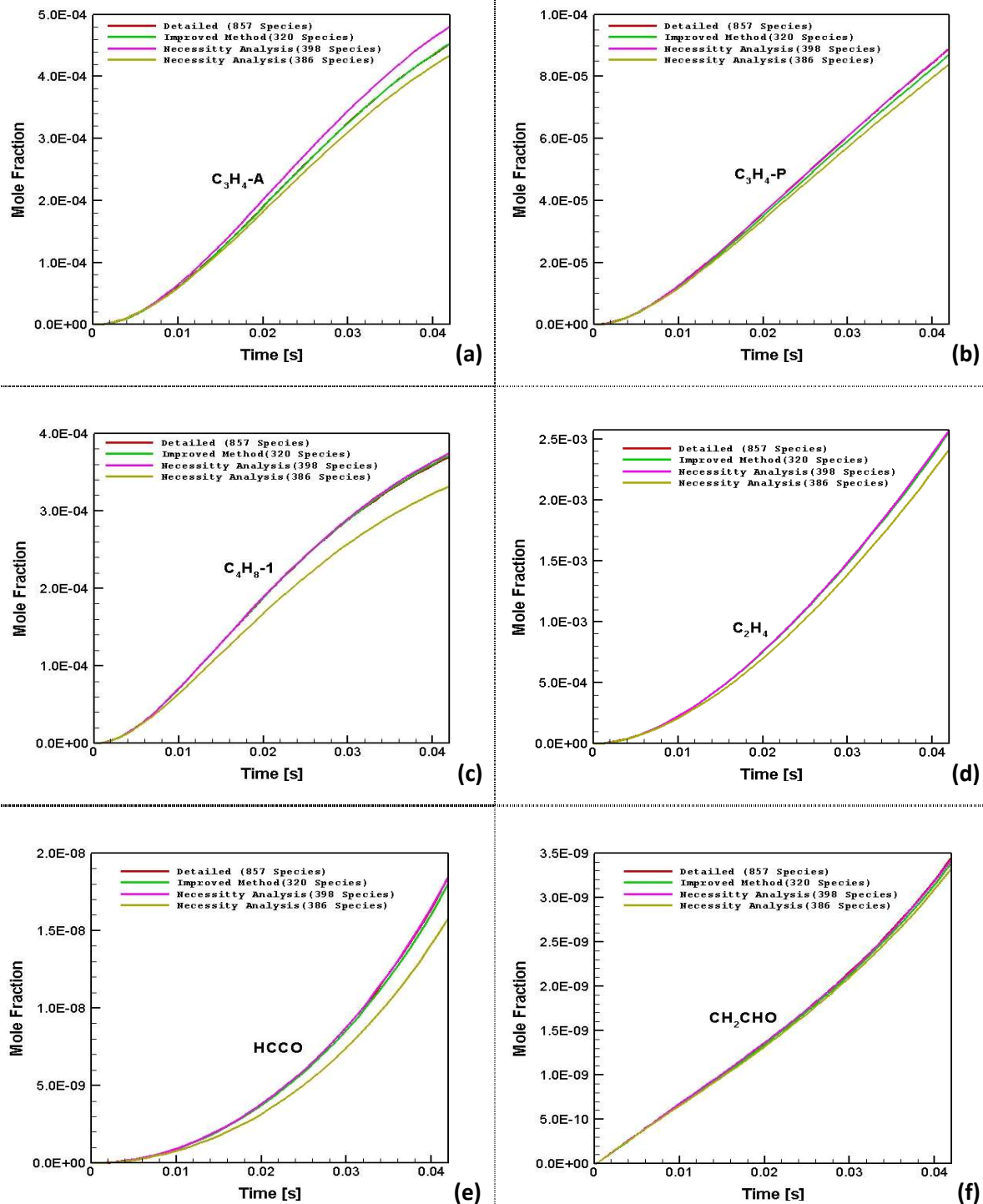
Figure A.9 : Comparison of the necessity analysis method and improved method for numerically predicted C_4H_8-2 distribution in CPOX of i-octane as a function of time in the batch reactor: C/O=1.2, 1017.86 K: (a) C_3H_4-A. (b) C_3H_4-P. (c) C_4H_8-1. (d) C_2H_4. (e) HCCO. (f) CH_2CHO
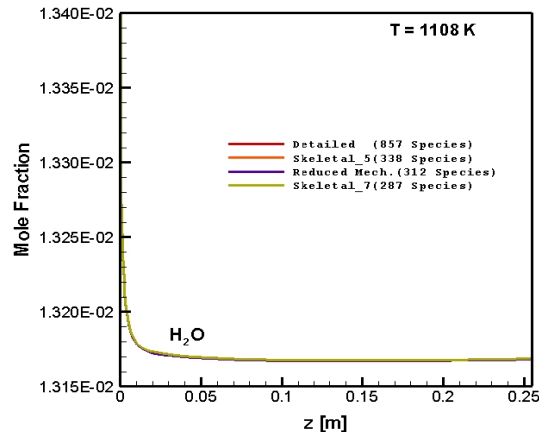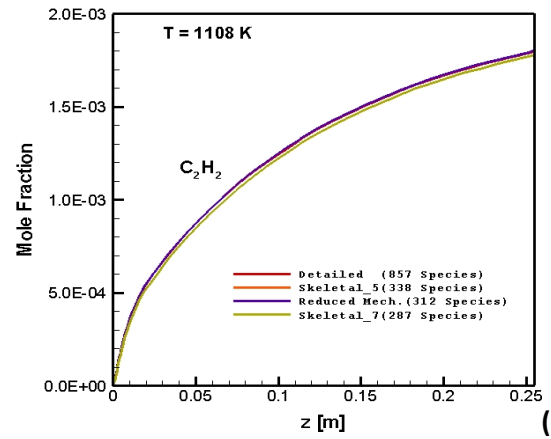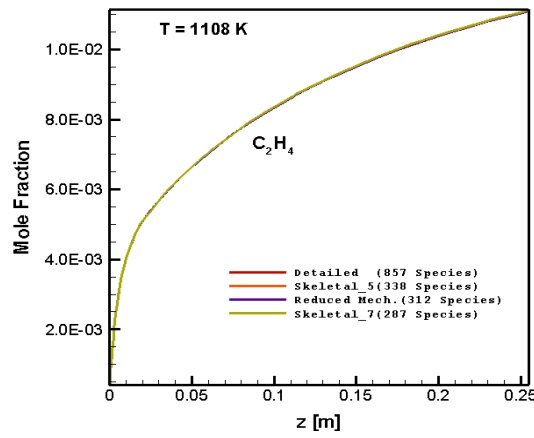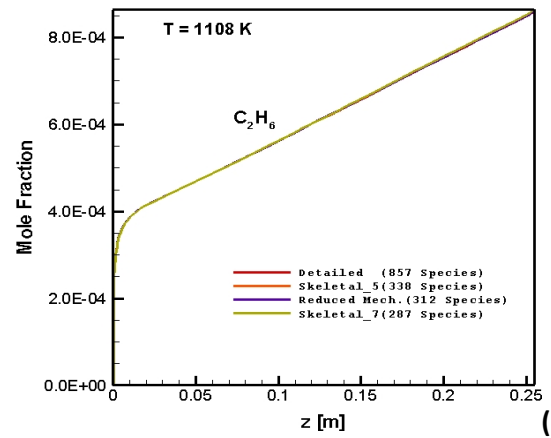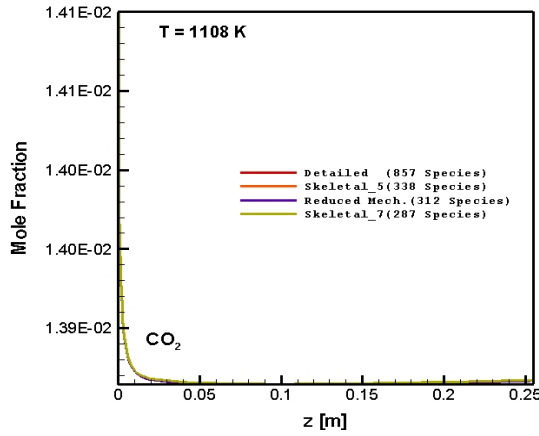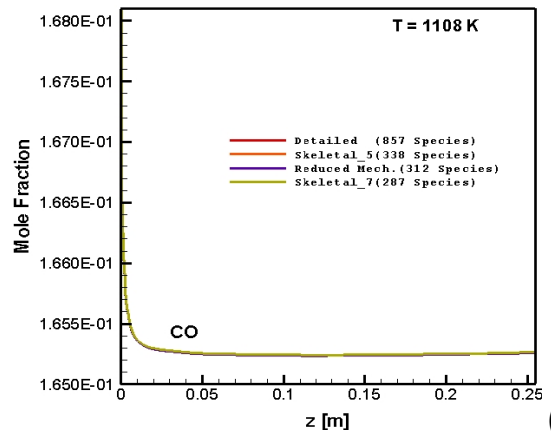
Figure A.10 : Numerically predicted species distribution as a function of axial position along the reactor: C/O=1.6, 1108 K: (a) H_2O. (b) C_2H_2. (c) C_2H_4. (d) C_2H_6. (e) CO_2. (f) CO
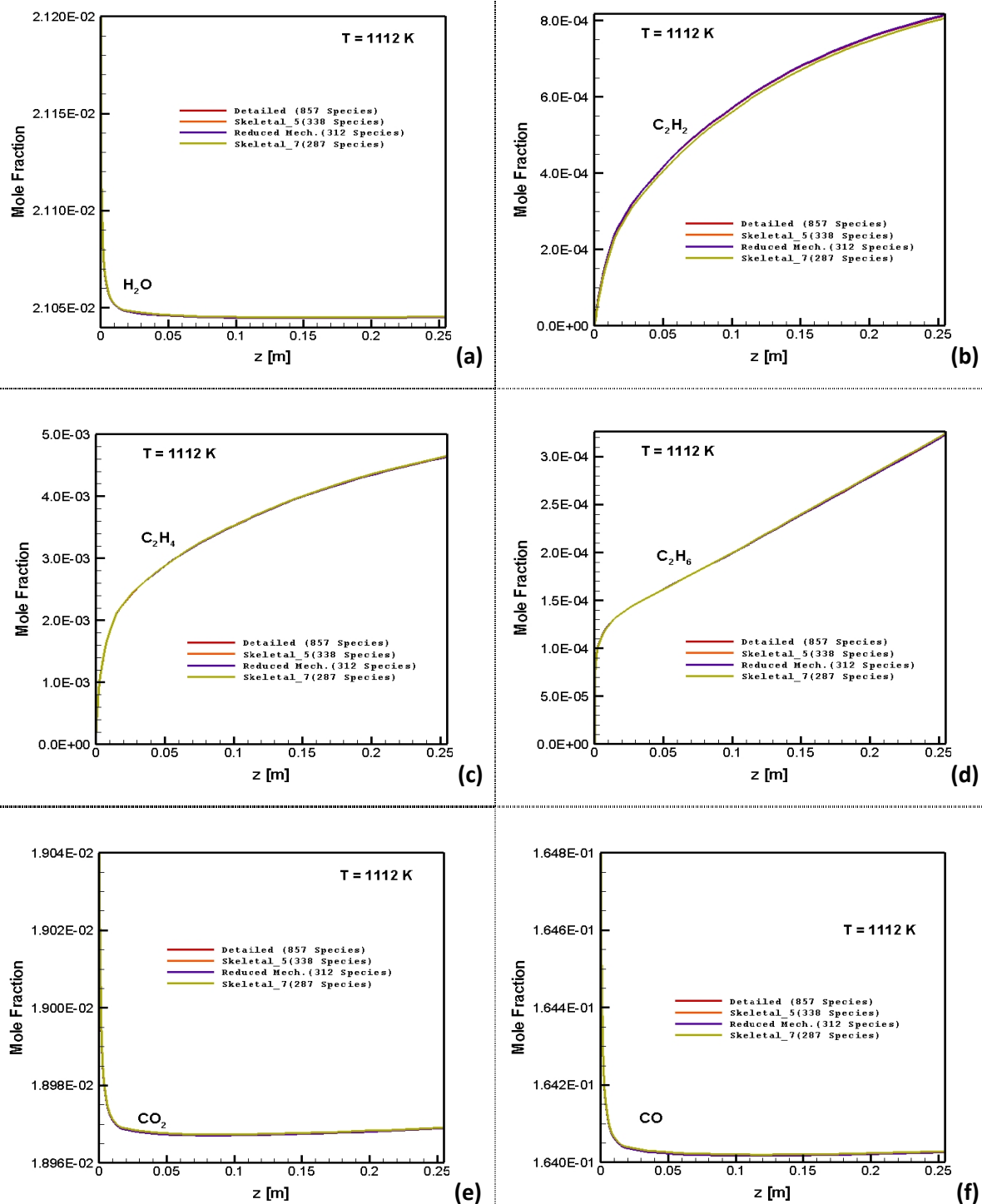
Figure A.11 : Numerically predicted species distribution as a function of axial position along the reactor: C/O=2.0, 1112 K: (a) H_2O. (b) C_2H_2. (c) C_2H_4. (d) C_2H_6. (e) CO_2. (f) CO
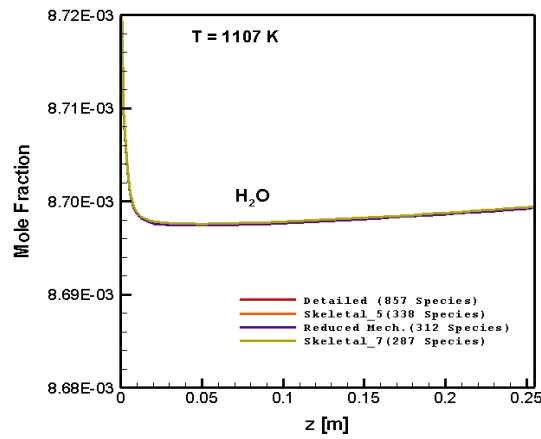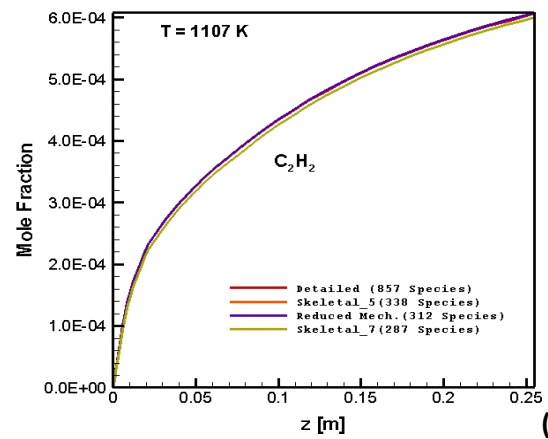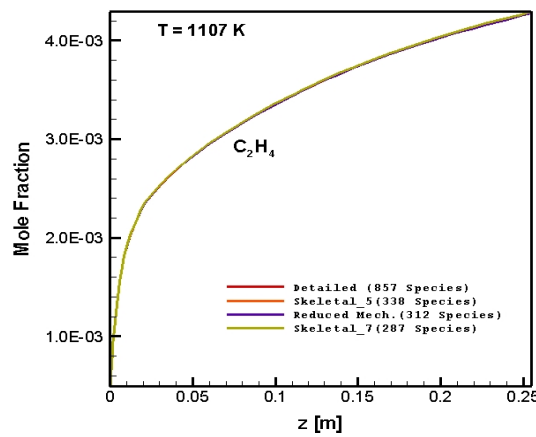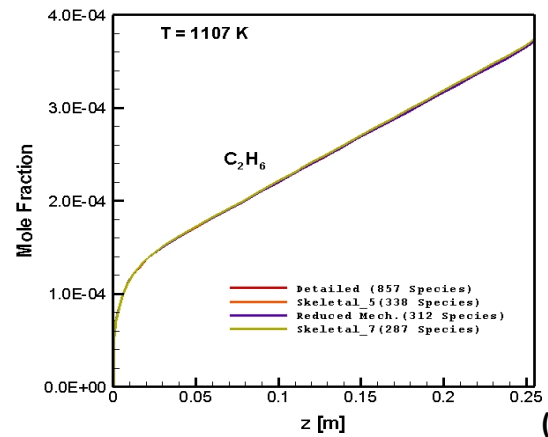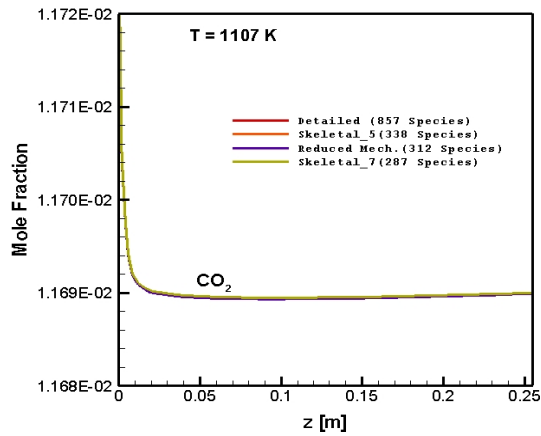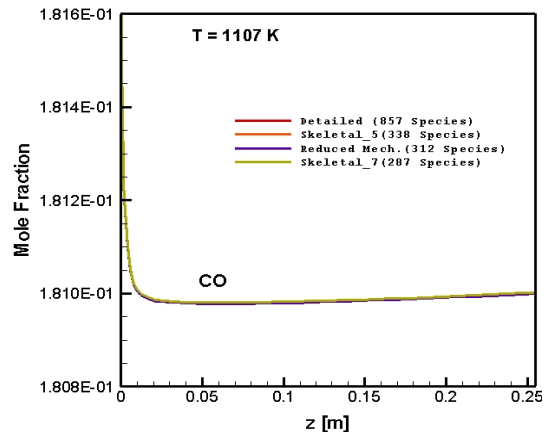
Figure A.12 : Numerically predicted species distribution as a function of axial position along the reactor: C/O=1.3, 1107 K: (a) H_2O. (b) C_2H_2. (c) C_2H_4. (d) C_2H_6. (e) CO_2. (f) CO
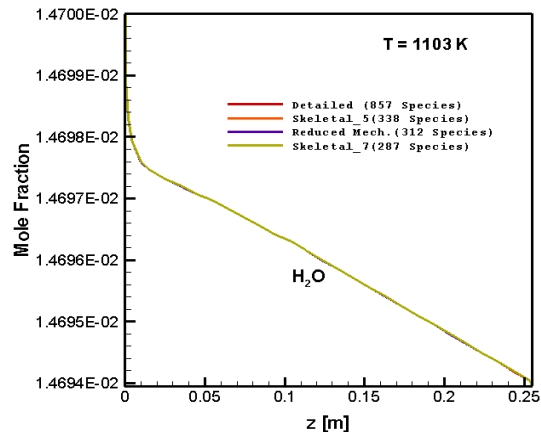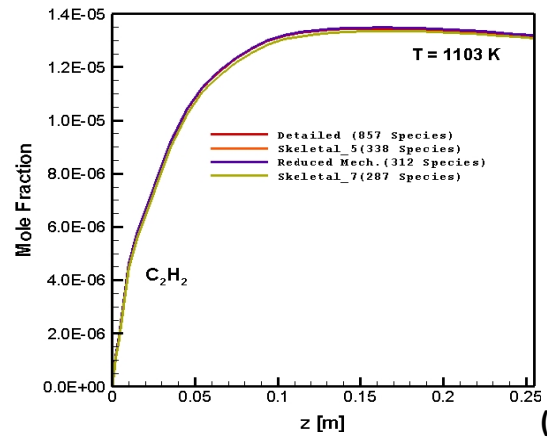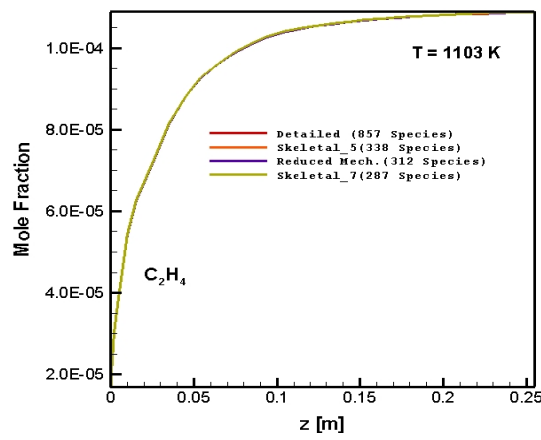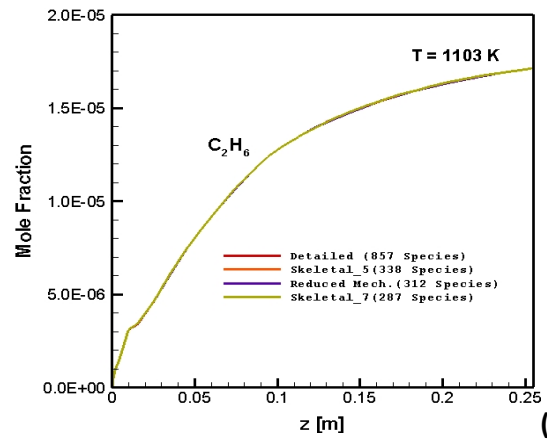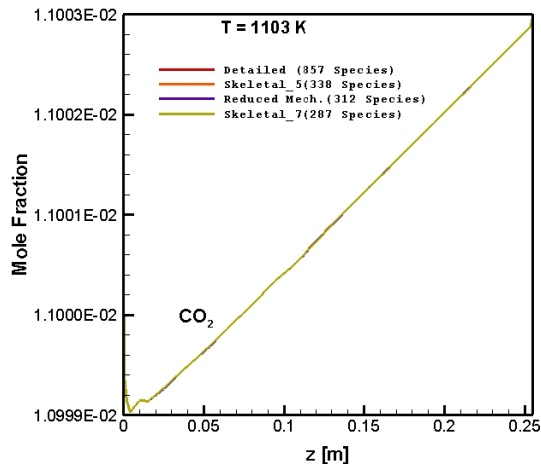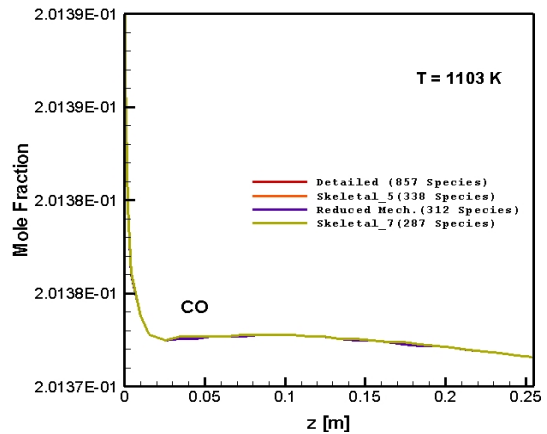
Figure A.13 : Numerically predicted species distribution as a function of axial position along the reactor: C/O=1.0, 1103 K: (a) H_2O. (b) C_2H_2. (c) C_2H_4. (d) C_2H_6. (e) CO_2. (f) CO

APPENDIX B

Table B.1 : List of 857 species of detailed LLNL i-octane reaction mechanism containing 7191 reactions

H	H2	O	O2	OH
H2O	N2	CO	HCO	CO2
CH3	CH4	HO2	H2O2	CH2O
CH3O	C2H6	C2H4	C2H5	CH2
CH	C2H	C2H2	C2H3	CH3OH
CH2OH	CH2CO	HCCO	C2H5OH	PC2H4OH
SC2H4OH	CH3CO	CH2CHO	CH3CHO	C3H4-A
C3H4-P	C3H6	C4H6	NC3H7	IC3H7
C3H8	IC4H7	IC4H8	C4H7	C4H8-2
C4H8-1	SC4H9	PC4H9	TC4H9	IC4H9
IC4H10	C4H10	CH3COCH3	CH3COCH2	C2H5CHO
C2H5CO	C5H9	C5H10-1	C5H10-2	IC5H12
AC5H11	BC5H11	CC5H11	DC5H11	AC5H10
BC5H10	CC5H10	IC5H9	NC5H12	C5H11-1
C5H11-2	C5H11-3	NEOC5H12	NEOC5H11	C2H5O
CH3O2	C2H5O2	CH3O2H	C2H5O2H	C2H3O1-2
CH3CO2	C2H4O1-2	C2H4O2H	O2C2H4OH	CH3CO3
CH3CO3H	C2H3CO	C2H3CHO	C3H5O	C3H6OOH1-2
C3H6OOH1-3	C3H6OOH2-1	C3H6OOH1-2O2	C3H6OOH1-3O2	C3H6OOH2-1O2
NC3H7O	IC3H7O	NC3H7O2H	IC3H7O2H	NC3H7O2
IC3H7O2	C3H6O1-3	IC4H8O	IC4H8OH	IO2C4H8OH
IC4H7O	C4H7O	C4H8OH-1	C4H8OH-2	C4H8OH-1O2
C4H8OH-2O2	C4H8OOH1-2O2	C4H8OOH1-3O2	C4H8OOH1-4O2	C4H8OOH2-1O2
C4H8OOH2-3O2	C4H8OOH2-4O2	TC4H8OOH-IO2	IC4H8OOH-IO2	IC4H8OOH-TO2
C4H8OOH1-2	C4H8OOH1-3	C4H8OOH1-4	C4H8OOH2-1	C4H8OOH2-3
C4H8OOH2-4	IC4H8O2H-I	IC4H8O2H-T	TC4H8O2H-I	C4H8O1-2

128

C4H8O1-3	C4H8O1-4	C4H8O2-3	CC4H8O	PC4H9O
SC4H9O	IC4H9O	TC4H9O	PC4H9O2H	SC4H9O2H
IC4H9O2H	TC4H9O2H	TC4H9O2	IC4H9O2	SC4H9O2
PC4H9O2	CH3COCH2O2	CH3COCH2O2H	CH3COCH2O	NEOC5KETOX
NEOC5KEJOL	AC5H11O2	BC5H11O2	CC5H11O2	DC5H11O2
AC5H11O2H	BC5H11O2H	CC5H11O2H	DC5H11O2H	AC5H11O
BC5H11O	CC5H11O	DC5H11O	AC5H10OOH-A	AC5H10OOH-B
AC5H10OOH-C	AC5H10OOH-D	BC5H10OOH-A	BC5H10OOH-C	BC5H10OOH-D
CC5H10OOH-A	CC5H10OOH-B	CC5H10OOH-D	DC5H10OOH-A	DC5H10OOH-B
DC5H10OOH-C	AC5H10OOH-AO2	AC5H10OOH-BO2	AC5H10OOH-CO2	AC5H10OOH-DO2
BC5H10OOH-AO2	BC5H10OOH-CO2	BC5H10OOH-DO2	CC5H10OOH-AO2	CC5H10OOH-BO2
CC5H10OOH-DO2	DC5H10OOH-AO2	DC5H10OOH-BO2	DC5H10OOH-CO2	A-AC5H10O
A-BC5H10O	A-CC5H10O	A-DC5H10O	B-CC5H10O	B-DC5H10O
C-DC5H10O	C5H11O2-1	C5H11O2-2	C5H11O2-3	C5H11O2H-1
C5H11O2H-2	C5H11O2H-3	C5H11O-1	C5H11O-2	C5H11O-3
C5H10OOH1-2	C5H10OOH1-3	C5H10OOH1-4	C5H10OOH1-5	C5H10OOH2-1
C5H10OOH2-3	C5H10OOH2-4	C5H10OOH2-5	C5H10OOH3-2	C5H10OOH3-1
C5H10OOH1-2O2	C5H10OOH1-3O2	C5H10OOH1-4O2	C5H10OOH1-5O2	C5H10OOH2-1O2
C5H10OOH2-3O2	C5H10OOH2-4O2	C5H10OOH2-5O2	C5H10OOH3-1O2	C5H10OOH3-2O2
C5H10O1-2	C5H10O1-3	C5H10O1-4	C5H10O1-5	C5H10O2-3
C5H10O2-4	NEOC5H11O2	NEOC5H11O2H	NEOC5H11O	NEOC5H10OOH
NEOC5H10OOH-O2	NEO-C5H10O	C3H5-A	C3H5-S	C3H5-T
C3H3	C3H2	C3H6O1-2	HO2CHO	O2CHO
OCHO	CH2(S)	C3KET12	C3KET13	C3KET21
NC4KET12	NC4KET13	NC4KET14	NC4KET21	NC4KET23
NC4KET24	IC4KETII	IC4KETIT	NEOC5KET	NC5KET12
NC5KET13	NC5KET14	NC5KET15	NC5KET21	NC5KET23
NC5KET24	NC5KET25	NC5KET31	NC5KET32	IC5KETAA
IC5KETAB	IC5KETAC	IC5KETAD	IC5KETCA	IC5KETCB

IC5KETCD	IC5KETDA	IC5KETDB	IC5KETDC	IC4H7-I1
C3H6OH	HOC3H6O2	O2C2H4O2H	CH2O2HCHO	IC4H7OOH
IC3H5CHO	TC3H6OCHO	TC3H6CHO	IC3H7CHO	IC4H7OH
IC3H6CO	IC4H6OH	IC3H5CO	IC3H7CO	TC3H6O2CHO
TC3H6O2HCO	IC3H5O2HCHO	TC3H6OHCHO	TC3H6OH	IC3H5OH
TC4H8CHO	O2C4H8CHO	O2HC4H8CO	O2HC4H7CHO	C3H5OH
CH2CCH2OH	NC3H7CHO	NC3H7CO	CH2CH2COCH3	C2H5COCH2
C2H5COCH3	CH2CHOOHCOCH3	CH3CHOOHCOCH3	CH3CHOOCOCH3	CH3CHCOCH3
C2H3COCH3	CH3CHCO	CH2CH2CHO	C3H6CHO-3	C3H6CHO-2
C2H5CHCO	IC3H5COCH3	IC3H5COCH2	AC3H4COCH3	SC3H5COCH2
CH3CHOCHO	CH3CHCHO	SC3H5CHO	SC3H5CO	IC3H6CHO
C3H6CHO-1	C2H5COC2H5	C2H5COC2H4P	C2H5COC2H4S	C2H5COC2H3
PC2H4COC2H3	SC2H4COC2H3	IC3H6CHCHO	IC3H6CHCO	AC3H5CHCHO
IC3H6CHCOCH3	AC3H5CHCOCH3	IC3H6CHCOCH2	NC3H7COCH3	NC3H7COCH2
C3H6COCH3-1	C3H6COCH3-2	C3H6COCH3-3	IC3H7COCH3	IC3H7COCH2
IC3H6COCH3	TC3H6COCH3	NC3H7COC2H5	C3H6COC2H5-1	C3H6COC2H5-2
C3H6COC2H5-3	NC3H7COC2H4P	NC3H7COC2H4S	IC3H7COC2H5	IC3H6COC2H5
TC3H6COC2H5	IC3H7COC2H4P	IC3H7COC2H4S	IC3H7COC2H3	IC3H6COC2H3
TC3H6COC2H3	IC3H5COC2H5	AC3H4COC2H5	IC3H5COC2H4P	IC3H5COC2H4S
NC4H9CHO	NC4H9CO	AC3H5CHO	AC3H5CO	C2H3CHCHO
C4H8CHO-1	C4H8CHO-2	C4H8CHO-3	C4H8CHO-4	NEOC5H9Q2
NEOC5H9Q2-N	IC4H6Q2-II	HOCH2O	HOCHO	IC6H14
AC6H13	BC6H13	CC6H13	DC6H13	EC6H13
AC6H12	BC6H12	CC6H12	DC6H12	IC6H11
AC6H13O2	BC6H13O2	CC6H13O2	DC6H13O2	EC6H13O2
AC6H13O2H	BC6H13O2H	CC6H13O2H	DC6H13O2H	EC6H13O2H
AC6H13O	BC6H13O	CC6H13O	DC6H13O	EC6H13O
AC6H12OOH-A	AC6H12OOH-B	AC6H12OOH-C	AC6H12OOH-D	AC6H12OOH-E
BC6H12OOH-A	BC6H12OOH-C	BC6H12OOH-D	BC6H12OOH-E	CC6H12OOH-A

CC6H12OOH-B	CC6H12OOH-D	CC6H12OOH-E	DC6H12OOH-A	DC6H12OOH-B
DC6H12OOH-C	DC6H12OOH-E	EC6H12OOH-A	EC6H12OOH-B	EC6H12OOH-C
EC6H12OOH-D	A-AC6H12O	A-BC6H12O	A-CC6H12O	A-DC6H12O
A-EC6H12O	B-CC6H12O	B-DC6H12O	B-EC6H12O	C-DC6H12O
C-EC6H12O	D-EC6H12O	AC6H12OOH-AO2	AC6H12OOH-BO2	AC6H12OOH-CO2
AC6H12OOH-DO2	AC6H12OOH-EO2	BC6H12OOH-AO2	BC6H12OOH-CO2	BC6H12OOH-DO2
BC6H12OOH-EO2	CC6H12OOH-AO2	CC6H12OOH-BO2	CC6H12OOH-DO2	CC6H12OOH-EO2
DC6H12OOH-AO2	DC6H12OOH-BO2	DC6H12OOH-CO2	DC6H12OOH-EO2	EC6H12OOH-AO2
EC6H12OOH-BO2	EC6H12OOH-CO2	EC6H12OOH-DO2	IC6KETAA	IC6KETAB
IC6KETAC	IC6KETAD	IC6KETAE	IC6KETCA	IC6KETCB
IC6KETCD	IC6KETCE	IC6KETDA	IC6KETDB	IC6KETDC
IC6KETDE	IC6KETEA	IC6KETEB	IC6KETEC	IC6KETED
NC4H9CHO-2	NC4H9CO-2	C4H8CHO1-2	C4H8CHO2-2	C4H8CHO3-2
C4H8CHO4-2	IC4H9CHO	IC4H9CO	IC3H6CH2CHO	TC3H6CH2CHO
IC3H7CHCHO	IC5H11CHO	IC5H11CO	AC5H10CHO	BC5H10CHO
CC5H10CHO	DC5H10CHO	C4H7CHO1-4	C4H7CO1-4	C4H6CHO1-43
C4H6CHO1-44	C4H7CHO2-1	C4H7CO2-1	C4H6CHO2-11	NC5H11CHO-2
NC5H11CO-2	C5H10CHO1-2	C5H10CHO2-2	C5H10CHO3-2	C5H10CHO4-2
C5H10CHO5-2	IC4H9COCH3	IC4H9COCH2	IC3H6CH2COCH3	IC3H7CHCOCH3
TC3H6CH2COCH3	NEOC6H14	FC6H13	GC6H13	HC6H13
NEOC6H12	NEOC6H11	FC6H13O2	GC6H13O2	HC6H13O2
FC6H13O2H	GC6H13O2H	HC6H13O2H	FC6H13O	GC6H13O
HC6H13O	FC6H12OOH-F	FC6H12OOH-G	FC6H12OOH-H	GC6H12OOH-F
GC6H12OOH-H	HC6H12OOH-F	HC6H12OOH-G	FC6H12OOH-FO2	FC6H12OOH-GO2
FC6H12OOH-HO2	GC6H12OOH-FO2	GC6H12OOH-HO2	HC6H12OOH-FO2	HC6H12OOH-GO2
F-FC6H12O	F-GC6H12O	F-HC6H12O	G-HC6H12O	NEOC6KETFF
NEOC6KETFG	NEOC6KETFH	NEOC6KETGF	NEOC6KETGH	NEOC6KETHF
NEOC6KETHG	TC4H9CHO	TC4H9CO	NEOC5H11CHO	NEOC5H11CO
TC4H9CHCHO	TC4H8CH2CHO	IC4H7CHO	IC4H7CO	AC3H4CH2CHO

131

IC3H5CHCHO	IC5H11CHO-B	IC5H11CO-B	IC5H10CHO-BA	IC5H10CHO-BC
IC5H10CHO-BD	C4H7CHO1-2	C4H7CO1-2	C4H6CHO1-23	C4H6CHO1-24
C4H7CHO2-2	C4H7CO2-2	C4H6CHO2-21	C4H6CHO2-24	CH2CCHCH3
TC4H9COCH3	TC4H9COCH2	TC4H8COCH3	CH2CCHO	C7H162-4
XC7H15	YC7H15	ZC7H15	XC7H14	YC7H14
XC7H13	XC7H15O2	YC7H15O2	ZC7H15O2	XC7H15O2H
YC7H15O2H	ZC7H15O2H	XC7H15O	YC7H15O	ZC7H15O
XC7H14OOH-X1	XC7H14OOH-Y1	XC7H14OOH-Z	XC7H14OOH-Y2	XC7H14OOH-X2
YC7H14OOH-X1	YC7H14OOH-Z	YC7H14OOH-Y2	YC7H14OOH-X2	ZC7H14OOH-X
ZC7H14OOH-Y	XC7H14OOH-X1O2	XC7H14OOH-X2O2	XC7H14OOH-Y1O2	XC7H14OOH-Y2O2
XC7H14OOH-ZO2	YC7H14OOH-X1O2	YC7H14OOH-X2O2	YC7H14OOH-Y2O2	YC7H14OOH-ZO2
ZC7H14OOH-XO2	ZC7H14OOH-YO2	X-X1C7H14O	X-X2C7H14O	X-Y1C7H14O
X-Y2C7H14O	X-ZC7H14O	Y-YC7H14O	Y-ZC7H14O	C7KET24XX1
C7KET24XY1	C7KET24XZ	C7KET24XY2	C7KET24XX2	C7KET24ZX
C7KET24ZY	NEOC7H16	NC7H15	OC7H15	PC7H15
QC7H15	OC7H14	PC7H14	PC7H13	NC7H15O2
OC7H15O2	PC7H15O2	QC7H15O2	NC7H15O2H	OC7H15O2H
PC7H15O2H	QC7H15O2H	NC7H15O	OC7H15O	PC7H15O
QC7H15O	NC7H14OOH-N2	NC7H14OOH-Q	QC7H14OOH-N	NC7H14OOH-O
NC7H14OOH-P	QC7H14OOH-O	QC7H14OOH-P	OC7H14OOH-N	OC7H14OOH-Q
PC7H14OOH-N	PC7H14OOH-Q	OC7H14OOH-P	PC7H14OOH-O	NC7H14OOH-N2O2
NC7H14OOH-QO2	QC7H14OOH-NO2	NC7H14OOH-OO2	NC7H14OOH-PO2	QC7H14OOH-OO2
QC7H14OOH-PO2	OC7H14OOH-NO2	OC7H14OOH-QO2	PC7H14OOH-NO2	PC7H14OOH-QO2
OC7H14OOH-PO2	PC7H14OOH-OO2	N-NC7H14O	N-OC7H14O	N-PC7H14O
N-QC7H14O	O-PC7H14O	O-QC7H14O	P-QC7H14O	NEOC7KETNN
NEOC7KETNO	NEOC7KETNP	NEOC7KETNQ	NEOC7KETON	NEOC7KETOP
NEOC7KETOQ	NEOC7KETPN	NEOC7KETPO	NEOC7KETPQ	NEOC7KETQN
NEOC7KETQO	NEOC7KETQP	IC8H18	AC8H17	BC8H17
CC8H17	DC8H17	IC8H16	JC8H16	IC8H14

IC8H15	AC8H17O2	BC8H17O2	CC8H17O2	DC8H17O2
AC8H17O2H	BC8H17O2H	CC8H17O2H	DC8H17O2H	AC8H17O
BC8H17O	CC8H17O	DC8H17O	AC8H16OOH-A	AC8H16OOH-B
AC8H16OOH-C	AC8H16OOH-D	BC8H16OOH-C	BC8H16OOH-A	BC8H16OOH-D
CC8H16OOH-D	CC8H16OOH-B	CC8H16OOH-A	DC8H16OOH-C	DC8H16OOH-D
DC8H16OOH-B	DC8H16OOH-A	IC8ETERAA	IC8ETERAB	IC8ETERAC
IC8ETERAD	IC8ETERBC	IC8ETERBD	IC8ETERCD	IC8ETERDD
AC8H16OOH-AO2	AC8H16OOH-BO2	AC8H16OOH-CO2	AC8H16OOH-DO2	BC8H16OOH-CO2
BC8H16OOH-AO2	BC8H16OOH-DO2	CC8H16OOH-DO2	CC8H16OOH-BO2	CC8H16OOH-AO2
DC8H16OOH-CO2	DC8H16OOH-DO2	DC8H16OOH-BO2	DC8H16OOH-AO2	IC8KETAA
IC8KETAB	IC8KETAC	IC8KETAD	IC8KETBA	IC8KETBC
IC8KETBD	IC8KETDA	IC8KETDB	IC8KETDC	IC8KETDD
IC6H13CHO-B	IC6H13CO-B	AC6H12CHO-B	CC6H12CHO-B	DC6H12CHO-B
EC6H12CHO-B	IC6H13CHO-D	IC6H13CO-D	AC6H12CHO-D	BC6H12CHO-D
CC6H12CHO-D	DC6H12CHO-D	EC6H12CHO-D	IC3H7COC3H7-I	IC3H7COC3H6-I
IC3H7COC3H6-T	TC4H9COC2H5	TC4H8COC2H5	TC4H9COC2H4S	TC4H9COC2H4P
NEOC5H11COCH3	NEOC5H10COCH3	TC4H9CHCOCH3	NEOC5H11COCH2	NEOC6H13CHO
NEOC6H13CO	FC6H12CHO	GC6H12CHO	HC6H12CHO	IC4H7COCH3
IC4H7COCH2	IC3H5CHCOCH3	AC3H4CH2COCH3	XC7H13OOH-X1	XC7H13O-X1
YC7H13OOH-X1	YC7H13O-X1	OC7H13OOH-N	OC7H13O-N	XC7H13OOH-Z
XC7H13O-Z	PC7H13OOH-O	PC7H13O-O	OC7H13OOH-Q	OC7H13O-Q
YC7H13OOH-X2	YC7H13O-X2	AC3H5OOH	NEOC6H11-H	CC6H11O-B
XC7H14OH-Y	YC7H14OH-X	ZC7H14OH-Y	YC7H14OH-Z	IC4H7OH-I1
OC7H14OH-P	PC7H14OH-O	QC7H14OH-P	PC7H14OH-Q	XC7H14OH-YO2
XC7H14O-YO2H	YC7H14OH-XO2	YC7H14O-XO2H	ZC7H14OH-YO2	ZC7H14O-YO2H
YC7H14OH-ZO2	YC7H14O-ZO2H	OC7H14OH-PO2	OC7H14O-PO2H	PC7H14OH-OO2
PC7H14O-OO2H	QC7H14OH-PO2	QC7H14O-PO2H	PC7H14OH-QO2	PC7H14O-QO2H
CC8H16OH-B	BC8H16OH-C	CC8H16OH-D	DC8H16OH-C	CC8H16OH-BO2
CC8H16O-BO2H	BC8H16OH-CO2	BC8H16O-CO2H	CC8H16OH-DO2	CC8H16O-DO2H

DC8H16OH-CO2   DC8H16O-CO2H

Table B.2 : List of 312 species of the reduced mechanism containing 2903 reactions for the description of catalytic partial oxidation of i-octane for C/O=1.6, T=1005.78 K

H	H2	O	O2	OH
H2O	N2	CO	HCO	CO2
CH3	CH4	HO2	H2O2	CH2O
CH3O	C2H6	C2H4	C2H5	CH2
C2H	C2H2	C2H3	CH3OH	CH2OH
CH2CO	HCCO	C2H5OH	PC2H4OH	SC2H4OH
CH3CO	CH2CHO	CH3CHO	C3H4-A	C3H4-P
C3H6	C4H6	NC3H7	IC3H7	C3H8
IC4H7	IC4H8	C4H7	C4H8-2	C4H8-1
SC4H9	PC4H9	TC4H9	IC4H9	IC4H10
C4H10	CH3COCH3	CH3COCH2	C2H5CHO	C2H5CO
C5H9	C5H10-1	C5H10-2	IC5H12	AC5H11
BC5H11	CC5H11	DC5H11	AC5H10	BC5H10
CC5H10	IC5H9	C5H11-1	C5H11-2	C5H11-3
NEOC5H12	NEOC5H11	C2H5O	CH3O2	C2H5O2
CH3O2H	C2H3O1-2	C2H4O1-2	C2H3CO	C2H3CHO
C3H5O	C3H6OOH1-2	C3H6OOH2-1	C3H6OOH1-2O2	C3H6OOH2-1O2
NC3H7O	IC3H7O	IC3H7O2H	NC3H7O2	IC3H7O2
C3H6O1-3	IC4H8O	IC4H8OH	IO2C4H8OH	IC4H7O
C4H7O	C4H8OH-1	C4H8OOH2-3O2	C4H8OOH2-4O2	IC4H8OOH-IO2
IC4H8OOH-TO2	C4H8OOH1-2	C4H8OOH2-1	C4H8OOH2-3	IC4H8O2H-T
TC4H8O2H-I	C4H8O1-2	C4H8O1-3	C4H8O1-4	CC4H8O
IC4H9O	TC4H9O	TC4H9O2	IC4H9O2	SC4H9O2
AC5H11O2	BC5H11O2	CC5H11O2	BC5H10OOH-A	BC5H10OOH-C
BC5H10OOH-D	CC5H10OOH-B	A-AC5H10O	A-BC5H10O	B-CC5H10O

134

B-DC5H10O	C5H10O1-3	NEOC5H11O2	NEOC5H11O	NEOC5H10OOH
NEOC5H10OOH-O2	NEO-C5H10O	C3H5-A	C3H5-S	C3H5-T
C3H3	C3H2	C3H6O1-2	OCHO	CH2(S)
NC4KET24	IC4KETII	IC4KETIT	IC4H7-I1	O2C2H4O2H
CH2O2HCHO	IC3H5CHO	TC3H6OCHO	TC3H6CHO	IC3H7CHO
IC4H7OH	IC3H6CO	IC4H6OH	IC3H5CO	IC3H7CO
TC3H6O2CHO	IC3H5O2HCHO	TC3H6OHCHO	TC3H6OH	IC3H5OH
O2C4H8CHO	O2HC4H7CHO	C3H5OH	CH2CCH2OH	CH2CHOOHCOCH3
CH3CHOOHCOCH3	C2H3COCH3	CH3CHCO	IC3H5COCH3	AC3H4COCH3
SC3H5COCH2	CH3CHCHO	IC3H6CHO	IC3H6CHCO	AC3H5CHCHO
AC3H5CHO	AC3H5CO	C4H8CHO-3	HOCH2O	HOCHO
AC6H13	BC6H13	DC6H13	EC6H13	AC6H12
BC6H12	CC6H12	DC6H12	IC6H11	CC6H13O
CC6H12OOH-B	CC6H12OOH-D	CC6H12OOH-E	DC6H12OOH-B	DC6H12OOH-C
DC6H12OOH-E	A-AC6H12O	A-BC6H12O	B-DC6H12O	C-DC6H12O
C-EC6H12O	D-EC6H12O	NEOC6H14	FC6H13	GC6H13
HC6H13	NEOC6H12	NEOC6H11	F-FC6H12O	TC4H9CHO
TC4H9CO	IC4H7CHO	IC4H7CO	C4H7CO2-2	XC7H15
YC7H15	ZC7H15	XC7H14	YC7H14	XC7H13
XC7H14OOH-Y1	XC7H14OOH-Z	XC7H14OOH-Y2	YC7H14OOH-X1	YC7H14OOH-Y2
ZC7H14OOH-X	ZC7H14OOH-Y	X-Y1C7H14O	X-Y2C7H14O	X-ZC7H14O
Y-ZC7H14O	C7KET24ZX	C7KET24ZY	NC7H15	OC7H15
PC7H15	QC7H15	OC7H14	PC7H14	PC7H13
OC7H15O	NC7H14OOH-O	OC7H14OOH-N	OC7H14OOH-Q	PC7H14OOH-N
OC7H14OOH-P	PC7H14OOH-OO2	N-OC7H14O	N-PC7H14O	O-PC7H14O
O-QC7H14O	NEOC7KETON	NEOC7KETOP	NEOC7KETPO	IC8H18
AC8H17	BC8H17	CC8H17	DC8H17	IC8H16
JC8H16	IC8H14	IC8H15	AC8H17O2H	BC8H17O2H
BC8H17O	AC8H16OOH-C	BC8H16OOH-C	BC8H16OOH-A	BC8H16OOH-D

135

| CC8H16OOH-B | DC8H16OOH-C | DC8H16OOH-D | IC8ETERAB | IC8ETERBC |
| CC8H16OOH-B | DC8H16OOH-C | DC8H16OOH-D | IC8ETERAB | IC8ETERBC |

CC8H16OOH-B	DC8H16OOH-C	DC8H16OOH-D	IC8ETERAB	IC8ETERBC
IC8ETERBD	IC8ETERCD	IC8ETERDD	NEOC5H11COCH3	IC4H7COCH3
IC4H7COCH2	XC7H13O-Z	PC7H13O-O	CC6H11O-B	XC7H14OH-Y
YC7H14OH-X	ZC7H14OH-Y	YC7H14OH-Z	IC4H7OH-I1	OC7H14OH-P
PC7H14OH-O	QC7H14OH-P	PC7H14OH-Q	XC7H14OH-YO2	YC7H14OH-XO2
ZC7H14OH-YO2	ZC7H14O-YO2H	YC7H14OH-ZO2	OC7H14OH-PO2	PC7H14OH-OO2
PC7H14O-OO2H	PC7H14OH-QO2	CC8H16OH-B	BC8H16OH-C	CC8H16OH-D
DC8H16OH-C	CC8H16OH-BO2	BC8H16OH-CO2	BC8H16O-CO2H	CC8H16OH-DO2
CC8H16O-DO2H	DC8H16OH-CO2			

Table B.3 : List of 320 species of the reduced mechanism containing 2933 reactions for the description of catalytic partial oxidation of i-octane for C/O=2.0, T=998.26 K

H	H2	O	O2	OH
H2O	N2	CO	HCO	CO2
CH3	CH4	HO2	H2O2	CH2O
CH3O	C2H6	C2H4	C2H5	CH2
C2H	C2H2	C2H3	CH3OH	CH2OH
CH2CO	HCCO	C2H5OH	PC2H4OH	SC2H4OH
CH3CO	CH2CHO	CH3CHO	C3H4-A	C3H4-P
C3H6	C4H6	NC3H7	IC3H7	C3H8
IC4H7	IC4H8	C4H7	C4H8-2	C4H8-1
SC4H9	PC4H9	TC4H9	IC4H9	IC4H10
C4H10	CH3COCH3	CH3COCH2	C2H5CHO	C2H5CO
C5H9	C5H10-1	C5H10-2	IC5H12	AC5H11
BC5H11	CC5H11	DC5H11	AC5H10	BC5H10
CC5H10	IC5H9	C5H11-1	C5H11-2	C5H11-3
NEOC5H12	NEOC5H11	C2H5O	CH3O2	C2H5O2
CH3O2H	C2H3O1-2	C2H4O1-2	C2H3CO	C2H3CHO
C3H5O	C3H6OOH1-2	C3H6OOH2-1	C3H6OOH1-2O2	C3H6OOH2-1O2

NC3H7O	IC3H7O	IC3H7O2H	NC3H7O2	IC3H7O2
C3H6O1-3	IC4H8O	IC4H8OH	IO2C4H8OH	IC4H7O
C4H7O	C4H8OH-1	C4H8OOH2-3O2	C4H8OOH2-4O2	IC4H8OOH-IO2
IC4H8OOH-TO2	C4H8OOH1-2	C4H8OOH2-1	C4H8OOH2-3	IC4H8O2H-T
TC4H8O2H-I	C4H8O1-2	C4H8O1-3	C4H8O1-4	CC4H8O
IC4H9O	TC4H9O	TC4H9O2	IC4H9O2	SC4H9O2
AC5H11O2	BC5H11O2	CC5H11O2	BC5H10OOH-A	BC5H10OOH-C
BC5H10OOH-D	CC5H10OOH-B	A-AC5H10O	A-BC5H10O	B-CC5H10O
B-DC5H10O	C5H10O1-3	NEOC5H11O2	NEOC5H11O	NEOC5H10OOH
NEOC5H10OOH-O2	NEO-C5H10O	C3H5-A	C3H5-S	C3H5-T
C3H3	C3H2	C3H6O1-2	OCHO	CH2(S)
NC4KET24	IC4KETII	IC4KETIT	IC4H7-I1	O2C2H4O2H
CH2O2HCHO	IC3H5CHO	TC3H6OCHO	TC3H6CHO	IC3H7CHO
IC4H7OH	IC3H6CO	IC4H6OH	IC3H5CO	IC3H7CO
TC3H6O2CHO	IC3H5O2HCHO	TC3H6OHCHO	TC3H6OH	IC3H5OH
O2C4H8CHO	O2HC4H7CHO	C3H5OH	CH2CCH2OH	CH2CHOOHCOCH3
CH3CHOOHCOCH3	C2H3COCH3	CH3CHCO	IC3H5COCH3	AC3H4COCH3
SC3H5COCH2	CH3CHCHO	IC3H6CHO	IC3H6CHCO	AC3H5CHCHO
AC3H5CHO	AC3H5CO	C4H8CHO-3	HOCH2O	HOCHO
AC6H13	BC6H13	DC6H13	EC6H13	AC6H12
BC6H12	CC6H12	DC6H12	IC6H11	CC6H13O
BC6H12OOH-C	CC6H12OOH-B	CC6H12OOH-D	CC6H12OOH-E	DC6H12OOH-B
DC6H12OOH-C	DC6H12OOH-E	A-AC6H12O	A-BC6H12O	B-DC6H12O
C-DC6H12O	C-EC6H12O	D-EC6H12O	NEOC6H14	FC6H13
GC6H13	HC6H13	NEOC6H12	NEOC6H11	F-FC6H12O
TC4H9CHO	TC4H9CO	NEOC5H11CHO	IC4H7CHO	IC4H7CO
C4H7CO2-2	XC7H15	YC7H15	ZC7H15	XC7H14
YC7H14	XC7H13	ZC7H15O2	XC7H14OOH-Y1	XC7H14OOH-Z
XC7H14OOH-Y2	YC7H14OOH-X1	YC7H14OOH-Z	YC7H14OOH-Y2	ZC7H14OOH-X

ZC7H14OOH-Y	X-Y1C7H14O	X-Y2C7H14O	X-ZC7H14O	Y-ZC7H14O
C7KET24ZX	C7KET24ZY	NC7H15	OC7H15	PC7H15
QC7H15	OC7H14	PC7H14	PC7H13	OC7H15O
NC7H14OOH-O	QC7H14OOH-P	OC7H14OOH-N	OC7H14OOH-Q	PC7H14OOH-N
OC7H14OOH-P	PC7H14OOH-O	PC7H14OOH-OO2	N-OC7H14O	N-PC7H14O
O-PC7H14O	O-QC7H14O	NEOC7KETON	NEOC7KETOP	NEOC7KETPO
IC8H18	AC8H17	BC8H17	CC8H17	DC8H17
IC8H16	JC8H16	IC8H14	IC8H15	DC8H17O2
AC8H17O2H	BC8H17O2H	BC8H17O	AC8H16OOH-C	BC8H16OOH-C
BC8H16OOH-A	BC8H16OOH-D	CC8H16OOH-D	CC8H16OOH-B	DC8H16OOH-C
DC8H16OOH-D	IC8ETERAB	IC8ETERBC	IC8ETERBD	IC8ETERCD
IC8ETERDD	NEOC5H11COCH3	IC4H7COCH3	IC4H7COCH2	XC7H13O-Z
PC7H13O-O	CC6H11O-B	XC7H14OH-Y	YC7H14OH-X	ZC7H14OH-Y
YC7H14OH-Z	IC4H7OH-I1	OC7H14OH-P	PC7H14OH-O	QC7H14OH-P
PC7H14OH-Q	XC7H14OH-YO2	YC7H14OH-XO2	ZC7H14OH-YO2	ZC7H14O-YO2H
YC7H14OH-ZO2	OC7H14OH-PO2	PC7H14OH-OO2	PC7H14O-OO2H	PC7H14OH-QO2
CC8H16OH-B	BC8H16OH-C	CC8H16OH-D	DC8H16OH-C	CC8H16OH-BO2
BC8H16OH-CO2	BC8H16O-CO2H	CC8H16OH-DO2	CC8H16O-DO2H	DC8H16OH-CO2

Table B.4 : List of 320 species of the reduced mechanism containing 3073 reactions for the description of catalytic partial oxidation of i-octane for C/O=1.2, T=1017.86 K

H	H2	O	O2	OH
H2O	N2	CO	HCO	CO2
CH3	CH4	HO2	H2O2	CH2O
CH3O	C2H6	C2H4	C2H5	CH2
C2H	C2H2	C2H3	CH3OH	CH2OH
CH2CO	HCCO	C2H5OH	PC2H4OH	SC2H4OH
CH3CO	CH2CHO	CH3CHO	C3H4-A	C3H4-P
C3H6	C4H6	NC3H7	IC3H7	C3H8

138

IC4H7	IC4H8	C4H7	C4H8-2	C4H8-1
SC4H9	PC4H9	TC4H9	IC4H9	IC4H10
C4H10	CH3COCH3	CH3COCH2	C2H5CHO	C2H5CO
C5H9	C5H10-1	C5H10-2	IC5H12	AC5H11
BC5H11	CC5H11	DC5H11	AC5H10	BC5H10
CC5H10	IC5H9	NC5H12	C5H11-1	C5H11-2
C5H11-3	NEOC5H12	NEOC5H11	C2H5O	CH3O2
C2H5O2	CH3O2H	C2H3O1-2	C2H4O1-2	C2H4O2H
C2H3CO	C2H3CHO	C3H5O	C3H6OOH1-2	C3H6OOH2-1
C3H6OOH1-2O2	C3H6OOH2-1O2	NC3H7O	IC3H7O	IC3H7O2H
NC3H7O2	IC3H7O2	C3H6O1-3	IC4H8O	IC4H8OH
IO2C4H8OH	IC4H7O	C4H7O	C4H8OH-1	C4H8OOH2-3O2
C4H8OOH2-4O2	IC4H8OOH-IO2	IC4H8OOH-TO2	C4H8OOH1-2	C4H8OOH2-1
C4H8OOH2-3	IC4H8O2H-T	TC4H8O2H-I	C4H8O1-2	C4H8O1-3
C4H8O1-4	CC4H8O	IC4H9O	TC4H9O	TC4H9O2
IC4H9O2	SC4H9O2	AC5H11O2	BC5H11O2	CC5H11O2
BC5H10OOH-A	BC5H10OOH-C	BC5H10OOH-D	CC5H10OOH-B	A-AC5H10O
A-BC5H10O	B-CC5H10O	B-DC5H10O	NEOC5H11O2	NEOC5H11O
NEOC5H10OOH	NEOC5H10OOH-O2	NEO-C5H10O	C3H5-A	C3H5-S
C3H5-T	C3H3	C3H2	C3H6O1-2	OCHO
CH2(S)	NC4KET24	IC4KETII	IC4KETIT	IC4H7-I1
HOC3H6O2	O2C2H4O2H	CH2O2HCHO	IC3H5CHO	TC3H6OCHO
TC3H6CHO	IC3H7CHO	IC4H7OH	IC3H6CO	IC4H6OH
IC3H5CO	IC3H7CO	TC3H6O2CHO	IC3H5O2HCHO	TC3H6OHCHO
TC3H6OH	IC3H5OH	O2C4H8CHO	O2HC4H7CHO	C3H5OH
CH2CCH2OH	CH2CHOOHCOCH3	CH3CHOOHCOCH3	CH3CHOOCOCH3	C2H3COCH3
CH3CHCO	IC3H5COCH3	AC3H4COCH3	SC3H5COCH2	CH3CHCHO
IC3H6CHO	IC3H6CHCO	AC3H5CHCHO	AC3H5CHO	AC3H5CO
C4H8CHO-3	HOCH2O	HOCHO	AC6H13	BC6H13

139

DC6H13	EC6H13	AC6H12	BC6H12	CC6H12
DC6H12	IC6H11	CC6H13O	BC6H12OOH-C	CC6H12OOH-B
CC6H12OOH-D	CC6H12OOH-E	DC6H12OOH-B	DC6H12OOH-C	DC6H12OOH-E
A-AC6H12O	A-BC6H12O	B-DC6H12O	C-DC6H12O	C-EC6H12O
D-EC6H12O	NEOC6H14	FC6H13	GC6H13	HC6H13
NEOC6H12	NEOC6H11	F-FC6H12O	TC4H9CHO	TC4H9CO
IC4H7CHO	IC4H7CO	C4H7CHO1-2	C4H7CO1-2	C4H7CO2-2
C7H162-4	XC7H15	YC7H15	ZC7H15	XC7H14
YC7H14	XC7H13	XC7H14OOH-Y1	XC7H14OOH-Z	XC7H14OOH-Y2
YC7H14OOH-X1	YC7H14OOH-Y2	ZC7H14OOH-X	ZC7H14OOH-Y	X-Y1C7H14O
X-Y2C7H14O	X-ZC7H14O	Y-ZC7H14O	C7KET24ZX	C7KET24ZY
NC7H15	OC7H15	PC7H15	QC7H15	OC7H14
PC7H14	PC7H13	OC7H15O	NC7H14OOH-O	OC7H14OOH-N
OC7H14OOH-Q	PC7H14OOH-N	OC7H14OOH-P	PC7H14OOH-OO2	N-OC7H14O
N-PC7H14O	O-PC7H14O	O-QC7H14O	NEOC7KETON	NEOC7KETOP
NEOC7KETPO	IC8H18	AC8H17	BC8H17	CC8H17
DC8H17	IC8H16	JC8H16	IC8H14	IC8H15
AC8H17O2H	BC8H17O2H	BC8H17O	AC8H16OOH-C	BC8H16OOH-C
BC8H16OOH-A	BC8H16OOH-D	CC8H16OOH-B	DC8H16OOH-C	DC8H16OOH-D
IC8ETERAB	IC8ETERBC	IC8ETERBD	IC8ETERCD	IC8ETERDD
NEOC5H11COCH3	IC4H7COCH3	IC4H7COCH2	XC7H13O-Z	PC7H13O-O
CC6H11O-B	XC7H14OH-Y	YC7H14OH-X	ZC7H14OH-Y	YC7H14OH-Z
IC4H7OH-I1	OC7H14OH-P	PC7H14OH-O	QC7H14OH-P	PC7H14OH-Q
XC7H14OH-YO2	YC7H14OH-XO2	ZC7H14OH-YO2	ZC7H14O-YO2H	YC7H14OH-ZO2
OC7H14OH-PO2	PC7H14OH-OO2	PC7H14O-OO2H	PC7H14OH-QO2	CC8H16OH-B
BC8H16OH-C	CC8H16OH-D	DC8H16OH-C	CC8H16OH-BO2	BC8H16OH-CO2
BC8H16O-CO2H	CC8H16OH-DO2	CC8H16O-DO2H	DC8H16OH-CO2	DC8H16O-CO2H

Table B.5 : List of 315 species of the reduced mechanism containing 3127 reactions for the description of catalytic partial oxidation of i-octane for C/O=0.8, T=1374.85 K

H	H2	O	O2	OH
H2O	N2	CO	HCO	CO2
CH3	CH4	HO2	H2O2	CH2O
CH3O	C2H6	C2H4	C2H5	CH2
C2H	C2H2	C2H3	CH3OH	CH2OH
CH2CO	HCCO	C2H5OH	PC2H4OH	SC2H4OH
CH3CO	CH2CHO	CH3CHO	C3H4-A	C3H4-P
C3H6	C4H6	NC3H7	IC3H7	C3H8
IC4H7	IC4H8	C4H7	C4H8-2	C4H8-1
SC4H9	PC4H9	TC4H9	IC4H9	IC4H10
C4H10	CH3COCH3	CH3COCH2	C2H5CHO	C2H5CO
C5H9	C5H10-1	C5H10-2	IC5H12	AC5H11
BC5H11	CC5H11	DC5H11	AC5H10	BC5H10
CC5H10	IC5H9	NC5H12	C5H11-1	C5H11-2
C5H11-3	NEOC5H12	NEOC5H11	C2H5O	CH3O2
C2H5O2	CH3O2H	C2H3O1-2	C2H4O1-2	C2H4O2H
CH3CO3H	C2H3CO	C2H3CHO	C3H5O	C3H6OOH1-2
C3H6OOH2-1	C3H6OOH1-2O2	C3H6OOH2-1O2	NC3H7O	IC3H7O
IC3H7O2H	NC3H7O2	IC3H7O2	C3H6O1-3	IC4H8O
IC4H8OH	IO2C4H8OH	IC4H7O	C4H7O	C4H8OOH2-3O2
C4H8OOH2-4O2	IC4H8OOH-IO2	IC4H8OOH-TO2	C4H8OOH1-2	C4H8OOH2-1
C4H8OOH2-3	IC4H8O2H-T	TC4H8O2H-I	C4H8O1-3	C4H8O1-4
C4H8O2-3	CC4H8O	PC4H9O	IC4H9O	TC4H9O
TC4H9O2	IC4H9O2	SC4H9O2	PC4H9O2	AC5H11O2
BC5H11O2	CC5H11O2	BC5H10OOH-A	BC5H10OOH-C	BC5H10OOH-D
CC5H10OOH-A	CC5H10OOH-B	CC5H10OOH-D	A-BC5H10O	A-CC5H10O
B-CC5H10O	B-DC5H10O	C-DC5H10O	NEOC5H11O2	NEOC5H11O

NEOC5H10OOH	NEOC5H10OOH-O2	NEO-C5H10O	C3H5-A	C3H5-S
C3H5-T	C3H3	C3H2	C3H6O1-2	OCHO
CH2(S)	NC4KET24	IC4KETII	IC4KETIT	IC4H7-I1
C3H6OH	HOC3H6O2	O2C2H4O2H	CH2O2HCHO	IC3H5CHO
TC3H6OCHO	TC3H6CHO	IC3H7CHO	IC4H7OH	IC3H6CO
IC4H6OH	IC3H5CO	IC3H7CO	TC3H6O2CHO	IC3H5O2HCHO
TC3H6OHCHO	TC3H6OH	IC3H5OH	O2C4H8CHO	O2HC4H7CHO
C3H5OH	CH2CCH2OH	C2H5COCH3	CH2CHOOHCOCH3	CH3CHOOHCOCH3
CH3CHOOCOCH3	CH3CHCOCH3	C2H3COCH3	CH3CHCO	C2H5CHO
IC3H5COCH3	IC3H5COCH2	AC3H4COCH3	SC3H5COCH2	CH3CHCHO
IC3H6CHO	IC3H6CHCO	AC3H5CHCHO	AC3H5CHO	AC3H5CO
C4H8CHO-3	C4H8CHO-4	HOCH2O	HOCHO	AC6H13
BC6H13	DC6H13	EC6H13	AC6H12	BC6H12
CC6H12	DC6H12	IC6H11	CC6H13O	CC6H12OOH-E
DC6H12OOH-B	DC6H12OOH-C	DC6H12OOH-E	A-AC6H12O	A-BC6H12O
B-DC6H12O	C-DC6H12O	C-EC6H12O	D-EC6H12O	NEOC6H14
FC6H13	GC6H13	HC6H13	NEOC6H12	NEOC6H11
F-FC6H12O	TC4H9CHO	TC4H8CH2CHO	IC4H7CHO	IC4H7CO
C4H7CHO1-2	C4H7CO1-2	C4H7CHO2-2	C4H7CO2-2	C7H162-4
XC7H15	YC7H15	ZC7H15	XC7H14	YC7H14
XC7H13	XC7H14OOH-Z	XC7H14OOH-Y2	YC7H14OOH-X1	YC7H14OOH-Y2
ZC7H14OOH-X	X-Y1C7H14O	X-Y2C7H14O	X-ZC7H14O	Y-ZC7H14O
C7KET24ZX	C7KET24ZY	OC7H15	PC7H15	QC7H15
OC7H14	PC7H14	PC7H13	OC7H15O	OC7H14OOH-N
OC7H14OOH-Q	OC7H14OOH-P	N-OC7H14O	O-PC7H14O	O-QC7H14O
NEOC7KETON	NEOC7KETOP	NEOC7KETPO	IC8H18	AC8H17
BC8H17	CC8H17	DC8H17	IC8H16	JC8H16
IC8H14	IC8H15	AC8H17O2H	BC8H17O2H	BC8H17O
AC8H16OOH-C	BC8H16OOH-C	BC8H16OOH-A	BC8H16OOH-D	CC8H16OOH-B

142

IC8ETERAB	IC8ETERBC	IC8ETERBD	NEOC5H11COCH3	XC7H13O-Z
PC7H13O-O	CC6H11O-B	XC7H14OH-Y	YC7H14OH-X	ZC7H14OH-Y
YC7H14OH-Z	OC7H14OH-P	PC7H14OH-O	QC7H14OH-P	PC7H14OH-Q
XC7H14OH-YO2	YC7H14OH-XO2	ZC7H14OH-YO2	YC7H14OH-ZO2	OC7H14OH-PO2
PC7H14OH-OO2	PC7H14O-OO2H	PC7H14OH-QO2	CC8H16OH-B	BC8H16OH-C
CC8H16OH-D	DC8H16OH-C	CC8H16OH-BO2	CC8H16O-BO2H	BC8H16OH-CO2
BC8H16O-CO2H	CC8H16OH-DO2	CC8H16O-DO2H	DC8H16OH-CO2	DC8H16O-CO2H

Table B.6 : List of 337 species of the reduced mechanism containing 3183 reactions for the description of catalytic partial oxidation of i-octane for C/O=1.6, T=1005.78 K, t=1.0s

H	H2	O	O2	OH
H2O	N2	CO	HCO	CO2
CH3	CH4	HO2	H2O2	CH2O
CH3O	C2H6	C2H4	C2H5	CH2
C2H	C2H2	C2H3	CH3OH	CH2OH
CH2CO	HCCO	C2H5OH	PC2H4OH	SC2H4OH
CH3CO	CH2CHO	CH3CHO	C3H4-A	C3H4-P
C3H6	C4H6	NC3H7	IC3H7	C3H8
IC4H7	IC4H8	C4H7	C4H8-2	C4H8-1
SC4H9	PC4H9	TC4H9	IC4H9	IC4H10
C4H10	CH3COCH3	CH3COCH2	C2H5CHO	C2H5CO
C5H9	C5H10-1	C5H10-2	IC5H12	AC5H11
BC5H11	CC5H11	DC5H11	AC5H10	BC5H10
CC5H10	IC5H9	NC5H12	C5H11-1	C5H11-2
C5H11-3	NEOC5H12	NEOC5H11	C2H5O	CH3O2
C2H5O2	CH3O2H	C2H3O1-2	C2H4O1-2	C2H4O2H
O2C2H4OH	C2H3CO	C2H3CHO	C3H5O	C3H6OOH1-2
C3H6OOH2-1	C3H6OOH1-2O2	C3H6OOH2-1O2	NC3H7O	IC3H7O
IC3H7O2H	NC3H7O2	IC3H7O2	C3H6O1-3	IC4H8O

143

IC4H8OH	IO2C4H8OH	IC4H7O	C4H7O	C4H8OH-1
C4H8OOH2-3O2	C4H8OOH2-4O2	IC4H8OOH-IO2	IC4H8OOH-TO2	C4H8OOH1-2
C4H8OOH2-1	C4H8OOH2-3	IC4H8O2H-T	TC4H8O2H-I	C4H8O1-2
C4H8O1-3	C4H8O1-4	CC4H8O	PC4H9O	IC4H9O
TC4H9O	TC4H9O2	IC4H9O2	SC4H9O2	AC5H11O2
BC5H11O2	CC5H11O2	BC5H10OOH-A	BC5H10OOH-C	BC5H10OOH-D
CC5H10OOH-A	CC5H10OOH-B	CC5H10OOH-D	A-BC5H10O	A-CC5H10O
B-CC5H10O	B-DC5H10O	C-DC5H10O	NEOC5H11O2	NEOC5H11O
NEOC5H10OOH	NEOC5H10OOH-O2	NEO-C5H10O	C3H5-A	C3H5-S
C3H5-T	C3H3	C3H2	C3H6O1-2	OCHO
CH2(S)	NC4KET24	IC4KETII	IC4KETIT	IC4H7-I1
C3H6OH	HOC3H6O2	O2C2H4O2H	CH2O2HCHO	IC4H7OOH
IC3H5CHO	TC3H6OCHO	TC3H6CHO	IC3H7CHO	IC4H7OH
IC3H6CO	IC4H6OH	IC3H5CO	IC3H7CO	TC3H6O2CHO
IC3H5O2HCHO	TC3H6OHCHO	TC3H6OH	IC3H5OH	TC4H8CHO
O2C4H8CHO	O2HC4H7CHO	C3H5OH	CH2CCH2OH	CH2CHOOHCOCH3
CH3CHOOHCOCH3	CH3CHOOCOCH3	C2H3COCH3	CH3CHCO	IC3H5COCH3
IC3H5COCH2	AC3H4COCH3	SC3H5COCH2	CH3CHCHO	IC3H6CHO
IC3H6CHCO	AC3H5CHCHO	AC3H5CHO	AC3H5CO	C4H8CHO-3
C4H8CHO-4	HOCH2O	HOCHO	AC6H13	BC6H13
DC6H13	EC6H13	AC6H12	BC6H12	CC6H12
DC6H12	IC6H11	CC6H13O	BC6H12OOH-C	CC6H12OOH-B
CC6H12OOH-D	CC6H12OOH-E	DC6H12OOH-A	DC6H12OOH-B	DC6H12OOH-C
DC6H12OOH-E	A-AC6H12O	A-BC6H12O	A-DC6H12O	B-DC6H12O
C-DC6H12O	C-EC6H12O	D-EC6H12O	C4H7CHO2-1	C4H6CHO2-11
NEOC6H14	FC6H13	GC6H13	HC6H13	NEOC6H12
NEOC6H11	F-FC6H12O	TC4H9CHO	TC4H9CO	NEOC5H11CHO
TC4H9CHCHO	TC4H8CH2CHO	IC4H7CHO	IC4H7CO	C4H7CHO1-2
C4H7CO1-2	C4H7CHO2-2	C4H7CO2-2	C7H162-4	XC7H15

YC7H15	ZC7H15	XC7H14	YC7H14	XC7H13
XC7H14OOH-Y1	XC7H14OOH-Z	XC7H14OOH-Y2	YC7H14OOH-X1	YC7H14OOH-Y2
ZC7H14OOH-X	ZC7H14OOH-Y	X-Y1C7H14O	X-Y2C7H14O	X-ZC7H14O
Y-ZC7H14O	C7KET24ZX	C7KET24ZY	NC7H15	OC7H15
PC7H15	QC7H15	OC7H14	PC7H14	PC7H13
OC7H15O	NC7H14OOH-O	OC7H14OOH-N	OC7H14OOH-Q	PC7H14OOH-N
OC7H14OOH-P	N-OC7H14O	N-PC7H14O	O-PC7H14O	O-QC7H14O
NEOC7KETON	NEOC7KETOP	NEOC7KETPO	IC8H18	AC8H17
BC8H17	CC8H17	DC8H17	IC8H16	JC8H16
IC8H14	IC8H15	AC8H17O2H	BC8H17O2H	BC8H17O
AC8H16OOH-C	BC8H16OOH-C	BC8H16OOH-A	BC8H16OOH-D	CC8H16OOH-B
DC8H16OOH-D	IC8ETERAB	IC8ETERBC	IC8ETERBD	IC8ETERDD
NEOC5H11COCH3	IC4H7COCH3	IC4H7COCH2	YC7H13OOH-X1	YC7H13O-X1
XC7H13O-Z	PC7H13O-O	CC6H11O-B	XC7H14OH-Y	YC7H14OH-X
ZC7H14OH-Y	YC7H14OH-Z	IC4H7OH-I1	OC7H14OH-P	PC7H14OH-O
QC7H14OH-P	PC7H14OH-Q	XC7H14OH-YO2	YC7H14OH-XO2	ZC7H14OH-YO2
ZC7H14O-YO2H	YC7H14OH-ZO2	OC7H14OH-PO2	PC7H14OH-OO2	PC7H14O-OO2H
PC7H14OH-QO2	CC8H16OH-B	BC8H16OH-C	CC8H16OH-D	DC8H16OH-C
CC8H16OH-BO2	CC8H16O-BO2H	BC8H16OH-CO2	BC8H16O-CO2H	CC8H16O-DO2H
DC8H16OH-CO2	DC8H16O-CO2H			

CURRICULUM VITAE

Personal Information:

Name: Hüseyin Karadeniz

Birth Location: Sakarya, TURKEY

Date of Birth: 22 / 05 / 1984

Marital Status: Single, No Children

Communication Information:

Home Address: Oppelner Strasse, 11   Plz:76139 Ort: Karlsruhe, GERMANY

Cell Phone: +49 (173) 188 06 31

E-mail: huseyinkaradeniz@gmail.com

Educational Information:

- Istanbul Technical University, Institute of Natural Sciences, Mechanical Engineering Department, Automative Master Programme (GPA: 3.38 / 4.00)

- Sakarya University, Institute of Natural Sciences, Mechanical Engineering Department (2003-2008)

  Bachelor Degree, Graduation Score (GPA): 3.08 / 4.00 (84,8 % success, in top 5 % interval among all the students in the department)

- Sakarya Anatolian High School (1998-2002)

  Graduation Score (GPA): 4.13 / 5.00

Attended Courses:

- Ansys, Sakarya University - Sausem* (2007)

- Pro Engineer, Sakarya University - Sausem (2007)

- Advanced English Course, Center Linguista Language School, Toronto / Canada (2006)

- Intermediate English Course, Center Linguista Language School, Toronto / Canada (2006)

- Catia V5, Sakarya University - Sausem (2005)

* Education center in Sakarya University for computer programs and languages

Certificates:

- Pro Engineer Wildfire 2.0 Attendance Certificate, 2007

- Ansys Attendance Certificate, 2007

- Advanced III English Certificate (77 % Grammar Success, 92 % Conversation Success), 2006

- Advanced II English Certificate (83 % Grammar Success, 89 % Conversation Success), 2006

- Advanced I English Certificate (86 % Grammar Success, 82 % Conversation Success), 2006

- Intermediate III English Certificate (87 % Grammar Success), 2006

- Catia V5 Attendance Certificate, 2006

Qualifications:

Computer Knowledge

- MS Office Programs (Advanced Level)

- Catia V5 (Intermediate Level)

- MS Adams (Intermediate Level)

- Fortran 90/95 (Advanced Level)

- Pro Engineer (Elementary Level)

- Ansys (Elementary Level)

- Matlab (Elementary Level)

- Microsoft Windows XP, Windows Vista (Advanced Level)

Languages

- Turkish (Native Language)

- Advanced in English

- Intermediate in German

Additional Exam Informations:

- UDS (Interuniversity Board Foreign Language Examination): 77.5 / 100

- ALES (Academic Staff and Graduate Education Entrance Examination): 82.663 / 100

Mandatory Work Experiences During Bachelor Studies:

- IETT Engine Renewing Factory, Ikitelli , Istanbul

  Trainee Engineer, Maintenance and Renovation, 2007

- Goodyear Lastikleri T.A.Ş. (Goodyear Tire & Rubber Factory)

  Trainee Engineer, Production, 2005

References:

- Prof. Dr. Olaf Deutschmann

  Institute für Technische Chemie und Polymerchemie

  Karlsruhe Institut für Technology

  Tel: +49 721 608-3064

  Fax: +49 721 608-4805

  olaf.deutschmann@kit.edu

- Prof. Dr. Cem Sorusbay

  Istanbul Technical University, Faculty of Mechanical Engineering

  Automotive Divison, Laboratory of Engines and Vehicles

  34390 Maslak – Istanbul / Turkey

  Tel. : +90 212 285 3466

  Fax : +90 212 285 3443

  sorusbay@itu.edu.tr

- Prof. Dr. Hakan Serhad Soyhan

  Sakarya University, Faculty of Mechanical Engineering

54187 Serdivan – Sakarya / Turkey

Tel: +90 264 295 58 69

hsoyhan@sakarya.edu.tr